

FILOVIRUS INFECTION IN THE EGYPTIAN ROUSETTE BAT (*ROUSETTUS AEGYPTIACUS*): PATHOLOGY, PATHOGENESIS, AND INVESTIGATION INTO A VIRUS-RESERVOIR HOST RELATIONSHIP

by

MEGAN E.B. JONES

(Under the Direction of Jonathan S. Towner and Corrie C. Brown)

ABSTRACT

Marburgviruses and ebolaviruses (*Filoviridae*) cause sporadic outbreaks of hemorrhagic fever in humans and nonhuman primates. Filoviruses are significant because of rapid spread, high fatality rate, and a lack of specific treatment or vaccine. Though the definitive identity of natural animal reservoir(s) for filoviruses remained elusive for decades, bats have been implicated as potential sources of infection. Several lines of evidence have shown that Egyptian rousette bats (*Rousettus aegyptiacus*) are natural hosts of marburgviruses and consistent sources of virus spillover. Cumulative evidence suggests various fruit bat species may also play a role in transmission of ebolaviruses. The goal of this research was to investigate the pathology and pathogenesis of filovirus infection in Egyptian rousette bats through a series of experimental infection and susceptibility studies.

In the first set of studies, we investigated the clinical and pathologic effects of experimental Marburg virus infection in Egyptian rousettes through a serial euthanasia study. Captive-born, juvenile rousettes were inoculated with a low-passage, wild-type

Marburg virus originally isolated from a naturally-infected bat. Results showed very mild liver lesions associated with viral antigen. Findings were consistent with patterns of Marburg virus infection in wild bats, showing that our experimental model replicates closely the natural Marburg virus-reservoir host relationship. This establishes the model as a useful tool for exploring the molecular and immunologic determinants of filovirus-natural host dynamics.

In the second set of experiments, we investigated the susceptibility of Egyptian rousettes to each of the five known ebolaviruses (Sudan virus, Ebola virus, Bundibugyo virus, Taï Forest virus, and Reston virus), and compared findings with Marburg virus. For four ebolaviruses, results showed that rousettes are generally refractory to infection. Sudan viral RNA was more disseminated, but tissue viral loads were low. In contrast, Marburg virus RNA was widely disseminated, with evidence of viremia, viral shedding, and antigen in spleen and liver. These results suggest that Egyptian rousettes are unlikely sources for ebolaviruses in nature.

Cumulatively, our results lend support to a possible single filovirus – single bat host relationship. A better understanding of virus-host dynamics will help guide public health efforts toward prevention and mitigation of filoviral disease outbreaks.

INDEX WORDS: Filoviruses, Marburgviruses, Ebolaviruses, Ebola virus, Marburg virus, Sudan virus, Bundibugyo virus, Taï Forest virus, Reston virus, Reservoir host, Viral pathogenesis, Hemorrhagic fever viruses, Emerging infectious diseases, Pathology, Histology, Immunohistochemistry, Bats, *Rousettus aegyptiacus*, Experimental infection

FILOVIRUS INFECTION IN THE EGYPTIAN ROUSETTE BAT (*ROUSETTUS
AEGYPTIACUS*): PATHOLOGY, PATHOGENESIS, AND INVESTIGATION INTO A
VIRUS-RESERVOIR HOST RELATIONSHIP

by

MEGAN E.B. JONES

BSc, The University of King's College / Dalhousie University, Canada, 1995

DVM, The University of Prince Edward Island, Canada, 2005

A Dissertation Submitted to the Graduate Faculty of The University of Georgia in Partial
Fulfillment of the Requirements for the Degree

DOCTOR OF PHILOSOPHY

ATHENS, GEORGIA

2015

© 2015

Megan E.B. Jones

All Rights Reserved

FILOVIRUS INFECTION IN THE EGYPTIAN ROUSETTE BAT (*ROUSETTUS
AEGYPTIACUS*): PATHOLOGY, PATHOGENESIS, AND INVESTIGATION INTO A
VIRUS-RESERVOIR HOST RELATIONSHIP

by

MEGAN E.B. JONES

Major Professors: Jonathan S. Towner
Corrie C. Brown

Committee: Elizabeth Howerth
Nicole Gottdenker

Electronic Version Approved:

Julie Coffield
Interim Dean of the Graduate School
The University of Georgia
May 2015

DEDICATION

I dedicate this dissertation to the memory of two women who shaped my love of science, encouraged excellence, and guided me through key junctions in my life: Deane Renouf and Linda Munson.

ACKNOWLEDGEMENTS

First and foremost, I'd like to express deep appreciation to Jon Towner, my co-major professor. The Virus Host Ecology Team in the Viral Special Pathogens Branch at CDC is a small and special group, composed of a people from disparate areas of expertise who share a similar sensibility, sense of humor, and work ethic. Jon leads the team with enthusiasm, common sense, great respect for his colleagues, and compassion for our unique study species, the "rosies". Brian Amman, Tara Sealy, Amy Schuh, and Luke Uebelhoer shouldered much of the burden of the day-to-day work and were integral to every step of this project.

My other colleagues in VSPB made me feel welcome from day one: Kim Dodd took me under her wing in the lab; Brian Bird consistently encouraged me to see things from a different point of view; and Anita McElroy's relentless productivity and positivity are an inspiration. I also thank Stuart Nichol, Pierre Rollin, Christina Spiropoulou, Andy Comer, Bobbie Erickson, Zach Reed, and all of VSPB.

My co-major professor, Corrie Brown, was incredibly supportive and I greatly appreciate her enthusiasm for my independent work and her "can-do" attitude. Nicole Gottdenker and Buffy Howerth have been wonderful to work with, as committee members and as pathologists. I'd also like to thank the administrative staff (Megan Troutman, Christy Morris, Jennifer Kempf, and Amanda Crawford) for always stepping up, as well as Keith Harris and my fellow grad students.

I could not have done any of my experiments without help, training, and equipment from the Infectious Diseases Pathology Branch at CDC: Sherif Zaki, Pat Greer, Chris Paddock, Libby White, Mitesh Patel, Cynthia Seales, Tara Jones, and Maureen Metcalfe all contributed directly to this work. Sherif and his wife Nadia were continually supportive both in and outside of work.

At CDC, I'd also like to thank the Animal Resources Branch (especially Abiola Aminu and Peter Eweronsky) for their many hours caring for the bats in the high-containment labs.

I am grateful to my current colleagues at the Wildlife Disease Laboratories at the San Diego Zoo. Bruce Rideout, Rebecca Papendick, Ilse Stalis, and Allan Pessier covered for my absences while I worked to finish this dissertation

Finally, I thank my husband, Clifton Drew for his essential support throughout my PhD.

TABLE OF CONTENTS

	Page
ACKNOWLEDGEMENTS	v
LIST OF TABLES	viii
LIST OF FIGURES.....	ix
CHAPTER	
1 INTRODUCTION.....	1
2 LITERATURE REVIEW.....	7
3 CLINICAL, HISTOPATHOLOGIC, AND IMMUNOHISTOCHEMICAL CHARACTERIZATION OF EXPERIMENTAL MARBURG VIRUS INFECTION IN A NATURAL RESERVOIR HOST, THE EGYPTIAN ROUSETTE BAT (<i>ROUSETTUS AEGYPTIACUS</i>).....	42
4 EXPERIMENTAL INOCULATION OF EGYPTIAN ROUSETTE BATS (<i>ROUSETTUS AEGYPTIACUS</i>) WITH FIVE EBOLAVIRUSES AND COMPARISON WITH MARBURG VIRUS	82
5 CONCLUSIONS	130
APPENDICES	
A: SUPPLEMENTAL DATA: VIREMIA, VIRAL TISSUE DISSEMINATION, AND EVIDENCE OF ORAL SHEDDING IN EGYPTIAN ROUSETTE BATS EXPERIMENTALLY INOCULTED WITH MARBURG VIRUS ..	133

LIST OF TABLES

	Page
Table 3.1: Liver viral load, liver histologic score, liver immunohistochemical staining results and alanine aminotransferase results for Egyptian rousette bats (<i>Rousettus aegyptiacus</i>) experimentally infected with Marburg virus in a serial euthanasia study	71
Table 3.2: Immunohistochemistry results for tissues other than liver, for Egyptian rousette bats (<i>Rousettus aegyptiacus</i>) experimentally infected with Marburg virus in a serial euthanasia study	73
Table 4.1: Pilot Study: Tissue viral loads as determined by quantitative reverse-transcriptase PCR (Q-RT-PCR) for Egyptian rousette bats (<i>Rousettus aegyptiacus</i>) experimentally inoculated with Marburg virus or one of five species of ebolavirus, and euthanized at days 5 or 10 post-inoculation.	116
Table 4.2: Tissue viral loads for Egyptian rousette bats (<i>Rousettus aegyptiacus</i>) inoculated with Sudan virus (Gulu) in a serial euthanasia study.	118
Table A.1: Viral loads in tissues from Egyptian rousette bats inoculated with Marburg virus in a serial euthanasia study.....	135

LIST OF FIGURES

Figure 3.1: Scatterplots and mean values of complete blood count and leukocyte differentials for <i>Rousettus aegyptiacus</i> bats experimentally inoculated with Marburg virus in a serial euthanasia study. A. Total leukocyte counts; B. Lymphocyte counts; C. Monocyte counts; D. Granulocyte counts.....	77
Figure 3.2: Blood chemistry values for <i>Rousettus aegyptiacus</i> bats experimentally inoculated with Marburg virus in a serial euthanasia study.....	78
Figure 3.3: Photomicrographs of tissues from Marburg-virus inoculated Egyptian rousette bats.	79
Figure 3.4: Graphical representation of liver viral load, immunohistochemical staining results, and liver score. Liver viral loads are represented as \log_{10} 50% tissue culture infective dose (TCID ₅₀) equivalents per gram, derived from quantitative reverse-transcriptase PCR.	80
Figure 3.5: Localization of Marburg viral antigen in tissues of Egyptian rousette bats. All stains are immunoalkaline phosphatase with naphthol fast red and hematoxylin counterstain.	81
Figure 4.1: Blood chemistry measurements for bats inoculated with six different filoviruses in the pilot study and euthanized at 5 and 10 days post inoculation (DPI).	122

Figure 4.2: Complete white blood cell (WBC) counts for bats inoculated with six different filoviruses in the pilot study and euthanized at 5 and 10 days post inoculation (DPI).....	123
Figure 4.3: Viral RNA, as determined by Q-RT-PCR, in four bats inoculated with Marburg virus and euthanized at 5 (n=2) and 10 (n=2) days post inoculation. ...	124
Figure 4.4: Photomicrographs of liver and spleen from Marburg-virus inoculated Egyptian rousette bats in a pilot study.	125
Figure 4.5: Complete blood count data for Egyptian rousette bats inoculated with Sudan virus, Marburg virus, and mock-inoculated controls in a serial euthanasia study.	126
Figure 4.6: Blood chemistry measurements Egyptian rousette bats inoculated with Sudan virus.	127
Figure 4.7: Serology results for Egyptian rousette bats inoculated with Sudan virus in a serial euthanasia study. Results for anti SUDV IgG measured by enzyme linked immunosorbent assay are shown as adjusted sum optical densities (OD) by day post-inoculation for 15 SUDV inoculated bats and 3 mock-inoculated control bats...	128
Figure 4.8: Comparison of SUDV and MARV RNA levels in Egyptian rousette tissues (skin at the inoculation site, liver, spleen, and kidney) compared at days 3, 6, 9, 12, and 15 post-infection. Viral loads are expressed as log ₁₀ 50% tissue culture infective dose (TCID ₅₀) equivalents per gram, derived from quantitative reverse-transcriptase PCR.	129

Figure A.1: Viral RNA load in blood (Q-RT –PCR derived 50% tissue culture infective dose (TCID₅₀) equivalents (eq.)/gram) in 27 bats inoculated with Marburg virus in a serial euthanasia study..... 139

Figure A.2: Viral RNA loads for spleen, liver, kidney, and skin at the inoculation site, compared with blood levels at the time of euthanasia.. 140

Figure A.3: Viral RNA loads for tissues potentially involved in viral shedding (large intestine, urinary bladder, and salivary gland) for 27 bats inoculated with Marburg virus in a serial euthanasia study..... 141

Figure A.4: Viral loads for oral and rectal swabs taken from bats experimentally inoculated with Marburg virus. 142

Figure A.5: Serology results for bats inoculated with Marburg virus in a serial euthanasia study. All bats had seroconverted by 12 days post-inoculation.. 143

CHAPTER 1

INTRODUCTION

Filoviruses (marburgviruses and ebolaviruses) are significant pathogens that can cause severe, highly transmissible hemorrhagic fever (known as filoviral disease, FVD) in humans and nonhuman primates (1–3). Though the total public health impact of filoviral disease is small relative to more common diseases such as malaria and tuberculosis, filoviruses are uniquely important because of their propensity for rapid spread, very high case fatality rate, and lack of specific preventive or therapeutic options. Furthermore, it is not possible to predict the timing or location of outbreaks of FVD because the natural histories of these viruses are incompletely understood. Among the most important outstanding questions is the identity of natural reservoir(s) of the viruses. While it is clear that human filoviral hemorrhagic fever outbreaks have resulted from direct exposure to a variety of animal species, the identity of species capable of maintaining the viruses in nature remains in question. In the four decades since the discovery of filoviruses, anecdotal and epidemiologic data have repeatedly suggested links between bats and outbreaks of filoviral disease (4–8). Recent ecological and molecular studies have demonstrated that the Egyptian rousette bat, *Rousettus aegyptiacus*, can be a natural source for marburgvirus spillover to humans, and preliminary experimental infection studies have demonstrated this species' susceptibility to infection (9–12). This bat species has also tested positive for ebolavirus-specific antibodies, in a single study and at low

prevalence, though infectious ebolavirus has never been isolated from any bat species (13).

A true reservoir host species is expected to be susceptible to infection, and to exhibit sustained viremia and viral shedding at sufficient rates to allow animal-to-animal transmission and maintain long-term circulation within the population (14,15). The goal of this research is to use experimental infection studies to investigate the potential for Egyptian rousette bats to act as reservoir hosts for filoviruses and to elucidate virus-reservoir host dynamics. Using experimental infection studies of Egyptian rousette bats, the aims of this research are to (1) investigate this species' susceptibility to infection by filoviruses; (2) investigate the clinical and pathologic features, and pathogenesis, of filovirus infection in bats; and, (3) compare findings across viruses representing different filovirus species. The end product of these studies is the development and characterization of an experimental system for studying filovirus dynamics in a true reservoir host. Our results contribute to a better understanding of virus-host dynamics that will, ultimately, guide public health efforts toward prevention and mitigation of human filoviral hemorrhagic fever outbreaks.

Hypotheses and Specific Objectives

We hypothesized that, if Egyptian rousette bats are the natural reservoir hosts of marburgviruses, then bats of this species should be susceptible to marburgvirus infection but not manifest clinical or pathologic evidence of significant disease. To address this hypothesis our objectives were to: 1) characterize the clinical and pathologic response of *Rousettus aegyptiacus* fruit bats to experimental infection with Marburg virus; 2)

demonstrate the tissue and cell-type distribution of Marburg viral antigen in experimentally-infected Egyptian rousette bats, and to correlate presence of antigen with pathologic lesions, if any; and, 3) compare histologic and immunohistochemical findings in experimentally infected bats to those found in wild-caught bats known to be infected with marburgviruses.

Regarding ebolaviruses, we hypothesized that, if Egyptian rousette bats are not a true reservoir host of any of the five ebolaviruses, then the response of this bat species to experimental infection with ebolaviruses will differ from the response to marburgvirus infection. Experimental inoculation of rousettes with ebolaviruses will result in either 1) abortive infection due to lack of susceptibility; or, 2) clinical and pathologic signs of such severe disease that long-term persistence in this species is unlikely. To address this, our objectives were to: 1) determine whether Egyptian rousette bats are susceptible to infection with representative strains of each of the five ebolavirus species, and to preliminarily characterize clinical and pathologic response to infection in a pilot study; and 2) investigate clinical and pathologic response to experimental ebolavirus infection of bats, and compare responses to different virus species, through complete blood count, clinical chemistry, gross pathology, histology, and immunohistochemistry.

References

1. Feldmann H, Sanchez A, Geisbert T. *Filoviridae*: Marburg and Ebola viruses. In: Knipe D, Howley P, editors. *Fields Virology*. Sixth Ed. Philadelphia: Lippincott, Williams, and Wilkins; 2012. p. 923–56.
2. Hartman AL, Towner JS, Nichol ST. Ebola and marburg hemorrhagic fever. *Clin Lab Med*. 2010;30(1):161–77.
3. Kuhn JH, Becker S, Ebihara H, Geisbert TW, Johnson KM, Kawaoka Y, et al. Proposal for a revised taxonomy of the family *Filoviridae*: classification, names of taxa and viruses, and virus abbreviations. *Arch Virol*. 2010 Dec;155(12):2083–103.
4. Food and Agriculture Organisation of the United Nations. Investigating the role of bats in emerging zoonoses: balancing ecology, conservation, and public health interest. Newman SH, Field H, Epstein JH, de Jong C, editors. Rome: FAO Animal Production and Health Manual No. 12.; 2011.
5. Arata A, Johnson B. Approaches towards studies on potential reservoirs of viral haemorrhagic fever in southern Sudan (1977). *Ebola Virus Haemorrhagic Fever*. 1978.
6. Olival KJ, Hayman DTS. Filoviruses in bats: current knowledge and future directions. *Viruses*. 2014 Apr;6(4):1759–88.

7. Bausch DG, Borchert M, Grein T, Roth C, Swanepoel R, Libande ML, et al. Risk factors for Marburg hemorrhagic fever, Democratic Republic of the Congo. *Emerg Infect Dis.* 2003 Dec;9(12):1531–7.
8. Swanepoel R, Smit SB, Rollin PE, Formenty P, Leman PA, Kemp A, et al. Studies of reservoir hosts for Marburg virus. *Emerg Infect Dis.* 2007;13(12):1847–51.
9. Towner JS, Amman BR, Sealy TK, Carroll SAR, Comer JA, Kemp A, et al. Isolation of genetically diverse Marburg viruses from Egyptian fruit bats. *PLoS Pathog.* 2009;5(7):e1000536.
10. Towner JS, Pourrut X, Albariño CG, Nkogue CN, Bird BH, Grard G, et al. Marburg virus infection detected in a common African bat. *PLoS One.* 2007;2(8).
11. Amman BR, Carroll SA, Reed ZD, Sealy TK, Balinandi S, Swanepoel R, et al. Seasonal pulses of Marburg virus circulation in juvenile *Rousettus aegyptiacus* bats coincide with periods of increased risk of human infection. *PLoS Pathog.* 2012;8(10):e1002877.
12. Paweska JT, Jansen van Vuren P, Masumu J, Leman PA, Grobbelaar AA, Birkhead M, et al. Virological and serological findings in *Rousettus aegyptiacus* experimentally inoculated with vero cells-adapted hogan strain of Marburg virus. *PLoS One.* 2012;7(9):e45479.
13. Pourrut X, Souris M, Towner JS, Rollin PE, Nichol ST, Gonzalez J-P, et al. Large serological survey showing cocirculation of Ebola and Marburg viruses in

Gabonese bat populations, and a high seroprevalence of both viruses in *Rousettus aegyptiacus*. BMC Infect Dis. 2009;9:159.

14. Viana M, Mancy R, Biek R, Cleaveland S, Cross PC, Lloyd-Smith JO, et al. Assembling evidence for identifying reservoirs of infection. Trends Ecol Evol. 2014;29(5):270–9.
15. Haydon DT, Cleaveland S, Taylor LH, Laurenson MK. Identifying reservoirs of infection: a conceptual and practical challenge. Emerg Infect Dis. 2002 Dec;8(12):1468–73.

CHAPTER 2

LITERATURE REVIEW

Taxonomy and History of Filoviruses

Filoviruses are negative-sense, single-stranded RNA viruses (order *Mononegavirales*). They are the etiologic agents of Marburg virus disease (MVD) and Ebola virus disease (EVD), which are characterized by rapid person-to-person transmission, high case fatality rates, and a lack of specific preventive or therapeutic options. All filoviruses are classified as Tier 1 Select Agents by the United States Department of Health and Human Services (HHS), and as Risk Group 4 Pathogens by the World Health Organization (WHO). As such, all work with infectious materials must be performed in high containment laboratories under biosafety level-4 (BSL-4) conditions, and strict regulations for storage, transfer, use, and inventory apply to all samples (1).

According to current taxonomic classification (2,3), the family *Filoviridae* is divided into three antigenically distinct genera: *Ebolavirus*, *Marburgvirus*, and the provisionally approved genus *Cuevavirus*, recently discovered in a European bat (4). At the nucleotide level, marburgvirus and ebolavirus genomes differ from each other by greater than 50% (2,5). Genus *Marburgvirus* contains a single species, *Marburg marburgvirus*, with two virus members, Marburg virus (MARV) and Ravn virus (RAVV), which are approximately 20% divergent (5). The genus *Ebolavirus* contains five species that each include a single virus member: *Sudan ebolavirus* (Sudan virus,

SUDV), *Zaire ebolavirus* (Ebola virus, EBOV), *Bundibugyo ebolavirus* (Bundibugyo virus, BDBV), *Tai Forest ebolavirus* (Tai Forest virus, TAFV), and *Reston ebolavirus* (Reston virus, RESTV). *Cuevavirus* consists of a single species and virus, *Lloviu cuevavirus* (Lloviu virus). Based on full-genome sequences, the ebolaviruses exhibit 31.7 to 42.3% divergence (6). Human disease caused by MARV and EBOV is associated with the highest fatality rates (up to 90%), followed by SUDV (42-65%) (7–9) and BDBV (36 to 40%) (6,10,11). TAFV has caused one non-fatal human infection (12) and RESTV is considered non-pathogenic to humans, but both can be highly pathogenic in nonhuman primates (13,14).

Marburg virus disease was first identified in 1967 in Germany and the former Yugoslavia, when laboratory workers acquired a fatal illness after exposure to primates imported from Uganda (15). Since that time, there have been 12 additional outbreaks originating in Zimbabwe, Kenya, DRC, Angola, and Uganda, as well as one laboratory-transmitted infection in Russia (5,11,16–18). The two largest outbreaks took place in Durba, DRC (154 cases, 83% mortality rate) and Uige Province, Angola (252 cases, 90% mortality rate).

Ebola virus disease was first documented in 1976, nine years after marburgviruses were discovered. EBOV and SUDV were identified as the causes of concurrent but unrelated outbreaks of hemorrhagic fever in Zaire (now Democratic Republic of the Congo, DRC) and southern Sudan (19,20). Since that time, several outbreaks of EVD due to SUDV have occurred in Uganda and Sudan (South Sudan) (8,11,21–23), with one additional case reported in England due to laboratory contamination. The largest ever outbreak of SUDV, and until recently the largest outbreak of any filoviral disease,

occurred in the Gulu district of Uganda in 2000-2001 and involved 425 cases and 224 deaths (21). Outbreaks of EVD due to EBOV have been similarly sporadic but more frequent than SUDV and with a different geographic distribution that includes DRC, Republic of the Congo (RC), and Gabon (summarized in (17) and (24)). The current EBOV outbreak in West Africa, which surpassed 25,000 cases in March of 2015, is the largest filovirus epidemic in history, and the first in West Africa (24,25). This significant expansion of case numbers and new geographic range for the virus clearly demonstrate the potential of filoviruses to become significant threats to public health on a global scale.

BDBV was discovered in 2007 in western Uganda, and emerged again in 2012 in DRC (6,11). Tai Forest virus was first documented in 1994 in Côte d'Ivoire, where it was associated with mortality in wild chimpanzees and caused one human infection (26,27). Reston virus has only been found in the Philippines, or in macaques imported from the Philippines (28–30). Human exposures have resulted in seroconversion without clinical signs of disease (13,14).

Genome Organization and Viral Proteins

Filoviral genome structure and organization are comprehensively summarized in multiple review articles (17,31–33). Briefly, filoviral genomes consist of approximately 19,000 bases and contain seven monocistronic genes in the order 3' untranslated region-nucleoprotein (NP)-VP35-VP40-glycoprotein (GP)-VP30-VP24-polymerase (L)-5' untranslated region (34,35). Relative to most other members of the order *Mononegavirales*, filovirus genomes are unique because of their large size and unusual intergenic regions, which include short overlaps between the transcription termination

sequence of the upstream gene and the transcription start sequence of the downstream gene (32,35,36). Marburgviruses have a single gene overlap site between VP30 and VP24, while ebolaviruses have two (VP35-VP40, VP24-L in RESTV) or three (VP35-VP40, GP-VP30, VP24-L EBOV, SUDV) overlapping sites (17,31,35,37).

The filoviral nucleocapsid complex is composed of viral RNA and four proteins, NP, VP30, VP35, and L (polymerase) (17,32,38). NP (major nucleoprotein) and VP30 (minor nucleoprotein) are phosphorylated proteins that interact with the genomic RNA molecule. The VP30 of ebolaviruses is involved with transcription initiation, but marburgvirus VP30 may not share this function (36). L is the RNA-dependent RNA polymerase enzyme. VP35 is a cofactor for the polymerase complex, and appears to influence the type of RNA synthesis (transcription vs. translation). VP35 also antagonizes interferon pathways (through inhibition of IRF3, and through other mechanisms) and contributes to the impairment of dendritic cell maturation that is a characteristic of filoviral pathogenesis. GP is an integral membrane glycoprotein that forms a trimeric surface peplomer (each peplomer is composed of a heterodimer of GP1 and GP2). GP functions as a receptor binding protein and membrane fusion protein, and also directs viral trafficking to and fusion with the late endosome. As a surface protein, GP is also a target for antibody binding. Ebolaviruses, but not marburgviruses, also produce a soluble form of the GP (sGP) that is biochemically and antigenically different from the structural GP. sGP, which is produced from transcriptionally edited transcript of the GP gene, is secreted from cells and circulates at relatively high levels in infected humans (17). Its function and definitive role in pathogenesis remain unclear, but hypothesized functions include acting as a decoy for antibodies, or eliciting a protective effect on the

endothelium (through antagonism of the effects of TNF-alpha). As the matrix protein, VP40 is involved in viral assembly and initiates and drives viral budding. In marburgviruses, VP40 antagonizes the type 1 and type 2 interferon pathway by inhibiting phosphorylation of STATs inhibiting multiple Janus Kinase 1-dependent pathways. This function does not appear to be present in ebolaviruses. VP24, the minor matrix protein, is also membrane-associated and appears to be involved in virion assembly. For ebolaviruses, VP24 is also an antagonist of type 1 and type 2 interferon pathways (39).

Clinical Findings in Humans

Human outbreaks of MVD and EVD occur sporadically, usually in remote locations, and clinical data from early stages of outbreaks are often sparse. Observations from a limited number of human outbreaks suggest an abrupt onset of non-specific clinical signs after an incubation period of 2 to 21 days (17,40). Reported initial signs include fever, myalgia, and general malaise, followed by fatigue, nausea, vomiting, diarrhea, abdominal pain, coughing, headache, maculopapular rash, and hypotension (17,40). Hemorrhagic symptoms occur late in the course of infection in only 30-50% of cases, and include petechiae, erythema, bleeding from venipuncture sites, and epistaxis. In fatal cases, time from symptom onset to death varies from 6 to 16 days; late stage disease is characterized by shock, coma, convulsions, generalized coagulopathy, and tachypnea (41,42). In general, levels of viral genomic-sense RNA tend to be 100 times higher in fatal than in nonfatal cases and high viral loads are associated with poor prognosis (9,43). Patients may exhibit a leukopenia characterized by lymphopenia (especially T cells), neutropenia with a left shift, and thrombocytopenia. Blood chemistry abnormalities often include

markedly elevated aspartate aminotransferase (AST) and alanine aminotransferase (ALT), increased amylase, hyperproteinemia, proteinuria, and increased PT, PTT, and fibrin split products. Fatal cases usually die without seroconversion, whereas non-fatal cases can develop relatively high IgM and IgG titers (43).

Pathology in Humans

Due to biosafety concerns with autopsy and risks of hemorrhage with biopsy, there have been limited comprehensive studies of the pathology of filoviral hemorrhagic fever in humans (44,45). Histopathologic lesions in both MVD and EVD are characterized by hemorrhage and widespread necrosis in multiple tissues, particularly the liver, but also spleen and lymph nodes. Eosinophilic, filamentous to oval, cytoplasmic inclusion bodies are often present in hepatocytes in cases of EVD, but inclusions are less distinct in MVD (44,45). In the lungs, there is evidence of diffuse alveolar damage without significant inflammatory response. Additional findings include myocardial edema and acute renal tubular necrosis. Viral antigen is often widely distributed and is readily detectable in hepatocytes, cells of the mononuclear phagocyte system (including alveolar macrophages and dendritic cells), fibroblasts, endothelial cells, and endocardium; very large amounts of viral antigen are also present extracellularly, in areas of necrosis and within hepatic sinusoids (44,46). In the skin, antigen is sufficiently abundant in fibroblasts and endothelial cells that immunohistochemical staining of skin biopsies can be used as a sensitive diagnostic test (46,47).

Pathogenesis

Much of what is known about filoviral pathogenesis is derived from experimental infections of animals, particularly nonhuman primates (see *Experimental Animal Models of Filoviral Disease*, below), and from *in vitro* studies. Filoviruses gain entry to the host through direct contact with infected body fluids, via openings in the skin or mucosal surfaces. Virus has been detected in a wide range of body fluids including saliva, breast milk, tears, stool, and semen, any of which could be infective during the acute illness (48). Aerosol transmission has been achieved in experimental settings (49–52), but is considered unlikely to be a mechanism of human-to-human transmission in an outbreak setting. Viral attachment, membrane fusion, and cell entry are mediated by the envelope glycoprotein (GP), and viral entry occurs via pH-dependent endocytic pathways including macropinocytosis (53–55). Likely candidate receptors include lectins (DC-SIGN, DC-SIGN-R, and L-SIGN); beta-1 integrins; human folate receptor alpha; members of the TAM receptor family; and/or, TIM-114 (55,56). Endosomal cysteine proteases and the Neimann-Pick C1 cholesterol transporter are also necessary for virus entry (57,58). Primary viral replication occurs in local (mucosal or dermal) macrophages and dendritic cells (59,60) which disseminate the virus to the spleen, liver, and lymph nodes. At these sites, productive infection of resident tissue macrophages leads to spread to surrounding parenchymal cells, uncontrolled virus replication, viremia, and, ultimately, broad tissue dissemination.

Immune dysregulation is a key component of the pathogenesis of FVD, and experimental and clinical studies have repeatedly provided evidence of significant immunosuppression in filovirus infected humans and nonhuman primates. Widespread

macrophage activation leads to massive release of proinflammatory cytokines and chemokines, likely contributing to rapid disease progression (61–63). In contrast, infection of dendritic cells results in their aberrant maturation and loss of function; consequences include loss of antigen-presenting capability and failure to stimulate T cells (64,65). Through a variety of mechanisms, viral proteins VP35 (polymerase cofactor), ebolavirus VP24 (minor matrix protein), and marburgvirus VP40 (matrix protein) function as interferon antagonists (66–69). Generalized, predominantly T-cell lymphoid depletion due to bystander apoptosis results in lymphopenia and decreased cell mediated immunity (70,71). However, despite cumulative evidence supporting filovirus-induced immunosuppression, clinical data from four human cases recently treated in the United States revealed unexpected immune activation during both acute and convalescent phases of infection (72). That study found high levels of activated, IgG-positive proliferating B cells, CD4 T cells, and, most prominently, CD8 T cells (72).

In primates, vascular impairment, hemorrhage, and disseminated intravascular coagulation (DIC) occur late in the course of disease. Though endothelial cells can be productively infected, vascular damage and DIC appear to be indirect effects of increased tissue factor expression on activated macrophages, rather than direct effects of endothelial cell damage due to virus infection (73). Hemorrhage may also be secondary to massive hepatocellular damage and associated loss of liver-origin coagulation factors.

Natural Filovirus Infections in Animals

In animals, naturally occurring cases of filoviral disease have been reported in nonhuman primates, which are very susceptible to infection and can exhibit high mortality rates (27–29,74). Reston ebolavirus caused nearly 100% fatality in cynomolgus macaques (*Macaca fascicularis*) and has been isolated several times from clinically ill monkeys transported from the Philippines to the United States and Europe for use in scientific research (28,29). In 1994, Taï Forest virus was identified as a cause of mortality in a population of chimpanzees (*Pan troglodytes*) in Ivory Coast (27). Ecological, epidemiologic, and molecular data implicate EBOV as a cause of large-scale mortality in western gorilla (*Gorilla gorilla*) and chimpanzees in Gabon and RC (74–76). Where data are available, clinical disease, lesions, and viral antigen distribution in natural outbreaks of non-human primate FHV are comparable to that seen in human disease and in experimentally infected nonhuman primates (28,29,77).

Experimental Animal Models of Filoviral Disease

Numerous animal models have been developed for the study of filoviral pathogenesis, prophylaxis, and therapy. Non-human primate models tend to replicate clinical and pathologic findings of human disease more completely than do other animal models, though with a more compressed course of disease, and macaques are considered to be the “gold standard” experimental model for a wide range of filovirus research (49,51,59,73,78–82). Rodent models using mice (BALB/c, C57BL/6, ICR), Syrian golden hamsters, and guinea pigs (Strain-13 or Hartley) require that viruses be serially passaged through the host species of interest, or another rodent species, in order to confer

significant virulence and recapitulate pathology and clinical findings of FVD (39,52,83–87).

Ecology, Natural History, and Reservoir Hosts

Spillover of filoviruses from animals to humans has been documented multiple times, and is often attributed to contact with animal (usually non-human primate) carcasses via hunting or bush meat consumption (88), or through contact with infected nonhuman primate tissues in a research capacity (12,15,89). However, nonhuman primates represent an unlikely reservoir host because of their high susceptibility to disease; it is more probable that infected primates act as intermediate or amplifying hosts that, in turn, acquire infection from a separate, long-term, reservoir species.

Since the discovery of filoviruses over four decades ago, cumulative epidemiologic, ecological, and molecular evidence have suggested a role for bats as natural reservoir hosts (comprehensively reviewed in (90,91). *Rousettus aegyptiacus*, the cave-roosting Egyptian rousette bat (also called the Egyptian fruit bat), has been identified as a natural reservoir host for marburgviruses and a source of virus spillover to humans (92,93). This discovery was based on identification of marburgvirus RNA and immunoglobulin G (IgG) (94,95) and the isolation of infectious marburgviruses (92,93,131) from wild rousettes inhabiting caves where human cases had recently occurred. Longitudinal studies have also demonstrated an association between the risk of human infection and the seasonal pulses of active marburgvirus infection in juvenile Egyptian rousettes during biannual reproductive cycles (93). Several studies have also shown that various fruit bat species may also play a role in the transmission cycle of

ebolaviruses. Early cases in the first SUDV outbreak in 1976 occurred in workers in a cotton factory where bats roosted (97,98). There were also epidemiologic links of bats to TAFV disease in chimpanzees in Côte d'Ivoire in 1994 (27). In 2005, in Gabon and the Republic of Congo, EBOV-specific IgG and RNA were detected in three species of fruit bats (*Hypsignathus monstrosus*, *Epomops franqueti*, and *Myonycteris torquata*), all of which were hunted and eaten by local people (99); this was the first and, thus far, only study in which ebolaviral RNA has been detected in any bat species. A subsequent investigation into a large EBOV outbreak in DRC in 2007 showed an association between regional EVD re-emergence and seasonal fruit bat migration (100). Since that time, several field studies have provided serologic evidence of EBOV exposure in a variety of fruit bat species in Ghana, Gabon, and RC (99,101–103)). Antibodies to RESTV were reported in fruit bats in the Philippines (104) and Bangladesh (105), and in eleven different species of insectivorous and fruit bats in China (106). However, despite multiple attempts, and in contrast to results for marburgviruses, isolation of infectious ebolaviruses from bats has been consistently unsuccessful.

Two recent, experimental infection studies of Marburg virus in Egyptian rousettes have demonstrated virus replication in blood and multiple tissues (96,107); oral shedding of infectious virus (96); and viral antigen in liver and spleen without evidence of significant disease, findings which are consistent with expectations for a reservoir host. Though numerous field studies have demonstrated potential associations between bats and ebolaviruses, only a single experimental ebolavirus infection study has been attempted in any bat species (108). In that experiment, a wide range of possible plant, invertebrate, and vertebrate hosts including two insectivorous bat (*Mops condylurus*,

Chaerephon pumilus) and one fruit bat species (*Epomophorous wahlbergi*) were inoculated with EBOV. Following inoculation, virus was successfully isolated from pooled viscera and blood from bats for up to three weeks, and was isolated from feces in one bat. There was also limited immunohistochemical staining for ebolavirus antigen in pulmonary endothelial cells in one insectivorous bat, without evidence of associated lesions (108).

Bats represent approximately 20% of known mammalian species, second only to rodents in mammalian species abundance (95). The role of rodents as natural reservoirs for both arenaviruses and hantaviruses is well-documented. These virus-rodent reservoir relationships tend to involve a high degree of virus-host species specificity which may be attributable to coevolution of virus and host or to preferential host switching and local adaptation (109–112). Given the diversity of bat species, and using rodent reservoirs as an example, this suggests the possibility of a one-filovirus, one-bat reservoir host relationship.

Bats as Reservoirs of Emerging and Zoonotic Infectious Diseases

Bats have received increasing attention as potential reservoirs of emerging or zoonotic infectious diseases (90,113). Significant or highly-pathogenic viruses known or suspected to be harbored by bats include rhabdoviruses (including rabies virus, European bat lyssaviruses (114)), paramyxoviruses (Hendra and Nipah viruses, as well as numerous other viruses (115–117)), coronaviruses (including SARS virus (118)), and filoviruses (92,93). As a result, there has been increasing research into potentially unique

immunological and ecological characteristics of bats that make them, possibly, more likely than other vertebrates to act as sources of virus spillover.

Historically, the bat immune system has been poorly studied, but data from existing research suggest many similarities with the innate and adaptive immune system of other vertebrates (comprehensively reviewed in (119)). For example, pattern recognition receptors (PRRs) including toll-like receptors (TLRs) and retinoic-acid inducible gene-like helicases, which are involved in inducing early antiviral immune responses, have been described in Pteropid bats (120,121). This includes TLR13, which has only previously been described in rodents and which is hypothesized to be involved with viral recognition. Interestingly, in bats, the TLR13 transcript is truncated, but the significance of this is not clear (120). Types I, II, and III interferons have also been described in bats (122,123). Bats appear to exhibit a full complement of adaptive immune cells and functions, though some studies have suggested possible differences in bats' ability to generate and maintain memory (124–126). Overall, further study and specific immunological tools will be required to clarify the presence of any unique features in the bat immune system.

Ecological characteristics proposed to explain bats' potentially increased ability to act as sources of virus spillover include flight and high dispersal distances; propensity of some species to roost in extremely dense aggregates; social behaviors; torpor and hibernation; relatively long lifespans; synchronous breeding behavior; and, across chiropterans, large species and life history diversity (90,113,127–129). For the Egyptian rousette, which roosts in very dense colonies of up to 100,000 individuals, biannual reproductive cycles likely play a role in maintenance and persistence of filoviruses in the

population. Longitudinal studies have demonstrated an association between the risk of human infection and the seasonal pulses of active marburgvirus infection in juvenile Egyptian rousettes during biannual reproductive cycles (93). Recently, a stochastic susceptible, infectious, and immune (SIR) model using available filovirus data showed that biannual birthing, rather than synchronous annual breeding, was necessary for filovirus persistence in colony sizes often found in nature (129).

Conservation and Public Health

When significant, emerging viral pathogens are discovered in various bat species, the initial public health response has sometimes led to calls for extermination of bat populations. However, virus-host dynamics are complex and, in many cases, spillover may be linked specifically to human disturbance or ecosystem change (128).

Furthermore, while culling efforts are in progress, there is an increased risk of direct and indirect contact between bats and humans; depending on the circumstances, it could be speculated that stress-related corticosteroid responses could lead to bat immunosuppression and increased shedding (128). Ecological models have shown that culling may select for viral strains that are more likely to become established in sparser populations (130). Thus, counter-intuitively, culling could cause increases in viral abundance (130). An example of a population eradication attempt that failed to eliminate a virus is found in marburgviruses and the Egyptian rousette. Following the 2007 discovery that bats were a source of marburgvirus spillover to miners in Kitaka cave, Uganda, the mine was closed and extensive efforts were made to completely exterminate the bat colony (131). Four years later, after a marburgvirus outbreak in the nearby town

that supports the mine, a small number of bats were found to have repopulated the cave, estimated to be approximately 1-5% of the previous population size. At that time, 13.3% of the population was found to be actively infected with marburgviruses, significantly greater than the previous level of 5.1% at that site, and the levels at other large colonies in Uganda and Gabon (2.5 and 4.8%, respectively; (131)). While the reason for the increased prevalence could not be confirmed, the authors speculated that culling and subsequent repopulation may have been important. Alternative strategies to prevent outbreaks might involve better personal protective equipment and a more complete understanding of the virus-reservoir host ecology and epidemiology.

References

1. Department of Health and Human Services, United States Department of Agriculture. Federal Select Agent Program: Regulations. [Internet]. [cited 2015 Oct 3]. Available from: www.selectagents.gov/regulations.html
2. Kuhn JH, Becker S, Ebihara H, Geisbert TW, Johnson KM, Kawaoka Y, et al. Proposal for a revised taxonomy of the family *Filoviridae*: classification, names of taxa and viruses, and virus abbreviations. *Arch Virol*. 2010 Dec;155(12):2083–103.
3. Kuhn JH, Bao Y, Bavari S, Becker S, Bradfute S, Brister JR, et al. Virus nomenclature below the species level: a standardized nomenclature for laboratory animal-adapted strains and variants of viruses assigned to the family *Filoviridae*. *Arch Virol*. 2013;158(6):1425–32.
4. Negrodo A, Palacios G, Vázquez-Morón S, González F, Dopazo H, Molero F, et al. Discovery of an ebolavirus-like filovirus in europe. *PLoS Pathog*. 2011 Oct;7(10):e1002304.
5. Towner JS, Khristova ML, Sealy TK, Vincent MJ, Erickson BR, Bawiec DA, et al. Marburgvirus genomics and association with a large hemorrhagic fever outbreak in Angola. *J Virol*. 2006 Jul;80(13):6497–516.

6. Towner JS, Sealy TK, Khristova ML, Albariño CG, Conlan S, Reeder SA, et al. Newly discovered ebola virus associated with hemorrhagic fever outbreak in Uganda. *PLoS Pathog.* 2008 Nov;4(11):e1000212.
7. World Health Organization. Ebola haemorrhagic fever in Sudan, 1976. *Bull World Health Organ.* 1978;56(2):247–70.
8. Baron RC, McCormick JB, Zubeir OA. Ebola virus disease in southern Sudan: Hospital dissemination and intrafamilial spread. *Bull World Health Organ.* 1983;61(6):997–1003.
9. Towner JS, Rollin PE, Bausch DG, Sanchez A, Crary SM, Vincent M, et al. Rapid Diagnosis of Ebola Hemorrhagic Fever by Reverse Transcription-PCR in an Outbreak Setting and Assessment of Patient Viral Load as a Predictor of Outcome. *J Virol.* 2004;78(8):4330–41.
10. MacNeil A, Farnon EC, Wamala J, Okware S, Cannon DL, Reed Z, et al. Proportion of deaths and clinical features in Bundibugyo Ebola virus infection, Uganda. *Emerg Infect Dis.* 2010 Dec;16(12):1969–72.
11. Albariño CG, Shoemaker T, Khristova ML, Wamala JF, Muyembe JJ, Balinandi S, et al. Genomic analysis of filoviruses associated with four viral hemorrhagic fever outbreaks in Uganda and the Democratic Republic of the Congo in 2012. *Virology.* 2013;442(2):97–100.

12. Formenty P, Hatz C, Le Guenno B, Stoll A, Rogenmoser P, Widmer A. Human infection due to Ebola virus, subtype Côte d'Ivoire: clinical and biologic presentation. *J Infect Dis.* 1999;179(Suppl 1):S48–53.
13. Miranda ME, Ksiazek TG, Retuya TJ, Khan SA, Sanchez A, Fulhorst CF, et al. Epidemiology of Ebola (subtype Reston) virus in the Philippines, 1996. *J Infect Dis.* 1999;179(Suppl):S115–9.
14. Barrette RW, Metwally SA, Rowland JM, Xu L, Zaki SR, Nichol ST, et al. Discovery of swine as a host for the Reston ebolavirus. *Science.* 2009;325(5937):204–6.
15. Siegert R, Shu HL, Slenczka HL, Peters D, Muller G. The aetiology of an unknown human infection transmitted by monkeys (preliminary communication). *Ger Med Mon.* 1968;13(1):1–2.
16. Bausch DG, Nichol ST, Muyembe-Tamfum JJ, Borchert M, Rollin PE, Sleurs H, et al. Marburg hemorrhagic fever associated with multiple genetic lineages of virus. *N Engl J Med.* 2006 Aug 31;355(9):909–19.
17. Feldmann H, Sanchez A, Geisbert T. *Filoviridae: Marburg and Ebola viruses.* In: Knipe D, Howley P, editors. *Fields Virology.* Sixth Ed. Philadelphia: Lippincott, Williams, and Wilkins; 2012. p. 923–56.

18. Centers for Disease Control and Prevention. Chronology of Marburg Hemorrhagic Fever Outbreaks [Internet]. 2015 [cited 2015 Mar 4]. Available from: <http://www.cdc.gov/vhf/marburg/resources/outbreak-table.html#seven>
19. Pattyn S, Jacob W, ven der Groen G, Piot P, Courteille G. Isolation of Marburg-like virus from a case of hemorrhagic fever in Zaire. *Lancet*. 1977;309:573–4.
20. Johnson KM, Lange J V, Webb PA, Murphy FA. Isolation and partial characterisation of a new virus causing acute haemorrhagic fever in Zaire. *Lancet*. 1977 Mar;1(8011):569–71.
21. Okware SI, Omaswa FG, Zaramba S, Opio A, Lutwama JJ, Kamugisha J, et al. An outbreak of Ebola in Uganda. *Trop Med Int Health*. 2002 Dec;7(12):1068–75.
22. World Health Organization. Outbreak of Ebola haemorrhagic fever in Yambio, south Sudan, April-June 2004. 2005;(43):370–5.
23. Shoemaker T, MacNeil A, Balinandi S, Campbell S, Wamala JF, McMullan LK, et al. Reemerging Sudan Ebola virus disease in Uganda, 2011. *Emerg Infect Dis*. 2012;18(9):1480–3.
24. CDC. Update: Ebola Virus Disease Epidemic - West Africa, January 2015. *MMWR Morb Mortal Wkly Rep*. 2015;64(4):109–10.
25. Centers for Disease Control and Prevention. 2014 Ebola Outbreak in West Africa - Case Counts [Internet]. 2015 [cited 2015 Apr 4]. Available from: <http://www.cdc.gov/vhf/ebola/outbreaks/2014-west-africa/case-counts.html>

26. Le Guenno B, Formenty P, Wyers M, Gounon P, Walker F, Boesch C. Isolation and partial characterisation of a new strain of Ebola virus. *Lancet*. 1995;345:1271–4.
27. Formenty P, Boesch C, Wyers M, Steiner C, Donati F, Walker F, et al. Ebola Virus Outbreak among Wild Chimpanzees Living in a Rain Forest of Côte d'Ivoire. *J Infect Dis*. 1999;179(Suppl 1):120–6.
28. Jahrling PB, Geisbert TW, Dalgard DW, Johnson ED, Ksiazek TG, Hall WC, et al. Preliminary report: isolation of Ebola virus from monkeys imported to USA. *Lancet*. 1990;335(8688):502–5.
29. Rollin PE, Williams RJ, Bressler DS, Pearson S, Cottingham M, Pucak G, et al. Ebola (subtype Reston) virus among quarantined nonhuman primates recently imported from the Philippines to the United States. *J Infect Dis*. 1999;179(Suppl):S108–14.
30. Miranda MEG, Yoshikawa Y, Manalo DL, Calaor AB, Miranda NLJ, Cho F, et al. Chronological and spatial analysis of the 1996 Ebola Reston virus outbreak in a monkey breeding facility in the Philippines. *Exp Anim*. 2002;51(2):173–9.
31. Kuhn JH. Filoviruses. A compendium of 40 years of epidemiological, clinical, and laboratory studies. *Arch Virol Suppl. Austria*; 2008;20:13–360.
32. Brauburger K, Hume AJ, Mühlberger E, Olejnik J. Forty-five years of Marburg virus research. *Viruses*. 2012;4(10):1878–927.

33. Feldmann H, Klenk HD, Sanchez A. Molecular biology and evolution of filoviruses. *Arch Virol Suppl.* 1993;7:81–100.
34. Sanchez A, Kiley MP, Holloway BP, Auperin DD. Sequence analysis of the Ebola virus genome: organization, genetic elements, and comparison with the genome of Marburg virus. *Virus Res.* 1993;29:215–40.
35. Feldmann H, Muhlberger E, Randolph A, Will C, Kiley MP, Sanchez A, et al. Marburg virus, a filovirus: Messenger RNAs, gene order, and regulatory elements of the replication cycle. *Virus Res.* 1992;24(1):1–19.
36. Mühlberger E. Filovirus replication and transcription. *Future Virol.* 2007;2(2):205–15.
37. Elliott LH, Sanchez A, Holloway BP, Kiley MP, McCormick JB. Ebola protein analyses for the determination of genetic organization. *Arch Virol.* 1993;133(3-4):423–36.
38. Elliott LH, Kiley MP, McCormick JB. Descriptive analysis of Ebola virus proteins. *Virology.* 1985 Nov;147(1):169–76.
39. Mateo M, Carbonnelle C, Reynard O, Kolesnikova L, Nemirov K, Page A, et al. VP24 is a molecular determinant of Ebola virus virulence in guinea pigs. *J Infect Dis.* 2011 Nov;204(Suppl 3):S1011–20.
40. Hartman AL, Towner JS, Nichol ST. Ebola and marburg hemorrhagic fever. *Clin Lab Med.* 2010;30(1):161–77.

41. Bwaka MA, Bonnet MJ, Calain P, Colebunders R, De Roo A, Guimard Y, et al. Ebola hemorrhagic fever in Kikwit, Democratic Republic of the Congo: clinical observations in 103 patients. *J Infect Dis.* 1999 Feb;179(Suppl 1):S1–7.
42. Colebunders R, Tshomba A, Van Kerkhove MD, Bausch DG, Campbell P, Libande M, et al. Marburg hemorrhagic fever in Durba and Watsa, Democratic Republic of the Congo: clinical documentation, features of illness, and treatment. *J Infect Dis.* 2007 Nov 15;196(Suppl 2):S148–53.
43. Ksiazek TG, West CP, Rollin PE, Jahrling PB, Peters CJ. ELISA for the detection of antibodies to Ebola viruses. *J Infect Dis.* 1999 Feb;179(Suppl):S192–8.
44. Zaki S, Goldsmith C. Pathologic features of filovirus infections in humans. *Curr Top Microbiol Immunol.* 1999;235:97–116.
45. Martines RB, Ng DL, Greer PW, Rollin PE, Zaki SR. Tissue and cellular tropism, pathology and pathogenesis of Ebola and Marburg viruses. *J Pathol.* 2015;153–74.
46. Zaki SR, Shieh W, Greer PW, Goldsmith CS, Katshitshi J, Tshioko FK, et al. A novel immunohistochemical assay for the detection of Ebola virus in skin: implications for diagnosis, spread, and surveillance of Ebola hemorrhagic fever. *J Infect Dis.* 1999;179(Suppl 1):S36–47.
47. Nkoghe D, Leroy E, Toung Mve M, Gonzalez J-P. Cutaneous manifestations of Filovirus infection. 2010;9(ii):1037–43.

48. Bausch DG, Towner JS, Dowell SF, Kaducu F, Lukwiya M, Sanchez A, et al. Assessment of the risk of Ebola virus transmission from bodily fluids and fomites. *J Infect Dis.* 2007;196(Suppl 2):S142–7.
49. Alves DA, Glynn AR, Steele KE, Lackemeyer MG, Garza NL, Buck JG, et al. Aerosol exposure to the angola strain of marburg virus causes lethal viral hemorrhagic Fever in cynomolgus macaques. *Vet Pathol.* 2010;47(5):831–51.
50. Weingartl HM, Embury-Hyatt C, Nfon C, Leung A, Smith G, Kobinger G. Transmission of Ebola virus from pigs to non-human primates. *Sci Rep.* 2012;2:811.
51. Twenhafel NA, Mattix ME, Johnson JC, Robinson CG, Pratt WD, Cashman KA, et al. Pathology of experimental aerosol Zaire ebolavirus infection in rhesus macaques. *Vet Pathol.* 2013;50(3):514–29.
52. Twenhafel NA, Shaia CI, Bunton TE, Shamblin JD, Wollen SE, Pitt LM, et al. Experimental Aerosolized Guinea Pig-Adapted Zaire Ebolavirus (Variant: Mayinga) Causes Lethal Pneumonia in Guinea Pigs. *Vet Pathol.* 2014;52(1):21–5.
53. Martinez O, Ndungo E, Tantral L, Miller EH, Leung LW, Chandran K, et al. A mutation in the Ebola virus envelope glycoprotein restricts viral entry in a host species- and cell-type-specific manner. *J Virol.* 2013;87(6):3324–34.

54. Bhattacharyya S, Mulherkar N, Chandran K. Endocytic pathways involved in filovirus entry: Advances, implications and future directions. *Viruses*. 2012;4(12):3647–64.
55. Takada A. Filovirus tropism: Cellular molecules for viral entry. *Front Microbiol*. 2012;3:1–9.
56. Olejnik J, Ryabchikova E, Corley RB, Mühlberger E. Intracellular Events and Cell Fate in Filovirus Infection. *Viruses*. 2011. p. 1501–31.
57. Carette JE, Raaben M, Wong AC, Herbert AS, Obernosterer G, Mulherkar N, et al. Ebola virus entry requires the cholesterol transporter Niemann-Pick C1. *Nature*. 2011;477(7364):340–3.
58. Misasi J, Chandran K, Yang J-Y, Considine B, Filone CM, Côté M, et al. Filoviruses require endosomal cysteine proteases for entry but exhibit distinct protease preferences. *J Virol*. 2012;86(6):3284–92.
59. Geisbert TW, Hensley LE, Larsen T, Young HA, Reed DS, Geisbert JB, et al. Pathogenesis of Ebola hemorrhagic fever in cynomolgus macaques: evidence that dendritic cells are early and sustained targets of infection. *Am J Pathol*. 2003;163(6):2347–70.
60. Hensley LE, Alves DA, Geisbert JB, Fritz EA, Reed C, Larsen T, et al. Pathogenesis of Marburg hemorrhagic fever in cynomolgus macaques. *J Infect Dis*. 2011;204(Suppl 3):S1021–31.

61. Ströher U, West E, Bugany H, Klenk HD, Schnittler HJ, Feldmann H. Infection and activation of monocytes by Marburg and Ebola viruses. *J Virol.* 2001;75(22):11025–33.
62. Hensley LE, Young HA., Jahrling PB, Geisbert TW. Proinflammatory response during Ebola virus infection of primate models: Possible involvement of the tumor necrosis factor receptor superfamily. *Immunol Lett.* 2002;80(3):169–79.
63. Bray M, Geisbert TW. Ebola virus: the role of macrophages and dendritic cells in the pathogenesis of Ebola hemorrhagic fever. *Int J Biochem Cell Biol.* 2005 Aug;37(8):1560–6.
64. Bosio CM, Aman MJ, Grogan C, Hogan R, Ruthel G, Negley D, et al. Ebola and Marburg viruses replicate in monocyte-derived dendritic cells without inducing the production of cytokines and full maturation. *J Infect Dis.* 2003 Dec 1;188(11):1630–8.
65. Jin H, Yan Z, Prabhakar BS, Feng Z, Ma Y, Verpooten D, et al. The VP35 protein of Ebola virus impairs dendritic cell maturation induced by virus and lipopolysaccharide. *J Gen Virol.* 2010 Mar;91(Pt 2):352–61.
66. Hartman AL, Bird BH, Towner JS, Antoniadou Z-A, Zaki SR, Nichol ST. Inhibition of IRF-3 activation by VP35 is critical for the high level of virulence of ebola virus. *J Virol.* 2008;82(6):2699–704.

67. Valmas C, Grosch MN, Schümann M, Olejnik J, Martinez O, Best SM, et al. Marburg virus evades interferon responses by a mechanism distinct from Ebola virus. *PLoS Pathog.* 2010;6(1).
68. Halfmann P, Neumann G, Kawaoka Y. The Ebolavirus VP24 protein blocks phosphorylation of p38 mitogen-activated protein kinase. *J Infect Dis.* 2011;204(Suppl 3):S953–6.
69. Bale S, Julien JP, Bornholdt Z A., Kimberlin CR, Halfmann P, Zandonatti MA, et al. Marburg Virus VP35 Can Both Fully Coat the Backbone and Cap the Ends of dsRNA for Interferon Antagonism. *PLoS Pathog.* 2012;8(9):1–12.
70. Baize S, Leroy EM, Georges-Courbot MC, Capron M, Lansoud-Soukate J, Debré P, et al. Defective humoral responses and extensive intravascular apoptosis are associated with fatal outcome in Ebola virus-infected patients. *Nat Med.* 1999;5(4):423–6.
71. Geisbert TW, Hensley LE, Gibb TR, Steele KE, Jaax NK, Jahrling PB. Apoptosis induced in vitro and in vivo during infection by Ebola and Marburg viruses. *Lab Invest.* 2000;80(2):171–86.
72. McElroy AK, Akondy RS, Davis CW, Ellebedy AH, Mehta AK, Kraft CS, et al. Human Ebola virus infection results in substantial immune activation. *Proc Natl Acad Sci.* 2015;201502619.

73. Geisbert TW, Young H a, Jahrling PB, Davis KJ, Larsen T, Kagan E, et al. Pathogenesis of Ebola hemorrhagic fever in primate models: evidence that hemorrhage is not a direct effect of virus-induced cytolysis of endothelial cells. *Am J Pathol.* 2003;163(6):2371–82.
74. Walsh P, Abernethy K, Bermejo M. Catastrophic ape decline in western equatorial Africa. *Nature.* 2003;422(April):611–4.
75. Bermejo M, Rodríguez-Teijeiro JD, Illera G, Barroso A, Vilà C, Walsh PD. Ebola outbreak killed 5000 gorillas. *Science (80-).* 2006 Dec 8;314(5805):1564.
76. Wittmann TJ, Biek R, Hassanin A, Rouquet P, Reed P, Yaba P, et al. Isolates of Zaire ebolavirus from wild apes reveal genetic lineage and recombinants. *Proc Natl Acad Sci U S A.* 2007 Oct 23;104(43):17123–7.
77. Ikegami T, Miranda MEG, Calaor AB, Manalo DL, Miranda NJ, Niikura M, et al. Histopathology of natural Ebola virus subtype Reston infection in cynomolgus macaques during the Philippine outbreak in 1996. *Exp Anim.* 2002;51(5):447–55.
78. Baskerville A, Bowen E, Platt G, McArdell L, Simpson D. The Pathology of Experimental Ebola Virus Infection in Monkeys. *J Pathol.* 1978;125:131–8.
79. Ryabchikova E, Kolesnikova L V, Netesov S. Animal Pathology of Filoviral infections. *Curr Top Microbiol Immunol.* 1999;235:145–73.
80. Geisbert TW, Daddario-DiCaprio KM, Geisbert JB, Young HA, Formenty P, Fritz EA, et al. Marburg virus Angola infection of rhesus macaques: pathogenesis and

- treatment with recombinant nematode anticoagulant protein c2. *J Infect Dis.* 2007 Nov 15;196(Suppl 2):S372–81.
81. Larsen T, Stevens EL, Davis KJ, Geisbert JB, Daddario-DiCaprio KM, Jahrling PB, et al. Pathologic findings associated with delayed death in nonhuman primates experimentally infected with Zaire Ebola virus. *J Infect Dis.* 2007 Nov 15;196(Suppl 2):S323–8.
 82. Rubins KH, Hensley LE, Wahl-Jensen V, Daddario DiCaprio KM, Young H a, Reed DS, et al. The temporal program of peripheral blood gene expression in the response of nonhuman primates to Ebola hemorrhagic fever. *Genome Biol.* 2007 Jan;8(8):R174.
 83. Bray M, Davis K, Geisbert T, Schmaljohn C, Huggins J. A mouse model for evaluation of prophylaxis and therapy of Ebola hemorrhagic fever. *J Infect Dis.* 1999 Feb;179(Suppl):S248–58.
 84. Gibb TR, Bray M, Geisbert TW, Steele KE, Kell WM, Davis KJ, et al. Pathogenesis of experimental Ebola Zaire virus infection in BALB/c mice. *J Comp Pathol.* 2001 Nov;125(4):233–42.
 85. Warfield KL, Bradfute SB, Wells J, Lofts L, Cooper MT, Alves DA, et al. Development and characterization of a mouse model for Marburg hemorrhagic fever. *J Virol.* 2009 Jul;83(13):6404–15.

86. Warfield KL, Alves DA, Bradfute SB, Reed DK, VanTongeren S, Kalina W V, et al. Development of a model for marburgvirus based on severe-combined immunodeficiency mice. *Virology*. 2007 Jan;4:108.
87. Wahl-Jensen V, Bollinger L, Safronetz D, de Kok-Mercado F, Scott DP, Ebihara H. Use of the Syrian hamster as a new model of ebola virus disease and other viral hemorrhagic fevers. *Viruses*. 2012 Dec;4(12):3754–84.
88. Leroy EM, Rouquet P, Formenty P, Souquière S, Kilbourne A, Froment J-M, et al. Multiple Ebola virus transmission events and rapid decline of central African wildlife. *Science* (80-). 2004;303(5656):387–90.
89. Kissling RE, Robinson RQ, Murphy FA, Whitfield SG. Agent of disease contracted from green monkeys. *Science* (80-). 1968 May 24;160(3830):888–90.
90. Food and Agriculture Organisation of the United Nations. Investigating the role of bats in emerging zoonoses: balancing ecology, conservation, and public health interest. Newman SH, Field H, Epstein JH, de Jong C, editors. Rome: FAO Animal Production and Health Manual No. 12.; 2011.
91. Olival KJ, Hayman DTS. Filoviruses in bats: current knowledge and future directions. *Viruses*. 2014 Apr;6(4):1759–88.
92. Towner JS, Amman BR, Sealy TK, Carroll SAR, Comer JA, Kemp A, et al. Isolation of genetically diverse Marburg viruses from Egyptian fruit bats. *PLoS Pathog*. 2009;5(7):e1000536.

93. Amman BR, Carroll SA, Reed ZD, Sealy TK, Balinandi S, Swanepoel R, et al. Seasonal pulses of Marburg virus circulation in juvenile *Rousettus aegyptiacus* bats coincide with periods of increased risk of human infection. *PLoS Pathog.* 2012;8(10):e1002877.
94. Towner JS, Pourrut X, Albariño CG, Nkogue CN, Bird BH, Grard G, et al. Marburg virus infection detected in a common African bat. *PLoS One.* 2007;2(8).
95. Swanepoel R, Smit SB, Rollin PE, Formenty P, Leman PA, Kemp A, et al. Studies of reservoir hosts for Marburg virus. *Emerg Infect Dis.* 2007;13(12):1847–51.
96. Amman BR, Jones MEB, Sealy TK, Uebelhoer LS, Schuh AJ, Bird BH, et al. Oral Shedding of Marburg Virus in Experimentally Infected Egyptian Fruit Bats (*Rousettus aegyptiacus*). *J Wildl Dis.* 2015;51(1):113–24.
97. Conrad JL, Isaacson M, Smith EB, Wulff H, Crees M, Geldenhuys P, et al. Epidemiologic investigation of Marburg virus disease, Southern Africa, 1975. *Am J Trop Med Hyg.* 1978;27(6):1210–5.
98. Arata A, Johnson B. Approaches towards studies on potential reservoirs of viral haemorrhagic fever in southern Sudan (1977). In: Pattyn S, editor. *Ebola Virus Haemorrhagic Fever.* New York: Elsevier; 1978. p. 191–200.
99. Leroy EM, Kumulungui B, Pourrut X, Rouquet P, Hassanin A, Yaba P, et al. Fruit bats as reservoirs of Ebola virus. *Nature.* 2005 Dec 1;438(7068):575–6.

100. Leroy EM, Epelboin A, Mondonge V, Pourrut X, Gonzalez J-P, Muyembe-Tamfum J-J, et al. Human Ebola outbreak resulting from direct exposure to fruit bats in Luebo, Democratic Republic of Congo, 2007. *Vector Borne Zoonotic Dis.* 2009 Dec;9(6):723–8.
101. Pourrut X, Souris M, Towner JS, Rollin PE, Nichol ST, Gonzalez J-P, et al. Large serological survey showing cocirculation of Ebola and Marburg viruses in Gabonese bat populations, and a high seroprevalence of both viruses in *Rousettus aegyptiacus*. *BMC Infect Dis.* 2009;9:159.
102. Hayman DTS, Emmerich P, Yu M, Wang L-F, Suu-Ire R, Fooks AR, et al. Long-term survival of an urban fruit bat seropositive for Ebola and Lagos bat viruses. *PLoS One.* 2010 Jan;5(8):e11978.
103. Pourrut X, Délicat A, Rollin PE, Ksiazek TG, Gonzalez J-P, Leroy EM. Spatial and temporal patterns of Zaire ebolavirus antibody prevalence in the possible reservoir bat species. *J Infect Dis.* 2007 Nov 15;196(Suppl 2):S176–83.
104. Taniguchi S, Watanabe S, Masangkay JS, Omatsu T, Ikegami T, Alviola P, et al. Reston Ebolavirus antibodies in bats, the Philippines. *Emerging infectious diseases.* 2011. p. 1559–60.
105. Olival KJ, Islam A, Yu M, Anthony SJ, Epstein JH, Khan SA, et al. Ebola virus antibodies in fruit bats, Bangladesh. *Emerg Infect Dis.* 2013;19(2):270–3.

106. Yuan J, Zhang Y, Li J, Zhang Y, Wang L-F, Shi Z. Serological evidence of ebolavirus infection in bats, China. *Virology Journal*. 2012. p. 236.
107. Paweska JT, Jansen van Vuren P, Masumu J, Leman PA, Grobbelaar AA, Birkhead M, et al. Virological and serological findings in *Rousettus aegyptiacus* experimentally inoculated with vero cells-adapted hogan strain of Marburg virus. *PLoS One*. 2012;7(9):e45479.
108. Swanepoel R, Leman PA, Burt FJ, Zachariades NA, Braack LE, Ksiazek TG, et al. Experimental inoculation of plants and animals with Ebola virus. *Emerg Infect Dis. Centers for Disease Control*; 1996;2(4):321–5.
109. Bowen MD, Peters CJ, Nichol ST. Phylogenetic analysis of the Arenaviridae: patterns of virus evolution and evidence for cospeciation between arenaviruses and their rodent hosts. *Mol Phylogenet Evol*. 1997 Dec;8(3):301–16.
110. Radoshitzky SR, Kuhn JH, Spiropoulou CF, Albariño CG, Nguyen DP, Salazar-Bravo J, et al. Receptor determinants of zoonotic transmission of New World hemorrhagic fever arenaviruses. *Proc Natl Acad Sci U S A*. 2008 Feb 19;105(7):2664–9.
111. Ramsden C, Holmes EC, Charleston MA. Hantavirus evolution in relation to its rodent and insectivore hosts: no evidence for codivergence. *Mol Biol Evol*. 2009 Jan;26(1):143–53.

112. Tayeh A, Tatard C, Kako-Ouraga S, Duplantier J-M, Dobigny G. Rodent host cell/Lassa virus interactions: evolution and expression of α -Dystroglycan, LARGE-1 and LARGE-2 genes, with special emphasis on the *Mastomys* genus. *Infect Genet Evol.* Elsevier B.V.; 2010 Dec;10(8):1262–70.
113. Calisher CH, Childs JE, Field HE, Holmes K V., Schountz T. Bats: Important reservoir hosts of emerging viruses. *Clin Microbiol Rev.* 2006;19(3):531–45.
114. Rupprecht CE, Turmelle A, Kuzmin I V. A perspective on lyssavirus emergence and perpetuation. *Curr Opin Virol.* Elsevier B.V.; 2011 Dec;1(6):662–70.
115. Drexler JF, Corman VM, Müller MA, Maganga GD, Vallo P, Binger T, et al. Bats host major mammalian paramyxoviruses. *Nat Commun.* 2012 Jan;3:796.
116. Halpin K, Hyatt AD, Fogarty R, Middleton D, Bingham J, Epstein JH, et al. Pteropid bats are confirmed as the reservoir hosts of henipaviruses: a comprehensive experimental study of virus transmission. *Am J Trop Med Hyg.* 2011;85(5):946–51.
117. Clayton BA, Wang LF, Marsh GA. Henipaviruses: An Updated Review Focusing on the Pteropid Reservoir and Features of Transmission. *Zoonoses Public Health.* 2013;60:69–83.
118. Wang LF, Shi Z, Zhang S, Field H, Daszak P, Eaton BT. Review of bats and SARS. *Emerg Infect Dis.* 2006;12(12):1834–40.

119. Baker ML, Schountz T, Wang L-F. Antiviral immune responses of bats: a review. *Zoonoses Public Health*. 2013 Mar;60(1):104–16.
120. Cowled C, Baker M, Tachedjian M, Zhou P, Bulach D, Wang LF. Molecular characterisation of Toll-like receptors in the black flying fox *Pteropus alecto*. *Dev Comp Immunol*. Elsevier Ltd; 2011;35(1):7–18.
121. Cowled C, Baker ML, Zhou P, Tachedjian M, Wang LF. Molecular characterisation of RIG-I-like helicases in the black flying fox, *Pteropus alecto*. *Dev Comp Immunol*. Elsevier Ltd; 2012;36(4):657–64.
122. Zhou P, Cowled C, Todd S, Crameri G, Virtue ER, Marsh G a, et al. Type III IFNs in pteropid bats: differential expression patterns provide evidence for distinct roles in antiviral immunity. *J Immunol*. 2011;186(5):3138–47.
123. Janardhana V, Tachedjian M, Crameri G, Cowled C, Wang LF, Baker ML. Cloning, expression and antiviral activity of IFN?? from the Australian fruit bat, *Pteropus alecto*. *Dev Comp Immunol*. Elsevier Ltd; 2012;36(3):610–8.
124. Baker KS, Suu-Ire R, Barr J, Hayman DTS, Broder CC, Horton DL, et al. Viral antibody dynamics in a chiropteran host. *J Anim Ecol*. 2013 Sep 23;415–28.
125. Butler JE, Wertz N, Zhao Y, Zhang S, Bao Y, Bratsch S, et al. The two suborders of chiropterans have the canonical heavy-chain immunoglobulin (Ig) gene repertoire of eutherian mammals. *Dev Comp Immunol*. Elsevier Ltd; 2011;35(3):273–84.

126. Bratsch S, Wertz N, Chaloner K, Kunz TH, Butler JE. The little brown bat, *M. lucifugus*, displays a highly diverse VH, DH and JH repertoire but little evidence of somatic hypermutation. *Dev Comp Immunol*. Elsevier Ltd; 2011;35(4):421–30.
127. Hayman DTS, Bowen RA, Cryan PM, McCracken GF, O’Shea TJ, Peel AJ, et al. Ecology of zoonotic infectious diseases in bats: current knowledge and future directions. *Zoonoses Public Health*. 2013 Mar;60(1):2–21.
128. Olival KJ, Epstein JH, Wang LF, Field HE, Daszak P. Are bats unique viral reservoirs? In: Aguirre AA, Ostfeld RS, Daszak P, editors. *New Directions in Conservation Medicine: Applied Cases of Ecological Health*. 2nd Ed. 2012. p. 195–212.
129. Hayman DTS. Biannual birth pulses allow filoviruses to persist in bat populations. *Proc R Soc B*. 2015;282(20142591).
130. Bolzoni L, De Leo GA. Unexpected consequences of culling on the eradication of wildlife diseases: the role of virulence evolution. *Am Nat*. 2013;181(3):301–13.
131. Amman BR, Nyakarahuka L, McElroy AK, Dodd KA, Sealy TK, Schuh AJ, et al. Marburgvirus resurgence in Kitaka Mine bat population after extermination attempts, Uganda. *Emerging infectious diseases*. 2014. p. 1761–4.

CHAPTER 3

CLINICAL, HISTOPATHOLOGIC, AND IMMUNOHISTOCHEMICAL
CHARACTERIZATION OF EXPERIMENTAL MARBURG VIRUS INFECTION IN A
NATURAL RESERVOIR HOST, THE EGYPTIAN ROUSETTE BAT (*ROUSETTUS
AEGYPTIACUS*)^{*}

^{*}Megan E.B. Jones, Brian R. Amman, Tara K. Sealy, Luke S. Uebelhoer, Amy J. Schuh,
Brian H. Bird, JoAnn D. Coleman-McCray, Brock E. Martin, Sherif R. Zaki, Stuart T.
Nichol, and Jonathan S. Towner. To be submitted to *PLoS Neglected Tropical Diseases*.

Abstract

Several lines of evidence have shown that Egyptian rousette bats (*Rousettus aegyptiacus*) are natural reservoir hosts of Marburg virus (MARV), and Ravn virus (RAVV; collectively called marburgviruses) and have linked human cases of Marburg hemorrhagic fever to spillover from this species. We investigated the clinical and pathologic effects of experimental MARV infection in Egyptian rousettes through a serial euthanasia study. Three groups of nine, captive-born, juvenile male bats were inoculated subcutaneously with 10,000 TCID₅₀ of Marburg virus strain Uganda 371Bat2007, a minimally passaged virus originally isolated from an Egyptian rousette. Control bats (n=3) were mock-inoculated. Three animals per day were euthanized at 3, 5-10, 12 and 28 days post-inoculation (DPI); controls were euthanized at 28 DPI. Blood chemistry analyses showed a mild, statistically significant elevation in alanine aminotransferase (ALT) at 3, 6 and 7 DPI. Liver histology revealed small foci of inflammatory infiltrate in infected bats, similar to lesions previously described in wild, naturally-infected bats. Liver lesion scores peaked at 7 DPI, and were correlated with both ALT and hepatic viral RNA levels. Immunohistochemical staining detected infrequent viral antigen in liver (3-8 DPI, n=8), spleen (3-7 DPI, n=8), skin (inoculation site; 3-12 DPI, n=20), lymph nodes (3-10 DPI, n=6), and oral submucosa (8-9 DPI, n=2). Antigen was present in histiocytes, hepatocytes and mesenchymal cells; in the liver, staining co-localized with inflammatory foci. These results contribute to the understanding of the pathogenesis of MARV infection in Egyptian rousettes, and provide support for our experimental model of this virus-reservoir host system.

Introduction

Marburgviruses (family *Filoviridae*; genus *Marburgvirus*; MARV) are non-segmented, negative-sense, single-stranded RNA viruses that cause sporadic outbreaks of severe hemorrhagic fever in humans. Marburg virus disease (MVD) is characterized by rapid person-to-person transmission and high case fatality rates. In humans and non-human primates, the clinical features and pathology of MVD are similar to, or indistinguishable from, Ebola virus disease (EVD) caused by several closely-related filoviruses in the genus *Ebolavirus* (Ebola virus, *Zaire ebolavirus*; Sudan virus, *Sudan ebolavirus*; Bundibugyo virus, *Bundibugyo ebolavirus*; and, Tai forest virus, *Tai forest ebolavirus*) (1–3). Gross and histologic pathology of filovirus disease (FVD) in humans and non-human primates is characterized by widely disseminated lesions including focal to widespread hepatocellular necrosis, often without inflammation; lymphoid depletion with lymphocyte apoptosis and accumulation of necrotic debris; acute renal tubular necrosis; and variably severe necrosis or apoptosis in the gastrointestinal tract, bone marrow, and other sites. A macular or maculopapular rash is a common clinical and gross finding (4). Hemorrhage, which is present in less than half of cases, is more often associated with fatal outcomes, and manifests as ecchymoses, melena, hematemesis, gingival bleeding, and bleeding from injection sites (5). Histologically, lesions compatible with disseminated intravascular coagulation and hemorrhage can be found in a wide range of tissues. Abundant viral antigen is present in hepatocytes, histiocytes (including Kupffer cells, dendritic cells, alveolar macrophages), fibroblasts, and endothelial cells in multiple tissues and is also present extracellularly in hepatic sinusoids, lymph nodes, spleen, and lung, usually associated with necrotic debris (1,3,6). Intracytoplasmic inclusion bodies

are present in hepatocytes, macrophages, and other cells, though these are more consistently identified in cases of EVD than MVD (1,3).

The first documented outbreak of MVD occurred in 1967 when laboratory workers in Germany and the former Yugoslavia became infected by exposure to African green monkeys (*Cercopithecidae*; now named *Chlorocebus tantalus*) imported from Uganda (7). In 2000-2001, a protracted outbreak of MVD in the Democratic Republic of the Congo (DRC) was epidemiologically linked to gold mining activity (8,9). MARV-specific RNA and IgG were identified in Egyptian rousettes (*Rousettus aegyptiacus*, also known as Egyptian fruit bats) that roosted in the mine in large numbers, and viral RNA sequences from bats matched those from human isolates (10). Genetic and serologic evidence of MARV infection was also found in Egyptian rousettes in Gabon (11). Longitudinal studies performed at two large Egyptian rousette colonies in southwest Uganda, prompted by cases of MVD in gold miners (Kitaka Mine) and tourists (Python Cave, Queen Elizabeth National Park) in 2007-8, identified seropositive and RNA-positive bats at both locations (12,13). IgG levels were highest in adult bats, RNA copy numbers were greatest in juveniles, and RNA sequences were similar to those from human cases. Furthermore, peaks of active viral infection of bats (as identified by presence of marburgviral RNA) coincided with seasonal timing of the majority of human cases of MVD and with the biannual breeding cycle of the rousettes (13). Infectious MARV has now been isolated from 21 bats at these two sites; these isolates represent the only reported successful virus isolation attempts for any filovirus from any bat species to date (12–14).

Ecological and epidemiologic findings confirmed a role for the Egyptian rousette as a natural marburgvirus host and a source of virus spillover to humans. However, fundamental aspects of this virus-host relationship remain incompletely characterized, including viral cell and tissue tropism in bats, and the clinical and pathologic effects of MARV infection on the bat host. Findings in wild Egyptian rousettes suggest that infection with MARV does not cause mortality or significant disease. Histologic examination of limited sets of tissues collected from MARV PCR-positive wild bats revealed very mild hepatitis, characterized by scattered foci of mononuclear inflammatory cells and hepatocyte necrosis (12). Marburgviral antigen was detected by immunohistochemical (IHC) staining in liver and spleen from PCR-positive bats from both Kitaka Mine (3/30) and Python Cave (4/40); in the liver, antigen was sometimes associated with inflammatory foci, and was only detected in bats with the highest viral RNA copy numbers (12,13). Given that these field data were collected from wild bats, there was no way to determine the duration of infection for any individual animal, or to correlate findings with length of infection.

To date, data from two experimental infection studies of Egyptian rousettes with MARV have been published. The first study used a cell culture-adapted, passage-38 (P38) Hogan strain of MARV to inoculate a mixed group of adult and juvenile bats via a combination of subcutaneous and intraperitoneal routes (15). That study confirmed that Egyptian rousettes are susceptible to experimental infection, demonstrated virus dissemination to multiple tissues, and documented seroconversion following inoculation. No lesions were identified grossly, but clinical or histopathologic investigations were not performed (15). The second experiment comprises the virological and serological

findings from the current study, which have been previously published ((16), and see Supplemental Data, Appendix A). We performed a serial euthanasia experiment using captive-bred, first generation, age- and sex-matched Egyptian rousettes inoculated subcutaneously with a low-passage (P2) wild-type ,MARV isolated from a naturally infected bat in Uganda (16). We documented viremia, widespread tissue dissemination of virus, seroconversion in all bats, and, for the first time, oral shedding of infectious MARV. Here, we present the clinical, histopathologic, and immunohistochemical findings from that serial euthanasia study. The objectives of this component of the study were to: 1) determine clinical and pathologic effects of experimental Marburg virus infection of Egyptian rousettes; 2) identify tissue- and cell type distribution of viral antigen and to associate antigen with lesions (if any); and, 3) compare findings in experimental infections to those found in wild-caught bats with evidence of infection. Our goal was to characterize the response of a reservoir host to experimental marburgvirus infection, which is a first step in understanding the mechanisms by which Egyptian rousettes might control marburgvirus infection. This work contributes to the validation of an experimental model of a unique virus-reservoir host relationship, and the only established reservoir model for any filovirus.

Materials and Methods

Ethics statement

All animal procedures and experiments were approved by the CDC Institutional Animal Care and Use Committee (IACUC) and conducted in strict accordance with the Guide for the Care and Use of Laboratory Animals (17). The CDC is fully accredited by the

Association for Assessment and Accreditation of Laboratory Animal Care International (AAALAC). No clinical materials derived from human patients were used in this study.

Biosafety

All work with infectious virus or infected animals was conducted at the Centers for Disease Control and Prevention (CDC, Atlanta, Georgia, USA) in a biological safety level-4 (BSL-4) laboratory in accordance with Select Agent regulations (HHS and USDA, cite website). All investigators and animal care personnel followed international biosafety practices appropriate to BSL-4 and strictly adhered to infection control practices to prevent cross contamination between groups of animals.

Animals and Husbandry

The study animals consisted of 30 juvenile (4-5 months old), first-generation, captive born, male Egyptian rousettes (*R. aegyptiacus*) from a MARV-free breeding colony founded from wild-caught animals imported from Uganda in 2011 (16). All bats were group-housed in flight cages until one week prior to experimental infection, when they were moved to experimental caging in the BSL-4 laboratory for acclimatization. Each bat was randomly assigned to one of three replicate groups (A, B, or C) of nine experimentally-inoculated animals housed in cages in separate isolator units (Duo-Flow Mobile Units, Lab Products Inc., Seaford, Delaware, USA) in climate-controlled rooms with a 12-hour light cycle. Three bats were randomly assigned as mock-inoculated control animals, and were maintained in identical caging in separate isolation units. All bats were fed a variety of fresh fruit, juice, and nutritional supplement (Lubee Bat

Conservancy, Gainesville, FL) *ad libitum* for the duration of the study. All animals in the breeding colony are individually identified using passive integrated transponder (PIT) tags (Biomark, Boise, ID) placed subcutaneously in the interscapular region.

Virus

The strain of Marburg virus used in all experimental infections (371bat virus) was originally isolated from a naturally infected Egyptian rousette caught at the Kitaka Mine, Uganda, in 2007 (12) and passaged twice on Vero E6 cells. The virus stock was titrated using a standard 50% tissue culture infective dose (TCID₅₀) protocol on Vero E6 cells and visualized by indirect fluorescent antibody assay (IFA) using a rabbit anti-MARV polyclonal antibody. For inoculations, virus stock was diluted to a concentration of 40,000 TCID₅₀/ml in sterile Dulbecco's Modified Eagles Medium (DMEM, Invitrogen) and each bat received 250 µl of diluted virus, for a dose of 10,000 TCID₅₀ per animal.

Experimental Inoculation, Serial Euthanasia, and Sampling Procedures

Experimental inoculation procedures are detailed in Amman *et al.* (2015). Briefly, bats were lightly anesthetized using isoflurane anesthetic administered via mask (RC² Rodent Anesthesia System, Vetequip, Pleasanton, CA). Bats were inoculated subcutaneously in the ventral abdomen with 250 µl of diluted virus stock, for a total dose of 10,000 TCID₅₀ of virus per bat. The 3 control animals were mock-inoculated with 250 µl of DMEM only. Three animals (one per replicate group) were scheduled for euthanasia on each of days 3, 5 to 10, 12, and 28 post-inoculation (PI) and the three mock-inoculated animals were euthanized on day 28. Blood was sampled for Q-RT-PCR

and complete blood count (CBC) prior to infection (day 0), on alternate days until day 14 or the scheduled day of euthanasia, and then on days 21 and 28 post-infection for remaining animals. Bats were observed at least once daily throughout the study so that any moribund animals could be scored according to a predetermined clinical illness / euthanasia algorithm. Body weight and rectal temperatures were obtained until day 14, and then on days 21 and 28 PI. Animals were euthanized by a combination of deep isoflurane anesthesia and exsanguination via cardiac puncture.

Clinical Laboratory Analysis

For CBCs, blood was collected into a 20 μ l, EDTA-coated capillary tube (True20 capillary tube) and analyzed using a Hematrue blood analyzer (HESKA, Loveland, CO, USA). For blood chemistry profiles, 100 μ l of whole blood was collected in lithium heparin tubes (Microtainer, BD) and analyzed using the Comprehensive Metabolic Panel Discs for the Piccolo point of care chemistry analyzer (Abaxis, Union City, CA, USA); analyses included alanine aminotransferase (ALT), albumin, alkaline phosphatase (ALP), aspartate aminotransferase (AST), calcium, chloride, creatinine, glucose, potassium, sodium, total bilirubin, total carbon dioxide, total protein, and blood urea nitrogen (BUN). Blood for CBCs was collected on day 0 (prior to infection), on alternate days until day 14 or the day of scheduled euthanasia, and then on day 21 and 28. Due to a larger volume requirement (100 μ l) and blood sampling volume limits for this species, sufficient blood for chemistry analysis was only available on the day of euthanasia, so only one chemistry analysis was available per bat.

Necropsy

Necropsies were performed immediately following euthanasia. Specimens of liver, spleen, skin from the inoculation site, skin from the antebrachium, lung, heart, kidney, adrenal gland, small intestine, large intestine, mesenteric lymph node, testis, urinary bladder, brain, and salivary gland were collected for RNA extraction using sterile technique and placed in 2 ml polycarbonate grinding vials (OPS Diagnostics, Lebanon, NJ) containing 1 ml viricidal lysis buffer (MagMax Lysis Binding Solution Concentrate, Life Technologies, Carlsbad, CA). Tissues were homogenized in a high-throughput tissue grinder (Genogrinder2000, BT&C Inc, Lebanon, NJ). Tissue samples collected for histologic examination were fixed by immersion in 10% neutral buffered formalin in the BSL-4 laboratory for a minimum of 7 days, and then formalin was completely replaced prior to further processing. Tissues collected and processed for histopathology included liver, spleen, lung, heart, trachea, thymus, tracheobronchial lymph nodes, tongue, tonsils, stomach, small intestine, pancreas, large intestine, mediastinal lymph nodes, kidney, adrenal gland, salivary gland, mandibular lymph node, superficial cervical lymph node, axillary lymph node, inguinal lymph node, pectoral muscle, skin from inoculation site, skin from antebrachium, skin from patagium (wing membrane), humerus including bone marrow, cross section of maxilla including nasal turbinates, and brain.

RNA Extraction and Q-RT-PCR

RNA extraction and Q-RT-PCR methods were performed as described in Amman *et al.*, 2015 (16). Briefly, total RNA was extracted from 125 µl aliquots of tissue homogenate using the MagMax-96 Total RNA Extraction Kit, per manufacturer's instructions, and the

AM1830_DW protocol pre-loaded on the MagMax express-96 Deep Well Magnetic Particle Processor (#4400077). The Q-RT-PCR assay targets VP40. To account for sample-to-sample variation, Q-RT-PCR results were normalized to 18s rRNA using a commercially available eukaryotic 18s rRNA assay (Applied Biosystems) according to manufacturer's instructions. Standard curves for Q-RT-PCR results were generated from ten-fold serial dilutions of the Bat 371 Marburg virus stock used in infections, and relative TCID₅₀/ml (fluids) or g (tissue) equivalents for experimental samples were interpolated from the standard curve.

Histology

Representative sections of all formalin-fixed tissues were embedded in paraffin, sectioned at 4 micrometers, mounted on glass slides, and routinely stained with hematoxylin and eosin (HE) for histologic examination. For each bat, at least four non-contiguous sections of liver were examined microscopically without knowledge of infection status or DPI. Liver lesions were assigned a semiquantitative score from 0-4 based on frequency and character, as follows: 0 = average of <1 focus of mononuclear inflammatory infiltrate per 100 high-powered fields (HPFs; 400x magnification); 1 = 1-2.9 foci of inflammatory infiltrate per 100 HPFs, with at least one focus containing hepatocellular degeneration and necrosis; 2 = 3-5.9 inflammatory foci per 100 HPFs, with multiple foci containing hepatocellular degeneration and necrosis; 3 = 6-10 inflammatory foci per 100 HPFs, with frequent hepatocellular degeneration and necrosis; and, 4 = >10 inflammatory foci per 100 HPFs, with frequent degeneration and necrosis. Prior to paraffin-embedding, bony sections (maxillary cross sections, humerus) were decalcified

by immersion in a commercial hydrochloric acid solution (Cal-Ex decalcifier, Fisher Chemical) for 4-6 hours.

Immunohistochemistry (IHC)

Immunohistochemical staining was performed using an alkaline-phosphatase (AP) polymer detection system (UltraVision Detection System, Thermo Scientific). Four-micron sections of formalin-fixed, paraffin-embedded tissues were deparaffinized and rehydrated using gradations of ethanol (100%, 95%, and 70%). Tissues were subjected to proteinase-K (Roche) digestion for 15 minutes at room temperature (RT), then Ultra V Block (Thermo Scientific) was applied for 10 minutes at RT. The primary antibody was a rabbit anti-Marburg virus polyclonal (Viral Special Pathogens Branch, Centers for Disease Control and Prevention, Atlanta, GA), diluted to 1:250 and incubated for 30 minutes at RT, followed by Primary Antibody Enhancer (Thermo Scientific; 10 minutes at RT). AP Polymer (Thermo Scientific) was used as the secondary antibody at manufacturer's dilution and incubated for 15 minutes at RT. The detector was Naphthol Phosphate Substrate/Fast Red (Thermo Scientific; 20 minutes at RT). Sections were counterstained with Mayer's modified hematoxylin (Poly Scientific, Bay Shore, NY). For negative controls, replicate sections from each block were deparaffinized and stained in parallel following an identical protocol, with the primary antibody replaced by normal rabbit serum (Centers for Disease Control and Prevention, Atlanta, GA).

Statistical Analyses

Statistical analyses were performed using Prism 6.0 (GraphPad Software, La Jolla, CA) or Stata 13 (StataCorp, College Station, TX). For each blood chemistry parameter, values from infected animals at each time point (n=3 per time point) were compared with those of mock-inoculated bats (n=3) using one-way analysis of variance (ANOVA), followed by Dunnett's multiple comparison test if the ANOVA demonstrated significant differences between groups ($p < 0.05$). Correlations between liver virus load, alanine aminotransferase, and liver lesion score were analyzed using the nonparametric Spearman rank test. Complete blood count data, which were obtained at multiple time points for each individual bat, were analyzed using repeated measures ANOVA.

Results

Clinical Presentation, Blood Chemistries, and Complete Blood Counts

There was no mortality and no behavioral or clinical evidence of morbidity in infected or uninfected bats from any group. No animal became febrile, body weights tended to increase over the course of the study, and there was no statistical difference in daily percent weight change between experimental groups or between infected and mock-infected animals (data not shown; also summarized in (16)). CBC data are presented in Fig. 1. There were no statistically significant differences in total WBC count between experimental groups ($F_{3,26}=2.6, p=0.055$), or between infected and mock-inoculated bats ($F_{1,28}=0.01; p=0.94$). However, overall, the total WBC count exhibited an increasing trend over time for infected bats, relative to mock-inoculated controls (Figure 3.1). Four animals exhibited mild, transient leukocytosis characterized by lymphocytosis and

monocytosis. In two of these animals, leukocytosis coincided with detection of viral RNA in the blood (16), while in the other two animals it lagged by several days.

Selected blood chemistry data are shown in Figure 3.2. When values from each DPI were compared with mock-infected bats, alanine aminotransferase (ALT) was the only chemistry parameter to show a significant difference ($F_{9, 20} = 3.191$; $p = 0.0147$). ALT was significantly increased in bats sampled on days 3, 6, and 7 post-infection, relative to mock-inoculated bats (Dunnet's multiple comparison test, $p < 0.01$, $p < 0.05$, $p < 0.05$, respectively). No statistically significant differences between groups were identified for any other chemistry parameter on any day, however one bat (Case 11 in Table 1; 7 DPI) with a liver score of 4 and a high liver viral load had a significantly elevated aspartate aminotransferase (554 U/L).

Q-RT-PCR

Detailed PCR results for tissues, blood, oral swabs, and rectal swabs are reported in Amman et al, 2015 and summarized in Appendix A: Supplemental Data. Briefly, bats were viremic (as indicated by the presence of viral RNA in blood) between days 1 and 9, with an average duration of 3 days (range 1-9 days). Viremia was not detected in three bats, though all individuals seroconverted (see ref (16) and Appendix A). Marburgviral RNA was identified most frequently in spleen, liver, and skin from the inoculation site, but was detected on at least two occasions from each of fifteen tissues tested (16). For some individual bats, virus was widely disseminated and could be detected simultaneously in multiple tissues. For comparison with liver lesion scores and IHC results, the viral loads for liver are reported in Table 1, as TCID₅₀ equivalents per gram.

Gross Necropsy and Histology

No significant gross lesions were identified in any animal. All animals had moderate to abundant abdominal and subcutaneous fat stores. Histologically, the subcutaneous tissues at the inoculation site of both infected and mock-infected bats were infiltrated by macrophage aggregates that tended to decrease in size and cell density over time from 3 to 12 DPI (Figure 3.3). Many lymph nodes in both control and inoculated bats exhibited mild subcapsular histiocytosis with erythrophagocytosis (iatrogenic, associated with repeated venipuncture). In all but three bats (one mock-inoculated, one from 5 DPI, and one from 28 DPI) there was zonal to diffuse, mild to moderate, lacy vacuolation of hepatocytes, consistent with glycogen accumulation.

Liver lesion scores are summarized in Table 1. An average of 368 HPFs (range 223-618 HPFs) of liver tissue from each bat were examined so lesions could be characterized and scored. Liver lesions included small, randomly-scattered aggregates of macrophages and lymphocytes, with occasional neutrophils (Figure 3.3). These foci also variably contained necrotic, apoptotic, or degenerating hepatocytes and karyorrhectic cell debris. For each animal, liver lesions were graded from 0 (absent) to 4 (most frequent, among samples examined). Foci were most numerous, and liver scores were highest, at 7 DPI, with slightly lower total scores on days 6 and 8 (Table 1; Figure 3.4). Grade 4 liver lesions were only present from 6-8 DPI, and at least one of three animals on each of days 3 and 10 had a liver score of 2 or greater. Liver lesion score and ALT were positively correlated with liver viral load (Spearman $r = 0.71$; $p < 0.0001$, and Spearman $r = 0.45$; $p = 0.0065$, respectively; figure 4). Significant liver lesions were not identified in mock-

inoculated animals. No significant lesions were identified in any other tissue examined in inoculated or mock-inoculated bats.

Immunohistochemistry (IHC)

Marburgviral antigen was identified rarely, but was most frequently present in spleen, liver, and skin and subcutaneous tissue from the inoculation site. In the liver, antigen was detected in 8 bats between 3 and 8 DPI (Table 1). Positive immunostaining was present in the cytoplasm of macrophages and hepatocytes within some liver inflammatory foci, and, rarely, in individual or small clusters of normal hepatocytes (Figure 3.5). The presence of antigen coincided with higher liver viral loads, with only one bat testing IHC positive with a liver load of less than 10^3 TCID₅₀ equivalents per gram (Table 1). Despite IHC being less sensitive than Q-RT-PCR, antigen was detected in all four bats with grade 4 liver lesions, as well as in bats with lower liver scores at 3 and 5 DPI (Table 1; Figure 3.4). IHC findings in other tissues are summarized in Table 2. In the spleen, antigen was present in the cytoplasm of cells in the red pulp morphologically consistent with macrophages in 8 bats between 3 and 7 DPI (Figure 3.5). In the skin from the inoculation site, antigen was present in subcutaneous macrophage aggregates in 20 bats from 3 to 12 DPI (Figure 3.3). Antigen was most often identified in the cytoplasm of infiltrating macrophages but was sometimes present in the cytoplasm of mesenchymal cells lining thin septa separating lobules of adipose tissue or adjacent to muscle bundles (fibrocytes or fibroblasts) (Figure 3.5). While antigen was most often localized to the subcutis at the inoculation site, in one bat (8 DPI, group C), there was a small focus of IHC-positive macrophages in the overlying superficial dermis. In the skin from the patagium in one bat

(10 DPI), a small cluster of dermal macrophages and associated dermal fibroblasts exhibited positive cytoplasmic labeling for antigen (Figure 3.5). In one animal from 3 DPI (case 2 on table 1), there was scant positive staining in perimyseal cells, arteriolar adventitial cells, and scattered histiocytes in subcutaneous and skeletal muscle tissue from the axillary region. Positive staining was present in mesenchymal cells (fibroblasts) and histiocytes comprising the loose collagenous connective tissue of the lamina propria and submucosa from the oropharynx adjacent to the tonsil in one bat at 8 DPI and from the ventral aspect of the tongue from one bat from 9 DPI (Figure 3.5). In six bats between 3 and 12 DPI, very small numbers of antigen-labeled cells were variably identified in lymph nodes (axillary, n=3; inguinal, n=2; internal iliac, n=1) (Figure 3.5). When present, antigen was granular and in the cytoplasm of macrophages in the subcapsular sinus or, less commonly, in the paracortical regions. Positive immunostaining consistently coincided with higher viral RNA levels. No antigen was identified in any tissue from mock-inoculated bats.

Discussion

This is the first description of clinical, histopathologic, and immunohistochemical findings of experimental filovirus infection in a natural host. We demonstrated that juvenile Egyptian rousettes experimentally inoculated with low-passage, wild-type MARV exhibited very mild hepatic disease, characterized by microscopic inflammatory foci in the liver and an increase in ALT, and that these lesions were not associated with mortality. Despite widespread virus dissemination, we observed no significant changes in daily food consumption, body weight, or body temperature, and no signs of overt

morbidity or behavioral changes such as waning appetite, overly aggressive behavior, separation from cage mates, lethargy, or reduced or abandoned grooming. Thus, histologic and hematologic results, daily weight and temperature data, and observational findings suggest that MARV infection does not cause significant disease in this bat species. This concurs with previous observations and necropsy findings from naturally infected bats (12,13), and meets expectations for Egyptian rousettes being a *bona fide* reservoir host.

We identified MARV antigen in liver, spleen, lymph nodes, skin, and, rarely, in the oral submucosa. Though the range of tissues available for histologic examination and IHC in this study was much greater than from field studies, liver lesions, antigen distribution, and cell and tissue tropism in liver and spleen in experimentally infected bats was comparable to those in naturally-infected bats (12). Previously published results from this experiment demonstrated viremia in 24 of 27 infected bats between days 3 and 9; seroconversion in all 27 bats after 12 DPI; widespread tissue dissemination of viral RNA; high viral loads in liver and spleen; and, viral shedding via oral and rectal routes (Appendix A; ref. 16). Widespread viral RNA dissemination and high tissue viral loads have been seen during the acute phase of infection in naturally infected bats (12,13). As a whole, these findings show that our experimental model appears to replicate closely the natural MARV-reservoir host relationship. This establishes the model as a useful tool for exploring the molecular and immunologic determinants of filovirus-natural host dynamics, especially in conjunction with a recently developed MARV reverse genetics system based on the bat371 virus isolate used in this experiment (18) .

Following inoculation, viral RNA and antigen were first detected in the liver and spleen, which were the most frequent sites of viral replication and dissemination (see Appendix A). Though infection was not associated with significant disease, tissue and cell tropism in experimentally infected bats shared some similarities with tropism in primates with MVD. In bat liver tissue, MARV antigen was present in hepatocytes and histiocytic cells. Filoviruses are known to exhibit tropism for hepatocytes, and hepatocellular necrosis is a hallmark lesion of both natural and experimental primate models of MVD (1,3,19–24). In bats, our semiquantitative liver grading scheme demonstrated a statistically significant association between the frequency of inflammatory foci and levels of viral RNA in liver tissue. The co-localization of antigen with inflammation was consistent with localized cytopathic effects of viral replication. Though liver lesions in bats were, overall, very mild, a statistical association between ALT levels and liver score lends validity to our grading system. Additionally, we did not identify liver inflammation in any of the three mock-inoculated control bats. However, given the small number of controls, and the presence of mild liver inflammation in the absence of antigen in some infected bats, it is possible some liver lesions were unrelated to viral infection. In the wild, active MARV infection most common in juvenile Egyptian rousettes, and viral spillover correlates with biannual seasonal reproductive cycles (13). In order to maximize the likelihood of faithfully replicating natural infection cycles, we chose single-cohort juvenile animals for these experiments. Animal numbers were therefore limited by the number of bats born in our colony at one time, and thus 3 controls were available to match the three bats euthanized per time point.

Antigen was most often identified in cells of monocyte/macrophage lineage in the liver, spleen, lymph nodes, skin, and oropharyngeal submucosa. Early and sustained filoviral tropism for cells of the mononuclear-phagocyte system, specifically macrophages, Kupffer cells, and dendritic cells, has been well documented (1,3,24–30). Monocytes, macrophages, and dendritic cells also appear to mediate dissemination of virus from the site of infection to regional lymph nodes (via lymphatics), liver, and spleen (via blood). In Egyptian rousettes in this study, viral antigen was most abundant in macrophages that accumulated in subcutaneous tissues at the site of inoculation. While some of this antigen likely represents phagocytized inoculum, Q-RT-PCR results for the inoculation site, liver, and spleen detected levels of viral RNA that were higher than the inoculated dose of 10^4 TCID₅₀, confirming that replication was occurring in these tissues (13). Antigen was relatively rare in lymph nodes, where it was identified most often in subcapsular sinus histiocytes and, occasionally, in paracortical regions (figure 3.5). In the spleen, MARV antigen was present in cells in red pulp macrophages. We also identified antigen in fibroblast- or fibrocyte-type cell in the connective tissues of the oropharyngeal submucosa, subcutis, and dermis. In previous studies of natural and experimental filoviral infection, immunopositive stromal cells have been described variably as fibrocytes, fibroblasts, fibroblast-like, fibrocyte-like, or perivascular spindle cells (1,3,6,22,29,31,32). In humans, antigen is sufficiently abundant in skin, including dermal fibroblasts, that postmortem skin punch biopsies have been used for EBOV diagnosis and surveillance in outbreak settings (6).

In previously published data from this study, oral shedding of MARV was confirmed through Q-RT-PCR (n=6) and virus isolation from oral swabs (n=3). Here, we

identified small amounts of viral antigen in the oropharyngeal or lingual submucosa in two bats; both these bats had had PCR-positive oral swabs on multiple days, and MARV was isolated from one oral swab (Appendix A; ref.(16)). Thus, two of the six bats with confirmed oral shedding had antigen in fibroblasts and macrophages in their oral submucosa. No MARV antigen was identified in multiple sections of salivary gland examined from each bat, despite the detection of RNA in salivary gland tissue from 8 bats, including one of the two with oral submucosal antigen (16; Appendix A). Our IHC findings suggests that viral replication in tissue macrophages, fibrocytes, or both may play a role in shedding. Based on both PCR and IHC findings, the tongue has been implicated as a possible site of virus transmission in Serotine bats (*Eptesicus serotinus*) infected with European lyssaviruses, and lingual lyssaviral antigen has been detected in intralingual glands and acini, nerves, skeletal muscle fibers, and lingual papillae in both experimentally and naturally infected bats (33,34).

Several mechanisms have been proposed to explain the tolerance or resistance of reservoir hosts to viruses that that are highly pathogenic in other species. These mechanisms are poorly understood in most virus-reservoir host systems, but hypotheses include differences in viral cytopathogenicity between natural and non-natural hosts, variations in cell surface receptors or other determinants of tropism, and differences in reservoir host immune responses (35). In other virus-reservoir host systems, mild histologic lesions have been observed with varying frequency, sometimes in association with the detection of viral antigen or nucleic acid. Sin Nombre virus (genus *Hantavirus*, family *Bunyaviridae*; SNV) causes Hantavirus pulmonary syndrome in humans (36,37) and is transmitted to humans from its reservoir host, the deer mouse (*Peromyscus*

maniculatus) (38). Lesions reported in deer mice experimentally or naturally infected with SNV include mild pulmonary edema (39) but often no abnormalities are identified despite the identification of antigen or viral RNA in tissue (40,41). Hendra and Nipah virus (genus *Henipavirus*, family *Paramyxoviridae*) infection of Pteropid fruit bat reservoir hosts has been associated with mild vasculitis without mortality or significant clinical disease, and intralésional viral antigen identification is variable (42–44). In the case of MARV and Egyptian rousettes, tropism for macrophages, connective tissue mesenchymal cells, and hepatocytes recapitulates to a small degree MARV tropism in susceptible hosts. However, despite early infection of macrophages, viremia, dissemination to lymph nodes, replication in spleen, skin, and liver, evidence of mild hepatic cytopathic effects, and oral and rectal shedding of virus, disease is minimal and the duration of infection appears to be limited. Our validation of this experimental model of the MARV-reservoir host relationship serves as a fundamental first step for understanding the innate and adaptive immunological mechanisms by which these bats control infection, and for addressing numerous still-unanswered questions such as the potential for bats to be persistently infected, dynamics of bat-to-bat transmission, and potential for long-term viral maintenance in the population.

References

1. Zaki S, Goldsmith C. Pathologic features of filovirus infections in humans. *Curr Top Microbiol Immunol*. 1999;235:97–116.
2. Kortepeter MG, Bausch DG, Bray M. Basic clinical and laboratory features of filoviral hemorrhagic fever. *J Infect Dis*. 2011 Nov;204(Suppl 3):S810–6.
3. Martines RB, Ng DL, Greer PW, Rollin PE, Zaki SR. Tissue and cellular tropism, pathology and pathogenesis of Ebola and Marburg viruses. *J Pathol*. 2015;153–74.
4. Martini G. Marburg virus disease. Clinical syndrome. In: Martini GA, Siegert R, editors. *Marburg virus disease*. Berlin: Springer-Verlag; 1971. p. 1–9.
5. Feldmann H, Sanchez A, Geisbert T. Filoviridae: Marburg and Ebola viruses. In: Knipe D, Howley P, editors. *Fields Virology*. Sixth Ed. Philadelphia: Lippincott, Williams, and Wilkins; 2012. p. 923–56.
6. Zaki SR, Shieh W, Greer PW, Goldsmith CS, Katshitshi J, Tshioko FK, et al. A novel immunohistochemical assay for the detection of Ebola virus in skin: implications for diagnosis, spread, and surveillance of Ebola hemorrhagic fever. *J Infect Dis*. 1999;179(Suppl 1):S36–47.
7. Siegert R, Shu HL, Slenczka HL, Peters D, Muller G. The aetiology of an unknown human infection transmitted by monkeys (preliminary communication). *Ger Med Mon*. 1968;13(1):1–2.

8. Bausch DG, Borchert M, Grein T, Roth C, Swanepoel R, Libande ML, et al. Risk factors for Marburg hemorrhagic fever, Democratic Republic of the Congo. *Emerg Infect Dis.* 2003 Dec;9(12):1531–7.
9. Bausch DG, Nichol ST, Muyembe-Tamfum JJ, Borchert M, Rollin PE, Sleurs H, et al. Marburg hemorrhagic fever associated with multiple genetic lineages of virus. *N Engl J Med.* 2006 Aug 31;355(9):909–19.
10. Swanepoel R, Smit SB, Rollin PE, Formenty P, Leman PA, Kemp A, et al. Studies of reservoir hosts for Marburg virus. *Emerg Infect Dis.* 2007;13(12):1847–51.
11. Towner JS, Pourrut X, Albariño CG, Nkogue CN, Bird BH, Grard G, et al. Marburg virus infection detected in a common African bat. *PLoS One.* 2007;2(8).
12. Towner JS, Amman BR, Sealy TK, Carroll SAR, Comer JA, Kemp A, et al. Isolation of genetically diverse Marburg viruses from Egyptian fruit bats. *PLoS Pathog.* 2009;5(7):e1000536.
13. Amman BR, Carroll SA, Reed ZD, Sealy TK, Balinandi S, Swanepoel R, et al. Seasonal pulses of Marburg virus circulation in juvenile *Rousettus aegyptiacus* bats coincide with periods of increased risk of human infection. *PLoS Pathog.* 2012;8(10):e1002877.
14. Amman BR, Nyakarahuka L, McElroy AK, Dodd KA, Sealy TK, Schuh AJ, et al. Marburgvirus resurgence in Kitaka Mine bat population after extermination attempts, Uganda. *Emerging infectious diseases.* 2014. p. 1761–4.

15. Paweska JT, Jansen van Vuren P, Masumu J, Leman PA, Grobbelaar AA, Birkhead M, et al. Virological and serological findings in *Rousettus aegyptiacus* experimentally inoculated with vero cells-adapted hogan strain of Marburg virus. PLoS One. 2012;7(9):e45479.
16. Amman BR, Jones MEB, Sealy TK, Uebelhoer LS, Schuh AJ, Bird BH, et al. Oral Shedding of Marburg Virus in Experimentally Infected Egyptian Fruit Bats (*Rousettus aegyptiacus*). J Wildl Dis. 2015;51(1):113–24.
17. National Research Council. Guide for the Care and Use of Laboratory Animals. 8th Ed. Washington, DC: National Academies Press; 2011.
18. Albariño CG, Uebelhoer LS, Vincent JP, Khristova ML, Chakrabarti AK, McElroy A, et al. Development of a reverse genetics system to generate recombinant Marburg virus derived from a bat isolate. Virology. 2013;446(1-2):230–7.
19. Oehlert. The Morphological Picture in Livers, Spleens, and Lymph Nodes of Monkeys and Guinea Pigs after Infection with the “Vervet Agent.” In: Martini GA, Siegert R, editors. Marburg virus disease. Berlin: Springer-Verlag; 1971. p. 144–56.
20. Bechtelsheimer H, Korb G, Gedigk P. The Morphology and Pathogenesis of “Marburg virus” hepatitis. Hum Pathol. 1972 Jan;3(2):255–64.

21. Carrion R, Ro Y, Hoosien K, Ticer A, Brasky K, de la Garza M, et al. A small nonhuman primate model for filovirus-induced disease. *Virology*. 2011;420(2):117–24.
22. Geisbert TW, Daddario-DiCaprio KM, Geisbert JB, Young HA, Formenty P, Fritz EA, et al. Marburg virus Angola infection of rhesus macaques: pathogenesis and treatment with recombinant nematode anticoagulant protein c2. *J Infect Dis*. 2007 Nov 15;196(Suppl 2):S372–81.
23. Warfield KL, Bradfute SB, Wells J, Lofts L, Cooper MT, Alves DA, et al. Development and characterization of a mouse model for Marburg hemorrhagic fever. *J Virol*. 2009 Jul;83(13):6404–15.
24. Hensley LE, Alves DA, Geisbert JB, Fritz EA, Reed C, Larsen T, et al. Pathogenesis of Marburg hemorrhagic fever in cynomolgus macaques. *J Infect Dis*. 2011 Dec;204(Suppl 3):S1021–31.
25. Geisbert TW, Jaax NK. Marburg hemorrhagic fever: report of a case studied by immunohistochemistry and electron microscopy. *Ultrastruct Pathol*. 1998;22(1):3–17.
26. Connolly BM, Steele KE, Davis KJ, Geisbert TW, Kell WM, Jaax NK, et al. Pathogenesis of experimental Ebola virus infection in guinea pigs. *J Infect Dis*. 1999 Feb;179(Suppl):S203–17.

27. Ryabchikova E, Kolesnikova L V, Netesov S. Animal Pathology of Filoviral infections. *Curr Top Microbiol Immunol*. 1999;235:145–73.
28. Gibb TR, Bray M, Geisbert TW, Steele KE, Kell WM, Davis KJ, et al. Pathogenesis of experimental Ebola Zaire virus infection in BALB/c mice. *J Comp Pathol*. 2001 Nov;125(4):233–42.
29. Geisbert TW, Hensley LE, Larsen T, Young HA, Reed DS, Geisbert JB, et al. Pathogenesis of Ebola hemorrhagic fever in cynomolgus macaques: evidence that dendritic cells are early and sustained targets of infection. *Am J Pathol*. 2003 Dec;163(6):2347–70.
30. Twenhafel NA, Mattix ME, Johnson JC, Robinson CG, Pratt WD, Cashman KA, et al. Pathology of experimental aerosol Zaire ebolavirus infection in rhesus macaques. *Vet Pathol*. 2013 May;50(3):514–29.
31. Ikegami T, Miranda MEG, Calaor AB, Manalo DL, Miranda NJ, Niikura M, et al. Histopathology of natural Ebola virus subtype Reston infection in cynomolgus macaques during the Philippine outbreak in 1996. *Exp Anim*. 2002;51(5):447–55.
32. Twenhafel NA, Shaia CI, Bunton TE, Shamblin JD, Wollen SE, Pitt LM, et al. Experimental Aerosolized Guinea Pig-Adapted Zaire Ebolavirus (Variant: Mayinga) Causes Lethal Pneumonia in Guinea Pigs. *Vet Pathol*. 2014;52(1):21–5.

33. Freuling C, Vos A, Johnson N, Kaipf I, Denzinger A, Neubert L, et al. Experimental infection of serotine bats (*Eptesicus serotinus*) with European bat lyssavirus type 1a. *J Gen Virol*. 2009;90:2493–502.
34. Schatz J, Teifke JP, Mettenleiter TC, Aue A, Stiefel D, Müller T, et al. Lyssavirus distribution in naturally infected bats from Germany. *Vet Microbiol*. 2014;169:33–41.
35. Mandl JN, Ahmed R, Barreiro LB, Daszak P, Epstein JH, Virgin HW, et al. Reservoir Host Immune Responses to Emerging Zoonotic Viruses. *Cell*. 2014;160(1-2):20–35.
36. Elliott LH, Ksiazek TG, Rollin PE, Spiropoulou CF, Morzunov S, Monroe M, et al. Isolation of the causative agent of hantavirus pulmonary syndrome. *Am J Trop Med Hyg*. 1994;51(1):102–8.
37. Zaki SR, Greer PW, Coffield LM, Goldsmith CS, Nolte KB, Foucar K, et al. Hantavirus pulmonary syndrome. Pathogenesis of an emerging infectious disease. *Am J Pathol*. 1995 Mar;146(3):552–79.
38. Childs JE, Ksiazek TG, Spiropoulou CF, Krebs JW, Morzunov S, Maupin GO, et al. Serologic and genetic identification of *Peromyscus maniculatus* as the primary rodent reservoir for a new hantavirus in the southwestern United States. *J Infect Dis*. 1994;169:1271–80.

39. Netski D, Thran BH, St Jeor SC. Sin Nombre virus pathogenesis in *Peromyscus maniculatus*. *J Virol*. 1999;73(1):585–91.
40. Botten J, Mirowsky K, Kusewitt D, Bharadwaj M, Yee J, Ricci R, et al. Experimental infection model for Sin Nombre hantavirus in the deer mouse (*Peromyscus maniculatus*). *Proc Natl Acad Sci U S A*. 2000;97(19):10578–83.
41. Botten J, Mirowsky K, Kusewitt D, Ye C, Gottlieb K, Prescott J, et al. Persistent Sin Nombre Virus Infection in the Deer Mouse (*Peromyscus maniculatus*) Model: Sites of Replication and Strand-Specific Expression. *J Virol*. 2003;77(2):1540–50.
42. Williamson M, Hooper P, Selleck P, Gleeson L, Daniels P, Westbury H, et al. Transmission studies of Hendra virus (equine morbillivirus) in fruit bats, horses and cats. *Aust Vet J*. 1998;76(12):813–8.
43. Williamson MM, Hooper PT, Selleck PW, Westbury HA, Slocombe RF. Experimental hendra virus infection in pregnant guinea-pigs and fruit bats (*Pteropus poliocephalus*). *J Comp Pathol*. 2000;122(2-3):201–7.
44. Middleton DJ, Morrissy CJ, van der Heide BM, Russell GM, Braun MA, Westbury H a, et al. Experimental Nipah virus infection in pteropid bats (*Pteropus poliocephalus*). *J Comp Pathol*. 2007 May;136(4):266–72.

Table 3.1. Liver viral load, liver histologic score, liver immunohistochemical staining results, and alanine aminotransferase (ALT) values for Egyptian rousette bats (*Rousettus aegyptiacus*) experimentally infected with Marburg virus in a serial euthanasia study.

Case Number	Group	DPI	Viral Load (TCID ₅₀ /g equivalents) ^a	HE Score ^b	IHC ^c	ALT (U/L)
1	A	3	++	++	+	166
2	B	3	++	-	-	138
3	C	3	++++	+	+	74
4	A	5	+++	+	-	110
5	B	5	++++	++	+	117
6	C	5	+++++	-	+	66
7	A	6	++	++	-	127
8	B	6	++++	++	-	131
9	C	6	+++++	++++	+	74
10	A	7	+++	++++	+	104
11	B	7	++++	++++	+	125
12	C	7	++++	+++	-	124
13	A	8	+++++	++++	+	108
14	B	8	++	++	-	122
15	C	8	++++	+++	-	62
16	A	9	+++	++	-	123
17	B	9	+	-	-	76
18	C	9	++	+	-	82
19	A	10	+	-	-	97
20	B	10	++	++	-	80
21	C	10	-	-	-	73
22	A	12	+	+	-	87
23	B	12	++	-	-	68
24	C	12	-	-	-	91
25	A	28	-	+	-	59
26	B	28	-	-	-	40
27	C	28	-	-	-	51
28	A	Control	-	-	-	52
29	B	Control	-	-	-	61
30	C	Control	-	-	-	26

Abbreviations: TCID₅₀, 50% tissue culture infective dose; DPI, days post-infection; HE, hematoxylin and eosin; IHC, immunohistochemistry; ALT, alanine aminotransferase.

^aViral loads are expressed as 50% tissue culture infective dose (TCID₅₀) equivalents per gram, derived from standard curves of the diluted stock viruses assayed using the identical Q-RT-PCR protocols as that for tissues: + <100 TCID₅₀ eq.; ++ 100-999 TCID₅₀ eq.; +++ 1000-9,999 TCID₅₀ eq.; ++++ 10,000-99,999 TCID₅₀ eq.; +++++ 100,000 to 1,000,000 TCID₅₀ eq.

^b Liver score based on average number and character of inflammatory foci per 100 high-powered fields: - = average of <1 focus of mononuclear inflammatory infiltrate per 100 high-powered fields (HPFs; 400x magnification); += 1-2.9 foci of inflammatory infiltrate per 100 HPFs, with at least one focus containing hepatocellular degeneration and necrosis; += 3-5.9 inflammatory foci per 100 HPFs, with multiple foci containing hepatocellular degeneration and necrosis; +++ = 6-10 inflammatory foci per 100 HPFs, with frequent hepatocellular degeneration and necrosis; and, ++++ = >10 inflammatory foci per 100 HPFs, with frequent degeneration and necrosis.

^cIHC staining was present in in hepatocytes and/ or macrophages, and was graded as - = no antigen detected; and, + = antigen detected.

Table 3.2. Immunohistochemistry results^a for tissues other than liver, for Egyptian rousette bats (*Rousettus aegyptiacus*) experimentally infected with Marburg virus in a serial euthanasia study.

DPI	Spleen	Skin (Inoculation Site)	Skin (Wing)	Lymph Node	Oropharyngeal Submucosa
3	2 M	3 M,F	0	1 (Il) M	0
5	3 M	3 M,F	0	1 (Ax) M	0
6	2 M	3 M,F	0	0	0
7	1 M	3 M,F	0	0	0
8	0	3 M	0	0	1 M,F
9	0	2 M,F	0	1 (In) M	1 M,F
10	0	2 M,F	1 M,S	2 (Ax) M	0
12	0	1 M,F	0	1 (In) M	0
28	0	0	0	0	0
Control	0	0	0	0	0

Abbreviations: DPI, days post-infection; M, macrophages; F = fibroblast-type cells

(fibroblasts or fibrocytes); Il = iliac lymph node; In = inguinal lymph node; Ax = axillary lymph node.

^a Results for each tissue are presented as the number of bats per day with antigen detected (of 3 bats sampled per day), with a summary of major cell types involved.

Figure Legends

Figure 3.1. Scatterplots (symbols) and mean values (lines) of complete blood count and leukocyte differentials for *Rousettus aegyptiacus* bats experimentally inoculated with Marburg virus in a serial euthanasia study; black circles = inoculated bats; open diamond = mock-inoculated control bats; solid line = mean cell count for inoculated bats; dashed line = mean cell count for mock-inoculated control bats: A. total leukocyte counts; B. lymphocyte counts; C. monocyte counts; D. granulocyte counts. Cell counts did not differ significantly between experimental groups, but there was an increasing trend over time for inoculated bats relative to control bats.

Figure 3.2. Blood chemistry values for Egyptian rousette bats experimentally inoculated with Marburg virus in a serial euthanasia study. Each point represents the chemistry parameter value measured for an individual bat on the day of euthanasia (3 bats euthanized per time point); bars represent mean \pm SEM per day. Alanine aminotransferase was significantly increased in bats tested on day 3, 5, and 7 relative to mock-inoculated bats (asterisks); ALT = alanine aminotransferase; AST = aspartate aminotransferase; ALP = alkaline phosphatase.

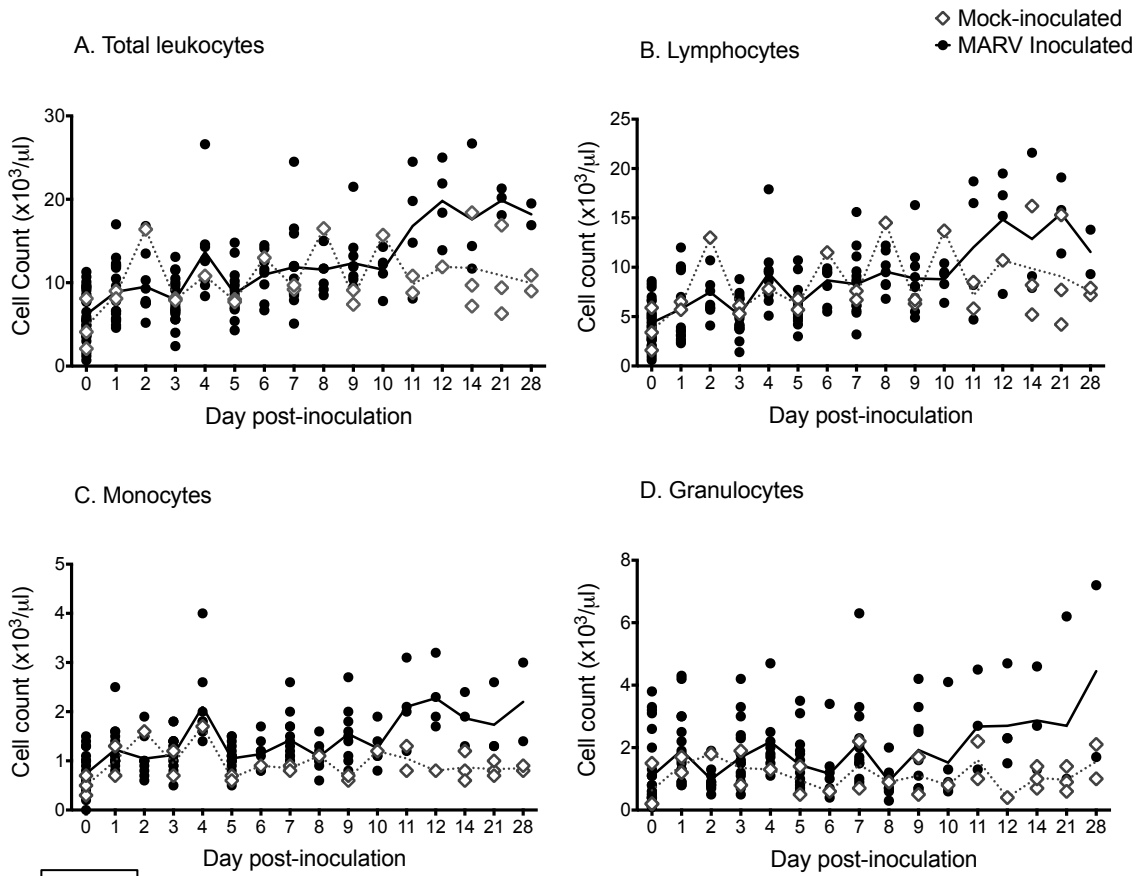
Figure 3.3. Photomicrographs of liver from Marburg-virus inoculated Egyptian rousette bats. **A.** Liver, 6 DPI. Randomly scattered foci of mixed cellular infiltrate disrupt the liver parenchyma (arrows) in a bat with a liver histologic score of 4 (see text for lesion scoring). There is also diffuse glycogen-type hepatocellular vacuolation. HE stain. **B.** Liver, 6 DPI. Higher magnification of (A) showing a focus of mixed inflammation with karyorrhectic debris and mild hemorrhage. HE stain. Inset: higher magnification of a necrotic hepatocyte in an adjacent liver inflammatory focus. HE stain. **C.** Liver, 7 DPI.

Immunohistochemical stain showing perimembranous and cytoplasmic Marburg virus antigen (red) in a hepatocyte. Immunoalkaline phosphatase with naphthol fast red and hematoxylin counterstain. **D.** Liver, 5 DPI. Marburg virus antigen (red) in macrophages and hepatocytes in a small focus of mixed cellular infiltrate. Immunoalkaline phosphatase with naphthol fast red and hematoxylin counterstain.

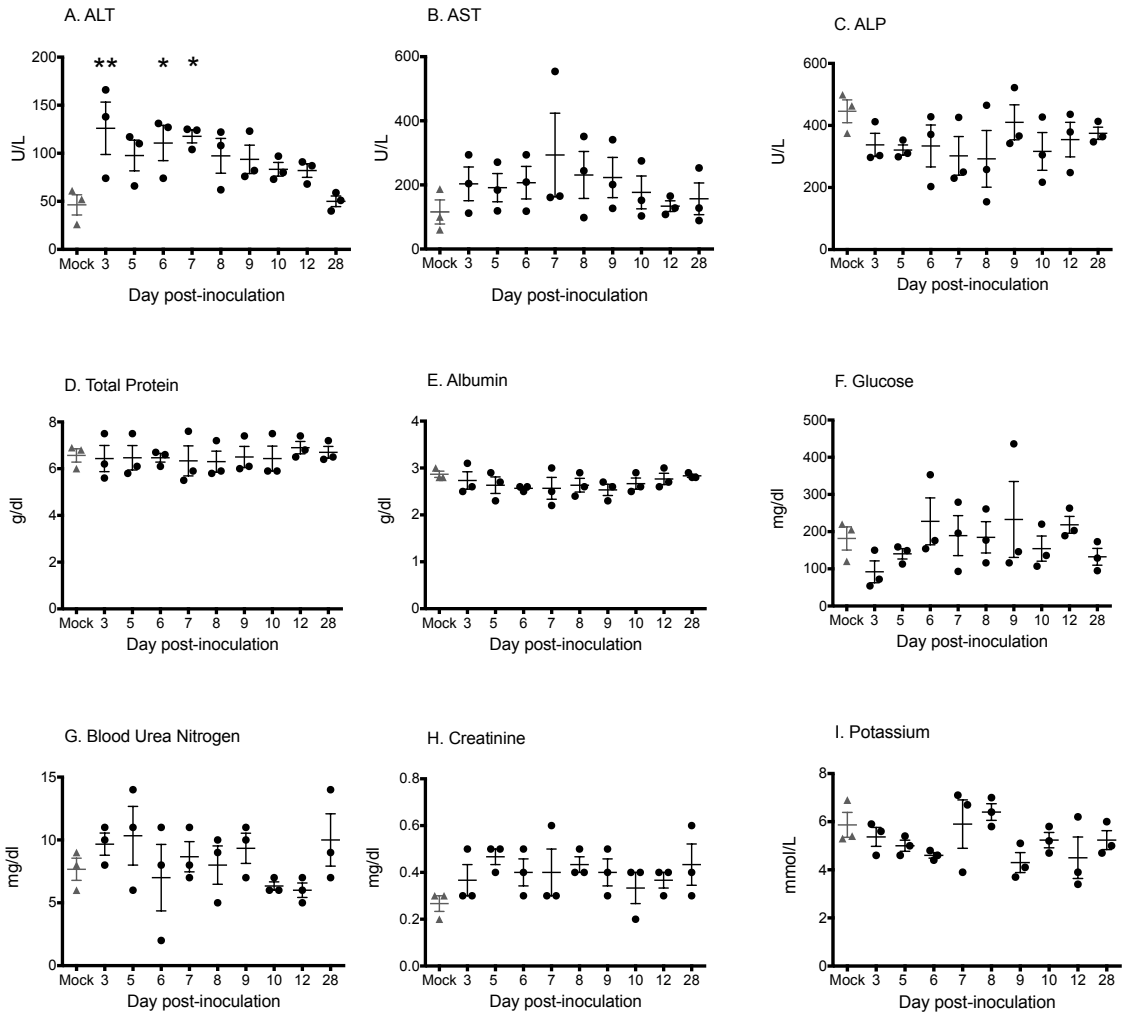
Figure 3.4. Graphical representation of liver viral load, immunohistochemical staining results, and liver lesion score. Top: Liver viral loads represented as \log_{10} 50% tissue culture infective dose (TCID₅₀) equivalents /g. Each point represents an individual bat. Bottom: Liver lesion scores per day post-inoculation. There were significant associations between liver viral load and liver lesion score.

Figure 3.5. Localization of Marburg viral antigen in tissues of Egyptian rousette bats. All IHC stains are immunoalkaline phosphatase with naphthol fast red and hematoxylin counterstain. **A.** Spleen, 5 DPI. MARV antigen (red) is present in the cytoplasm of small numbers of red pulp histiocytes. Inset: higher magnification of a histiocyte showing granular to globular, cytoplasmic staining of antigen. **B.** Axillary lymph node; 10 DPI. Marburg viral antigen is localized to the cytoplasm of histiocytes in the subcapsular sinus (top of image) and in the paracortical region (arrows). **C.** Tongue (mucosa, submucosa, and skeletal muscle); 9 DPI. Marburg virus antigen (red) is present in a small number of histiocytes and fibroblast-type cells. **D.** Skin, patagium (wing membrane), 10 DPI. Cytoplasmic antigen (red) is present in a focus of dermal histiocytes. **E.** Skin and subcutaneous tissue from the MARV inoculation site, 3 DPI. The subcutis is infiltrated by a dense aggregate of macrophages at the site of viral inoculation. HE stain. **F.** Skin and subcutaneous tissue from the MARV inoculation site (replicate of section in C).

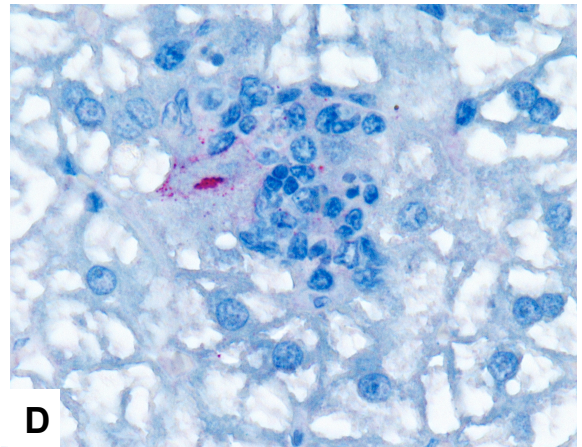
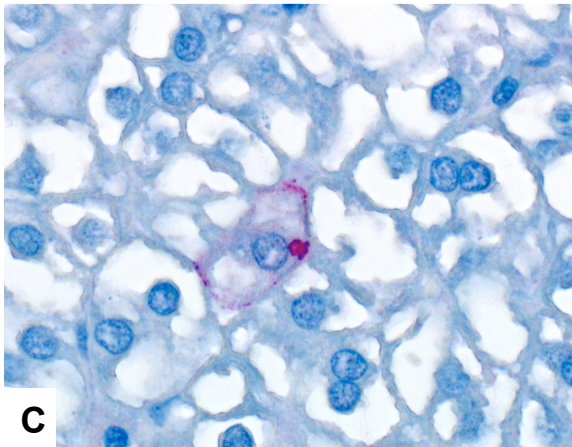
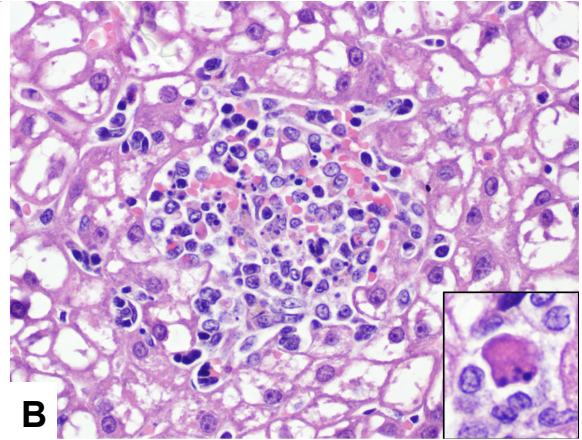
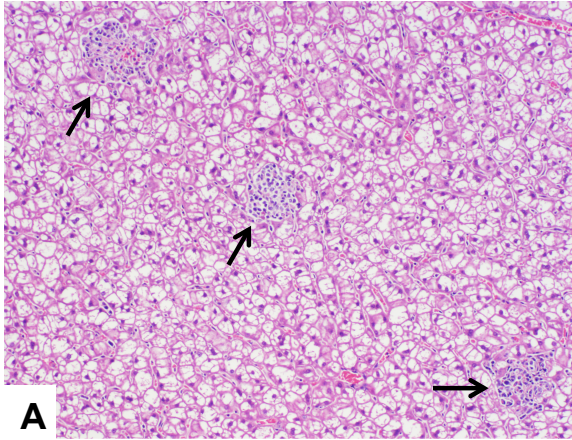
Immunohistochemical stain demonstrating Marburg viral antigen (red) in macrophages in the subcutaneous tissues. Immunoalkaline phosphatase stain with naphthol fast red and hematoxylin counterstain.



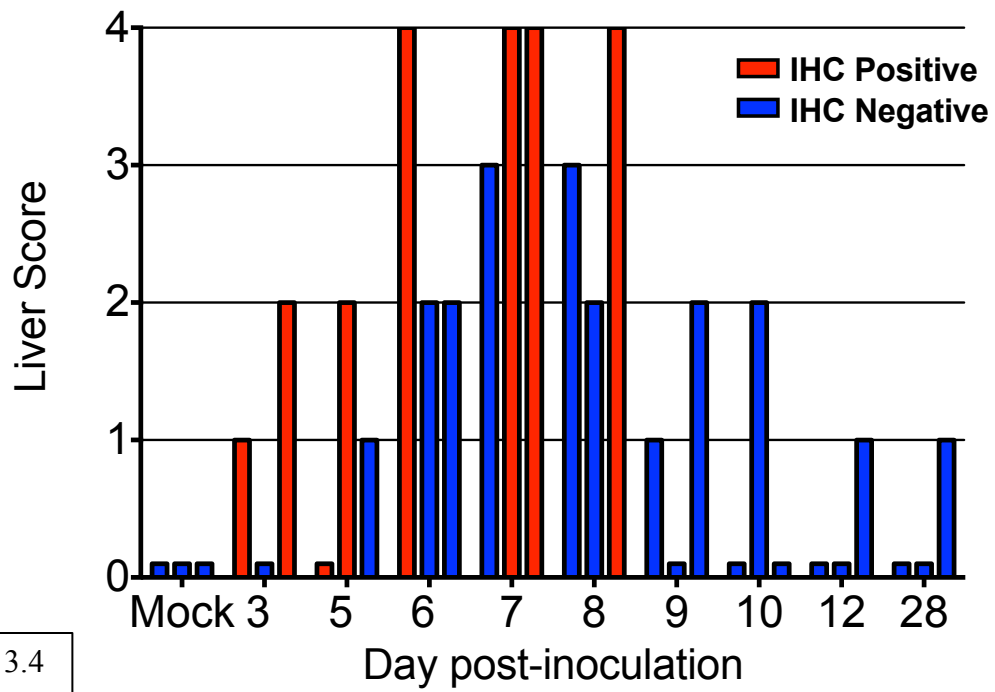
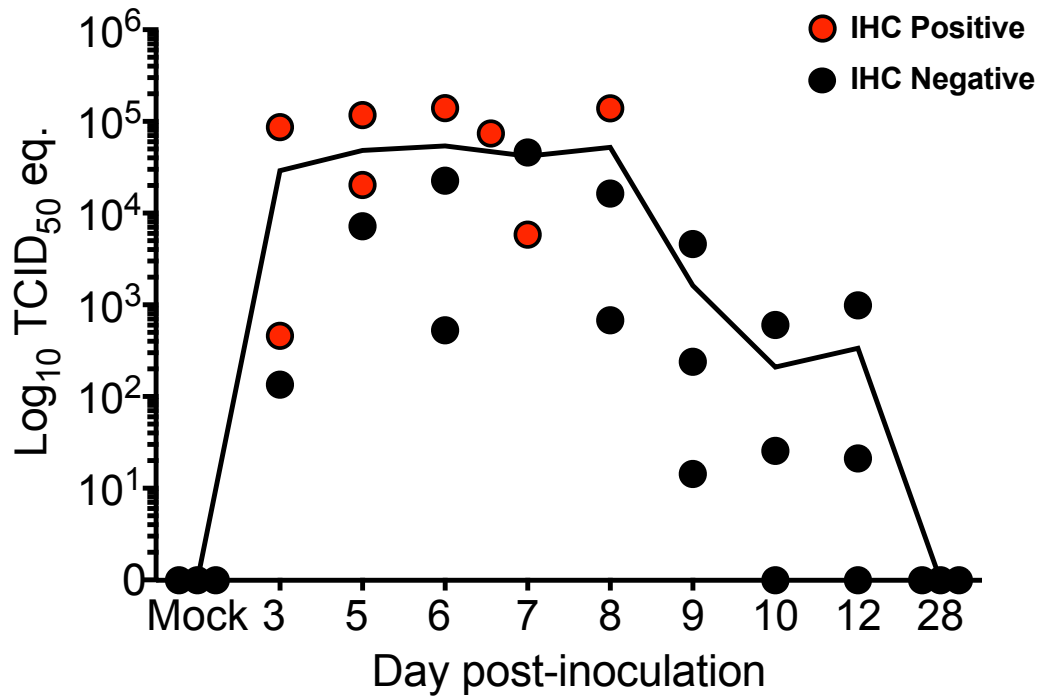
3.1



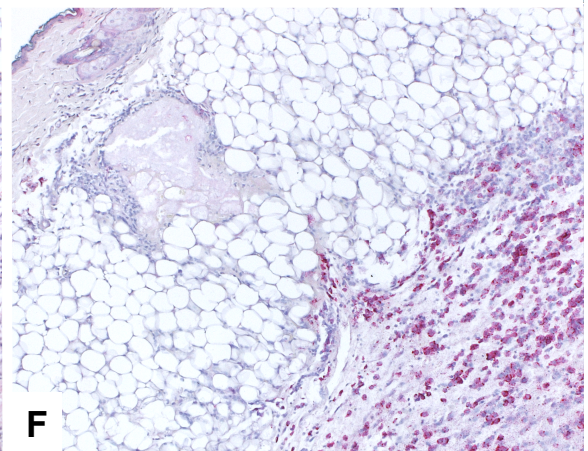
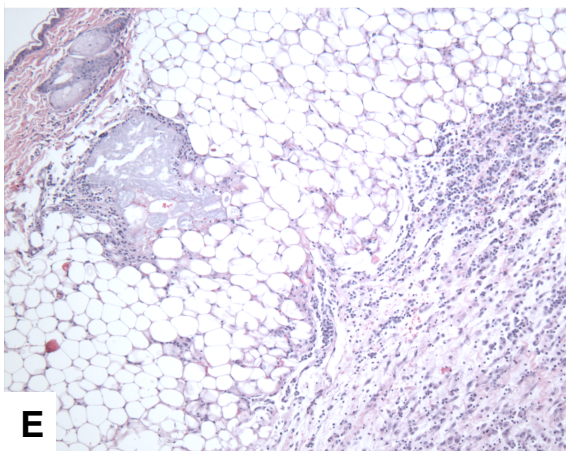
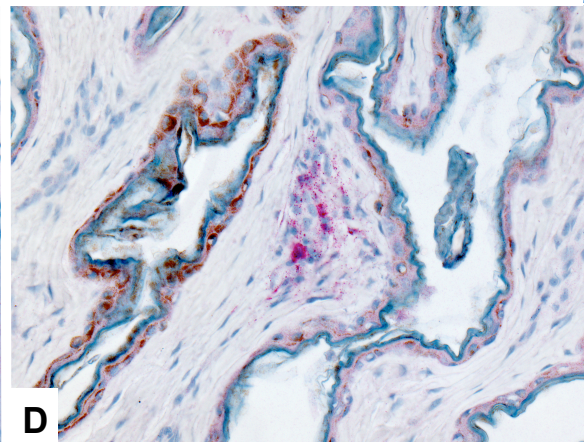
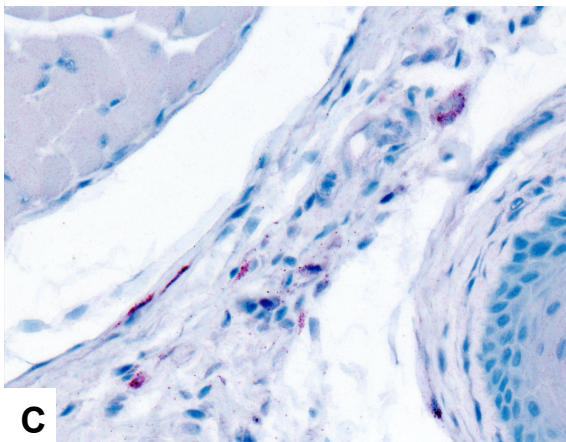
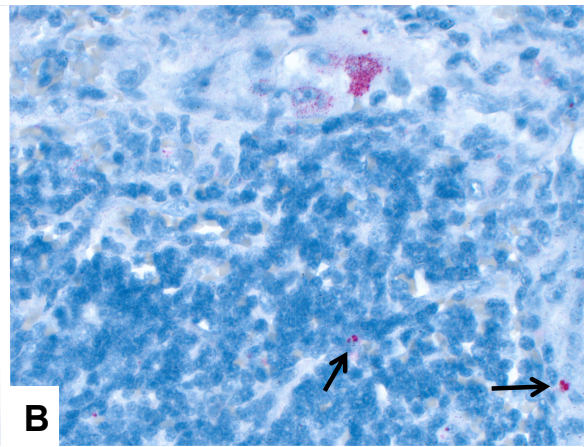
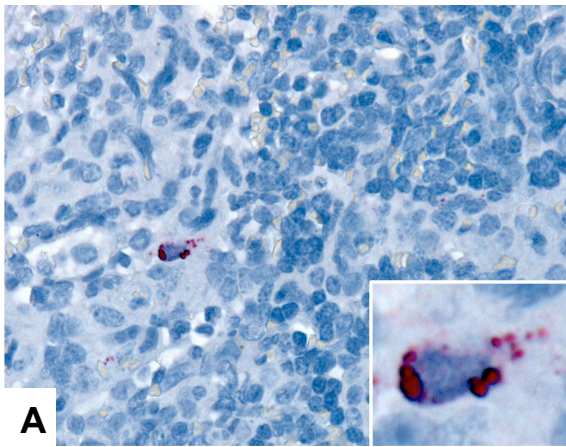
3.2



3.3



3.4



3.5

CHAPTER 4
EXPERIMENTAL INOCULATION OF EGYPTIAN ROUSETTE BATS (*ROUSETTUS
AEGYPTIACUS*) WITH FIVE EBOLAVIRUSES AND COMPARISON WITH
MARBURG VIRUS*

*Megan E.B. Jones, Amy J. Schuh, Brian R. Amman, Tara K. Sealy, Sherif R. Zaki,
Stuart T. Nichol, and Jonathan S. Towner. To be submitted to *Viruses, Special Issue
"Advances in Ebolavirus, Marburgvirus, and Cuevavirus Research 2014-2015"*

Abstract

Ebolaviruses and marburgviruses (*Filoviridae*) cause sporadic outbreaks of hemorrhagic fever in humans and non-human primates, with case fatality rates up to 90%. The Egyptian rousette bat (*Rousettus aegyptiacus*) has been identified as a natural reservoir for marburgviruses and a consistent source of virus spillover to humans. Cumulative evidence suggests various fruit bat species also play a role in the transmission cycle of ebolaviruses. There are five known ebolaviruses (Sudan, Ebola, Bundibugyo, Taï Forest, and Reston), and one study found antibodies from Egyptian rousettes to be reactive to Ebola virus antigen. Through a two-part experimental infection study, we investigated the susceptibility of Egyptian rousettes to viruses representing each of the five ebolavirus species, and compared findings with Marburg virus. In a 10-day pilot study, groups of four juvenile, captive-bred bats were inoculated with a low-passage stock of one of the ebolaviruses or Marburg virus. There were no mortalities and no significant hematologic or histopathologic abnormalities. In ebolavirus groups, viral RNA distribution in tissues was limited, and no bat became viremic. Viral RNA was slightly more widespread in the Sudan virus group, and liver and spleen were PCR-positive at day 5 post-inoculation, spurring a second, 15-day serial euthanasia study where 15 bats were inoculated with Sudan virus. Sudan viral RNA was found in multiple tissues, especially at early time points, but tissue viral loads were low, with no detected viremia or viral shedding. In contrast, Marburg virus RNA was widely disseminated, with evidence of viremia, oral and rectal viral shedding, and antigen in spleen and liver. This is the first reported experimental infection study comparing tissue tropism, potential for viral shedding, and clinical and pathologic effects of six different filoviruses in the Egyptian rousette, a

known marburgvirus reservoir. Our results suggest that Egyptian rousettes are unlikely sources for ebolaviruses in nature, and lend support to a possible single filovirus – single bat host relationship, analogous to that of hantaviruses in rodent reservoirs.

Introduction

Ebolaviruses and marburgviruses (*Filoviridae*) are negative-sense, single-stranded RNA viruses that cause severe hemorrhagic fever in humans and non-human primates. Filoviral disease is characterized by rapid person-to-person transmission, high case fatality rates, and a lack of approved treatments or vaccines. All filoviruses are classified as Tier 1 Select Agents by the United States Department of Health and Human Services (HHS), and as Risk Group 4 Pathogens by the World Health Organization (WHO). As such, all work with infectious materials must be performed in high containment laboratories under biosafety level-4 (BSL-4) conditions.

According to recently updated taxonomic classification (1), the family *Filoviridae* is divided into three antigenically distinct genera: *Ebolavirus*, *Marburgvirus*, and the provisionally approved genus *Cuevavirus*, recently discovered in a European bat (2). Genus *Marburgvirus* contains a single species, *Marburg marburgvirus*, with two virus members, Marburg virus (MARV) and Ravn virus (RAVV), which are approximately 20% divergent (3). The genus *Ebolavirus* includes five species that each contains a single virus member: *Sudan ebolavirus* (Sudan virus, SUDV), *Zaire ebolavirus* (Ebola virus, EBOV), *Bundibugyo ebolavirus* (Bundibugyo virus, BDBV), *Tai Forest ebolavirus* (Tai Forest virus, TAFV), and *Reston ebolavirus* (Reston virus, RESTV). *Cuevavirus* consists of a single species and virus, *Lloviu cuevavirus* (Lloviu virus). Disease caused by MARV and EBOV have the highest fatality rates (up to 90% in some outbreaks), followed by SUDV (42-65%), (4-6) and BDBV (36 to 40%) (7-9). TAFV has caused one non-fatal human infection and RESTV is considered non-pathogenic to humans, but both can be highly pathogenic in nonhuman primates.

Marburg virus disease (MVD) was first identified in 1967 in Germany and the former Yugoslavia, when laboratory workers acquired a fatal illness after exposure to primates imported from Uganda (10). Ebola virus disease (EVD) first emerged in 1976 in Zaire (now Democratic Republic of the Congo, DRC) and Sudan (now South Sudan), during concurrent but unrelated outbreaks caused by EBOV and SUDV(11,12). Since that time, sporadic outbreaks of both MVD and EVD have been recorded, usually involving dozens to hundreds of cases in relatively remote locations in Africa. The largest ever outbreak of SUDV, and until recently the largest outbreak of any filovirus, occurred in the Gulu district of Uganda in 2000-2001 and involved 425 cases and 224 deaths (13). The most recently discovered ebolavirus, BDBV, caused an outbreak of EVD in 2007 in western Uganda, and emerged again in 2012 in DRC (7,9). TAFV was first documented in 1994 in Côte d'Ivoire, where it was associated with mortality in wild chimpanzees and caused one human infection (14,15). RESTV has only been found in the Philippines, or in macaques imported from the Philippines (16–18). Human exposures to RESTV have resulted in seroconversion without clinical signs of disease (19,20). The current EBOV outbreak in West Africa, which surpassed 25,000 cases in March of 2015 (21), represents a significant expansion of case numbers and a new geographic range for the virus, and clearly demonstrates the potential of filoviruses to become significant threats to public health on a global scale.

Rousettus aegyptiacus, the cave-roosting Egyptian rousette bat (also called the Egyptian fruit bat), has been identified as a natural reservoir host for marburgviruses and consistent source of virus spillover to humans (22,23). This discovery was based on identification of marburgvirus RNA and immunoglobulin G (IgG) (24,25) and the

isolation of infectious marburgviruses (22,23,26) from wild rousettes inhabiting caves where human cases had recently occurred. Longitudinal studies have also demonstrated an association between the risk of human infection and the seasonal pulses of active marburgvirus infection in juvenile Egyptian rousettes during biannual reproductive cycles (23). Cumulative evidence suggests various fruit bat species also play a role in the transmission cycle of ebolaviruses. Epidemiologic links between ebolaviruses and fruit bats were identified in the first SUDV outbreak in 1976 (27) and in TAFV disease in chimpanzees in Côte d'Ivoire in 1994 (14). In 2005, in Gabon and the Republic of Congo (RC), EBOV-specific IgG and RNA were detected in three species of fruit bats (*Hypsignathus monstrosus*, *Epomops franqueti*, and *Myonycteris torquata*) that were hunted for food (28); this was the first and only study in which ebolaviral RNA was detected in any bat species. Subsequently, an investigation into a large EBOV outbreak in DRC in 2007 showed a possible link between regional EVD re-emergence and seasonal fruit bat migration (29). Since that time, several field studies have provided serologic evidence of EBOV exposure in a variety of fruit bat species, including the Egyptian rousette, in Ghana, Gabon, and RC (28–31). Antibodies to RESTV were reported in fruit bats in the Philippines (32) and Bangladesh (33), and in eleven different species of insectivorous and fruit bats in China (34). However, in contrast to results for marburgviruses, repeated attempts at isolation of infectious ebolaviruses from bats have been unsuccessful.

Two recent experimental infection studies of Marburg virus in Egyptian rousettes have demonstrated virus replication in blood and multiple tissues (35,36); oral shedding of infectious virus (36); and viral antigen in liver and spleen without evidence of

significant disease, findings which are consistent with expectations for a reservoir host. Though numerous field studies have demonstrated potential associations between bats and ebolaviruses, only a single experimental ebolavirus infection study has been attempted in any bat species (37). In that experiment, a wide range of possible plant, invertebrate, and vertebrate hosts including two insectivorous bat (*Mops condylurus*, *Chaerephon pumilus*) and one fruit bat species (*Epomophorous wahlbergi*) were inoculated with EBOV. Following inoculation, virus was successfully isolated from pooled viscera and blood from bats for up to three weeks, and was isolated from feces in one bat. There was also limited immunohistochemical staining for ebolavirus antigen in pulmonary endothelial cells in one insectivorous bat, without evidence of associated lesions (37). Recently, a colony of *Mops condylurus* bats was found near the reported index case of the current West African EBOV outbreak (38).

EBOV antibodies have been detected in wild Egyptian rousette bats in Gabon (29), and a *R. aegyptiacus*-derived cell line was shown to support EBOV replication *in vitro* (39). Other *Rousettus* spp. bats have been seropositive for RESTV and EBOV in the Philippines and China (32–34). However, the capacity for Egyptian rousettes to become infected with ebolaviruses and act as a potential source of infectious virus is not known. Here, we report the findings of an experimental inoculation study of Egyptian rousette bats in which we compare the viral kinetics, tissue and cell tropism, potential for viral shedding, and clinical and pathologic effects of all five known ebolaviruses with findings from Marburg virus. This was a two-part study, consisting of a pilot study to investigate all six filoviruses concurrently, followed by a serial euthanasia study to compare the effects of SUDV infection with our previous findings for MARV. We hypothesized that,

if Egyptian rousettes are not a true reservoir host of any of the five species of ebolavirus, then the response of this bat species to experimental infection with ebolaviruses will differ significantly from the response to Marburg virus infection. Inoculation of Egyptian rousette bats with ebolaviruses would result in either 1) abortive infection due to lack of susceptibility; or, 2) clinical and pathologic signs of severe disease. We show that Egyptian rousettes are generally refractory to ebolavirus infection and are unlikely to act as sources of infectious virus in nature.

Materials and Methods

Ethics Statement

All animal procedures and experiments were approved by the CDC Institutional Animal Care and Use Committee (IACUC) and conducted in strict accordance with the Guide for the Care and Use of Laboratory Animals (40). The CDC is fully accredited by the Association for Assessment and Accreditation of Laboratory Animal Care International (AAALAC).

Biosafety

All work with infectious virus or infected animals was conducted at the Centers for Disease Control and Prevention (CDC, Atlanta, Georgia, USA) in a biological safety level-4 (BSL-4) laboratory in accordance with Select Agent regulations (HHS and USDA, cite website). All investigators and animal care personnel followed international biosafety practices appropriate to BSL-4 and strictly adhered to infection control practices to prevent cross contamination between groups of animals.

Animals and Husbandry

The study animals consisted of juvenile (4-5 months old), first-generation, captive born, Egyptian rousettes (*R. aegyptiacus*) from a marburgvirus and ebolavirus-free breeding colony founded from wild-caught animals imported from Uganda in 2011 (36). All bats were group-housed in large flight cages until one week prior to experimental infection, when they were moved to experimental caging in the BSL-4 laboratory for acclimatization. In the BSL-4 laboratory, cages housing each experimental group (minimum of two, maximum of nine bats per cage, depending on the study) were maintained in separate isolator units (Duo-Flow Mobile Units, Lab Products Inc., Seaford, Delaware, USA) in temperature- and humidity-controlled rooms with a 12-hour light-dark cycle. All bats were fed a variety of fresh fruit, juice, and nutritional supplement (Lubee Bat Conservancy, Gainesville, FL) *ad libitum* for the duration of the study. All animals in the breeding colony are individually identified at weaning using passive integrated transponder (PIT) tags (Biomark, Boise, ID) placed subcutaneously in the interscapular region.

Viruses

All virus stocks used in this experiment were titrated using a standard 50% tissue culture infective dose (TCID₅₀) protocol on Vero E6 cells and visualized by indirect fluorescent antibody assay (IFA) using appropriate rabbit polyclonal antibodies. For bat inoculations, virus stock was diluted to a concentration of 4×10^4 TCID₅₀/ml in sterile Dulbecco's Modified Eagles Medium (DMEM, Invitrogen) and each bat received 250 μ l of diluted virus, for a dose of 10^4 TCID₅₀ per animal. The strain of Marburg virus used in this and

previous experimental infections (371bat virus; see (36)), was originally isolated from a naturally infected Egyptian rousette caught at the Kitaka Mine, Uganda, in 2007 (22) and passaged twice on Vero E6 cells. The ebolavirus stocks used were grown from low-passage seed stocks at the Viral Special Pathogens Branch, Centers for Disease Control and Prevention, as follows: Ebola virus variant Mayinga, originally isolated in 1976 and passaged twice on Vero E6 cells; Sudan virus variant Gulu, originally isolated during the outbreak in Gulu, Uganda in 2000-2001 and passaged three times on Vero E6 cells; Bundibugyo virus originally isolated during the 2007 outbreak in Uganda and passaged twice on Vero E6 cells; Tai forest virus isolated in 1994 and passaged five times on Vero E6 cells, and Reston virus originally isolated from a Rhesus macaque in 1989, and passaged on MA104 cells (x1) and Vero E6 cells (x7). This virus had also been plaque picked and confirmed negative for Simian Hemorrhagic Fever virus.

Ebolavirus Pilot Study

This was a 10-day pilot study to investigate the response of Egyptian rousettes to experimental infection of each of the five ebolavirus species, and to identify potential ebolavirus candidate(s) for further investigation. Four bats (2 male and 2 female) were randomly assigned to each experimental group, to be inoculated with either MARV, EBOV, SUDV, BDBV, TAFV, or RESTV; two bats (1 male and 1 female) were randomly assigned as mock-inoculated controls. Experimental inoculation procedures were performed as in in Amman *et al.* (2015). Briefly, bats were lightly anesthetized using isoflurane anesthetic administered via mask (RC² Rodent Anesthesia System, Vetequip, Pleasanton, CA). Bats were inoculated subcutaneously in the ventral abdomen

with 250 µl of virus stock diluted in DMEM, for a total dose of 10,000 TCID₅₀ of virus per animal. Control animals were inoculated with 250 µl of DMEM only. Two animals (one male, one female) from each group were scheduled for euthanasia at 5 and 10 days post-inoculation (DPI), and both mock-inoculated animals were euthanized on day 10. Body weights, rectal temperatures, and blood samples for PCR and complete blood counts (CBC) were obtained prior to infection and then daily from 1 DPI until the time of euthanasia. Oral and rectal swab samples were taken daily. Polyester-tipped applicators (Fisher Scientific, Pittsburgh, PA, USA) were used to swab the inside of the mouth of each bat and placed into 500 µl of MagMax lysis buffer (Life Technologies) for RNA extraction. After use, plastic sheaths covering rectal temperature probes (MABIS Healthcare, Waukegan, Illinois, USA) were cut and placed in 500 µl of MagMax lysis buffer (#AM8500, Life Technologies, Grand Island, NY) for RNA extraction. Due to a larger volume requirement (100µl) and blood sampling limits for this species, sufficient blood for chemistry analysis was only available on the day of euthanasia. Bats were observed at least once daily throughout the study so that any moribund animals could be scored according to a predetermined clinical illness / euthanasia algorithm. Animals were euthanized under deep isoflurane anesthesia by exsanguination via cardiac puncture.

Sudan Virus (Variant Gulu) Serial Euthanasia Study

This was a 15-day serial euthanasia study to investigate viral infection kinetics, tissue and cell tropism, potential for viral shedding, and clinical and pathologic findings, of Egyptian rousette bats inoculated with Sudan virus (variant Gulu). Twenty-one juvenile (4-5 month old) Egyptian rousettes were randomly assigned to be inoculated with 10⁴

TCID₅₀ of Sudan virus (n=15 bats), 10⁴ TCID₅₀ of Marburg virus (n=3), or mock inoculated (n=3). Inoculation procedures, dosages, and volumes were identical to those in the pilot study, above. Rectal temperatures, oral swabs, and blood samples for Q-RT-PCR and CBC were obtained prior to infection and then daily starting at 1 DPI until euthanasia, as described above. Body weights were obtained prior to infection and then on days 3, 6, 9, 12, and 15. Three Sudan virus inoculated bats (2 males, 1 female; sex ratios were determined by available animals of appropriate age in our breeding colony) were scheduled for euthanasia on each of 3, 6, 9, 12, and 15 DPI, and euthanasia procedures were as described above. MARV-inoculated and mock-inoculated bats were euthanized at 15 DPI. Blood was sampled for chemistry analysis from each bat on the day of euthanasia. Blood was taken for serology at 0, 5, 10, and 15 DPI.

Hematology and Clinical Chemistry

For daily CBCs, blood was collected from the cephalic vein into a 20µl, EDTA-coated capillary tube (True20 capillary tube) and analyzed using a Hematrue blood analyzer (HESKA, Loveland, CO, USA). For blood chemistry profiles, 100µl of whole blood was collected at the time of euthanasia, placed in lithium heparin tubes (Microtainer, BD) and analyzed using Comprehensive Metabolic Panel Discs for the Piccolo point of care chemistry analyzer (Abaxis, Union City, CA, USA). Chemistry analyses included alanine aminotransferase (ALT), albumin, alkaline phosphatase (ALP), aspartate aminotransferase (AST), calcium, chloride, creatinine, glucose, potassium, sodium, total bilirubin, total carbon dioxide, total protein, and blood urea nitrogen (BUN).

Necropsy

Complete necropsies were performed immediately following euthanasia. For RNA extraction, approximately 100 mg samples of each tissue were collected with sterile instruments to prevent cross-contamination. For the ebolavirus pilot study, this included liver, spleen, skin from the inoculation site, skin from the antebrachium, axillary lymph node, lung, heart, kidney, adrenal gland, small intestine, large intestine, mesenteric lymph node, gonad, urinary bladder, and salivary gland. For the Sudan virus serial euthanasia study, tissues collected for RNA extraction were liver, spleen, skin from the inoculation site, axillary lymph node, lung, heart, kidney, small intestine, large intestine, gonad, urinary bladder, and salivary gland. Tissue samples collected for histologic examination were fixed by immersion in 10% neutral buffered formalin in the BSL-4 laboratory for a minimum of 7 days, and then formalin was completely replaced prior to further processing. Tissues collected and processed for histopathology for both the pilot study and the serial euthanasia study included liver, spleen, lung, heart, trachea, thymus, tongue, tonsils, stomach, small intestine, pancreas, large intestine, mediastinal lymph nodes, kidney, adrenal gland, salivary gland, mandibular lymph node, axillary lymph node, pectoral muscle, skin from inoculation site, skin from antebrachium, and skin from patagium (wing membrane).

RNA Extraction and Q-RT-PCR

RNA extraction was performed as described in Amman *et al.* (2015). Approximately 100 mg samples of each tissue were placed in 2 ml polycarbonate grinding vials (OPS Diagnostics, Lebanon, NJ) containing 1 ml viricidal lysis buffer concentrate (#AM8500;

MagMax Lysis Binding Solution Concentrate, Life Technologies, Carlsbad, CA). Specimen sizes of some tissues (e.g., gonad, adrenal gland, urinary bladder) were less than 100 mg due to availability, but remained consistent within a tissue type. Tissues were homogenized in a high-throughput tissue grinder (Genogrinder2000, BT&C Inc, Lebanon, NJ). Total RNA was extracted from 125 μ l aliquots of tissue homogenate using the MagMax-96 Total RNA Isolation Kit (Life Technologies) per manufacturer's instructions, and the AM1830_DW protocol pre-loaded on the MagMax express-96 Deep Well Magnetic Particle Processor (#4400077). Blood samples (20 μ l whole blood) were added to 130 μ l of lysis binding solution (1:1 ratio of MagMax Lysis Binding Solution concentrate and 100% isopropanol) and RNA was extracted using the MagMax-96 Total RNA Isolation Kit and the AM1836_DW_50v2 protocol preloaded on the MagMax Express Deep Well Magnetic Particle Processor. To account for sample-to-sample variation in tissue and blood, Q-RT-PCR results were normalized to 18s rRNA using a commercially available eukaryotic 18s rRNA assay (Applied Biosystems/Life Technologies) according to the manufacturer's instructions.

Polyester-tipped applicators used as oral swabs and plastic probe covers used as rectal swabs were placed in 500 μ l MagMax lysis buffer, as for blood, above, and RNA was extracted using the 5x MagMax Pathogen RNA/DNA kit per manufacturer's instructions, and the 44262359_DW_HV protocol for low-cell-content samples preloaded on the MagMax Express-96 Deep Well Magnetic Particle Processor. Gamma-irradiated Rift Valley Fever Virus (RVFV) was added to swab samples as an extraction control (5 μ l per well).

Quantitative reverse-transcriptase PCR (Q-RT-PCR) was performed using the SuperScript III Platinum One-Step qRT-PCR kit, Invitrogen/Life Technologies) and routine diagnostic protocols targeting Marburg virus VP40, NP of Ebola virus, Sudan virus, Reston virus, and the VP40 of Bundibugyo and Taï Forest viruses. For swab samples, a Q-RT-PCR assay targeting the L segment of RVFV was performed as in Bird et al, 2007.

Standard curves for Q-RT-PCR results for the Sudan virus serial sacrifice study were generated from ten-fold serial dilutions of the Marburg and Sudan virus stocks used in infections, and added to blood, tissue (calf liver) homogenate, or DMEM in the same proportions as experimental blood, tissue, or swab samples, respectively. The relative TCID₅₀/ml (fluids) or g (tissue) equivalents for experimental samples were interpolated from the relevant standard curve.

Histology and Immunohistochemistry

Representative sections of all formalin-fixed tissues were embedded in paraffin, sectioned at 4 micrometers, mounted on glass slides, and routinely stained with hematoxylin and eosin (HE) for histologic examination.

Immunohistochemical staining was performed using an alkaline-phosphatase (AP) polymer detection system (UltraVision Detection System, Thermo Scientific). Four-micron sections of formalin-fixed, paraffin-embedded tissues were deparaffinized and rehydrated using gradations of ethanol (100%, 95%, and 70%). Tissues were subjected to proteinase-K (Roche) digestion for 15 minutes at room temperature (RT), then Ultra V Block (Thermo Scientific) was applied for 10 minutes at RT. The primary antibody was

either a rabbit anti-Marburg virus polyclonal or a rabbit anti-ebolavirus polyclonal antibody (Viral Special Pathogens Branch, Centers for Disease Control and Prevention, Atlanta, GA). The primary antibody was diluted to 1:250 and incubated for 30 minutes at RT, followed by Primary Antibody Enhancer (Thermo Scientific; 10 minutes at RT). AP Polymer (Thermo Scientific) was used as the secondary antibody at manufacturer's dilution and incubated for 15 minutes at RT. The detector was Naphthol Phosphate Substrate/Fast Red (Thermo Scientific; 20 minutes at RT). Sections were counterstained with Mayer's modified hematoxylin (Poly Scientific, Bay Shore, NY). For negative controls, replicate sections from each block were deparaffinized and stained in parallel following an identical protocol, with the primary antibody replaced by normal rabbit serum (Centers for Disease Control and Prevention, Atlanta, GA).

Serology

In the SUDV serial euthanasia study, blood samples taken for serologic analysis were tested by ELISA for the presence of IgG antibodies reactive to SUDV, as described in Ksiazek et al. (41,42) with the modification that 96-well plates were coated with 50 ng/well of recombinant SUDV nucleocapsid (NP) protein expressed in *E. coli* and sum ODs adjusted by subtracting reactivity at each 4-fold dilution (1:100 to 1:6400) to MARV NP protein similarly expressed and purified from *E. coli*.

Statistical Analyses

Statistical analyses were performed using Prism 6.0 (GraphPad Software, La Jolla, CA) and Stata 13 (StataCorp, College Station, TX). For each blood chemistry parameter,

values from infected animals at each time point (n=3 per time point) were compared with those of mock-inoculated bats (n=3) using one-way analysis of variance (ANOVA), followed by Dunnett's multiple comparison test if the ANOVA demonstrated significant differences between groups ($p < 0.05$). Complete blood count data, which were obtained at multiple time points for each individual bat, were analyzed using repeated measures ANOVA.

Results

Ebolavirus Pilot Study

Clinical and Hematologic Findings

No clinical signs or behavioral changes suggestive of morbidity were observed in any animal, and there were no mortalities. Bats included in the pilot study weighed $109.9 \text{g} \pm 11.5$ (mean \pm SD), with a range of 80.8g to 129.1g, and there was no mean weight difference between experimental groups ($F_{6,19} = 2.491$, $p > 0.05$). Change in percent daily body weight did not significantly differ between groups ($F_{6,19} = 1.212$, $p > 0.05$). Over the course of the experiment, most bats tended to gain weight, with a maximum gain of 10.1% over 10 days, and no individual animal lost more than 2% body weight, relative to initial weight. Rectal temperatures remained within normal ranges in all animals.

Blood chemistry data for the pilot study are shown in Figure 4.1. AST was significantly elevated (269 U/L; normal range 26-136 for juvenile bats in our colony) in one BDBV-inoculated bat at 5 DPI. Other parameters remained within normal limits for all bats. CBC data are shown in Figure 4.2. Overall, WBC counts for EBOV, TAFV, and RESTV bats were significantly higher than those for controls, MARV, or SUDV, though

all WBC parameters remained within the normal range for all but two bats ($F_{6,19} = 4.31$, $p=0.007$). One TAVF-inoculated bat and one RESTV bat exhibited mild leukocytosis characterized by monocytosis and lymphocytosis on days 4 and 6 and days 6 and 8 post-inoculation, respectively. Platelet and erythrocyte counts remained within normal limits for all bats (data not shown).

Q-RT-PCR

All four MARV-inoculated bats became viremic (as determined by the presence of viral RNA in blood) at 4 DPI, and MARV RNA was detected for at least two days in each bat (Figure 4.3). Both bats euthanized at 5 DPI were viremic at the time of euthanasia, and viremia was detected until days 7 and 8 in the two MARV bats euthanized on day 10. Viral RNA was never detected in the blood of any of the ebolavirus-inoculated or mock-inoculated bats.

The viral tissue distribution and levels of viral RNA for the pilot study are summarized in Table 1. MARV was widely disseminated in bats euthanized at 5 and 10 DPI, with RNA detected in a total 11 of 16 tissue types tested. RNA was most frequently detected in skin at the inoculation site (n=4), liver (n=4), spleen (n=3), and salivary gland (n=3), but was also found in axillary lymph node (n=1), urinary bladder (n=2), small intestine (n=2), mesenteric lymph node (n=1), gonad (n=2, both males), heart (n=1), and kidney (n=1). SUDV RNA was detected in a total of five of 16 different tissue types tested from four bats (Table 1), including skin from the inoculation site (n=3), liver (n=2), spleen (n=2), axillary lymph node (n=3), and urinary bladder (n=1). For EBOV, BDBV, and RESTV, RNA dissemination was limited to skin from the inoculation site

and axillary lymph node, and for TAFV, only the inoculation site was PCR-positive (Table 1). All oral and rectal swabs from all five ebolavirus groups and mock-inoculated bats were negative by Q-RT-PCR. In contrast, MARV RNA was detected in oral and rectal swabs from both MARV-inoculated bats euthanized at 10 DPI (Figure 4.3).

Necropsy, Histopathology, and Immunohistochemistry

Necropsy revealed no significant gross lesions in any bat. All animals had abundant abdominal and subcutaneous adipose tissue. On histologic examination of the liver, most bats exhibited moderate to marked, midzonal to diffuse hepatocellular vacuolation, consistent with glycogen accumulation, a common incidental finding in in our colony. The distribution and degree of vacuolation was similar in all experimental groups including controls. In the livers of MARV-inoculated bats, there were small, randomly scattered aggregates of cellular infiltrate composed predominantly of histiocytes and lymphocytes admixed with few neutrophils (Figure 4.4). These foci sometimes contained necrotic or apoptotic hepatocytes and karyorrhectic debris. Foci were most frequent in animals with higher viral load in the liver. IHC staining for MARV in the liver revealed antigen in a small proportion of these foci in both bats from 5 DPI (Figure 4.4; Table 1). Positive, cytoplasmic, granular to globular immunostaining was localized to histiocytes or hepatocytes, and was rarely perimembranous in hepatocytes. Very rarely, foci of similar liver infiltrate were also present in one SUDV bat (10 DPI), one EBOV bat (10 DPI), one BDBV bat (10 DPI), two TAFV bats (both from 10 DPI), two RESTV bats (5 and 10 DPI), and one control bat (10 DPI), but immunohistochemical stains of liver were negative for all ebolavirus-inoculated and mock-inoculated bats.

In the spleen, small amounts of MARV antigen were present in the cytoplasm of red pulp histiocytes in both bats from 5 DPI (Figure 4.4). No splenic lesions were identified in any bat, and no antigen was detected in spleen in any ebolavirus-inoculated or mock-inoculated bat.

In all experimental groups, histologic examination of skin from the inoculation site revealed small aggregates of macrophages in the deep subcutaneous tissues that decreased in cell density from 5 to 10 DPI. These aggregates were present in all MARV and all SUDV-inoculated bats, but were larger in MARV bats than in other groups. In other virus-inoculated groups, only three of four bats had comparable lesions. Immunohistochemical staining of inoculation site skin sections demonstrated MARV antigen in the cytoplasm of subcutaneous histiocytes and fibroblast-type in all four MARV-inoculated bats, though antigen was sparse at 10 DPI. Very small amounts of virus-specific antigen was also present in histiocytes and, rarely, fibroblasts at 5 DPI in bats inoculated with SUDV (n=1), EBOV (n=2), and RESTV (n=1). All other tissues examined by immunohistochemical staining were negative in all bats.

Sudan Virus Serial Euthanasia Study

Based on pilot study Q-RT-PCR results, which showed SUDV to be more widely disseminated than the other ebolavirus species, SUDV was further investigated in a serial euthanasia study. This study was designed to complement our previous Marburg virus serial euthanasia study (36), while also taking into account the limited number of juvenile, single-cohort bats available from the breeding colony at one time. Euthanasia

and other sampling time points were chosen for direct comparison with days 3, 6, 9, and 12 of the MARV study, and an additional time point was added at 15 DPI.

Clinical and Hematologic Findings

As in the pilot study, there were no mortalities and no evidence of significant clinical disease. Bats included in the study weighed 99.0 ± 12.2 g (mean \pm SD), with a range of 72.0 to 120.6 g, and there was no significant weight difference between groups ($F_{2,18}=0.29$; $p=0.750$). Percent weight change per time point (every 3 days) did not significantly differ between groups, and average weights for each group tended to increase over time. CBC results are shown in Figure 4.5. CBC parameters remained within the normal range for all bats. Relative to day 0, average counts of total white blood cells, lymphocytes, and monocytes for all groups tended to decrease until approximately 4-5 DPI, then increase to peak at day 9-11. Granulocytes, platelets, and erythrocyte counts remained relatively stable from day to day. There were no statistical differences in any CBC parameter between virus groups. Blood chemistry results are shown in Figure 4.6. AST was significantly elevated in SUDV bats at 3 DPI relative to all other days ($F_{6,14} = 6.411$, $p=0.002$). No other chemistry value was significantly elevated.

Q-RT-PCR

RNA was never detected in the blood of any SUDV-inoculated bat. All 3 MARV bats became viremic (as indicated by detection of MARV RNA in blood) at 5 DPI and remained so for 2 (n=2) to 3 (n=1) days (data not shown). Q-RT-PCR results for tissues for SUDV bats from days 3-15 are shown in Table 2. SUDV RNA was most frequently

detected in the skin from the inoculation site (n=13), axillary lymph node (n=7), large intestine (n=5), and urinary bladder (n=4). Liver was PCR positive in 4 bats, at 3, 6, and 15 DPI, at lower viral loads than in MARV-inoculated bats in our previous study (36). SUDV RNA was detected in spleen in three bats total, two at 3 DPI and one at 6 DPI. Tissue viral loads were greatest in skin from the inoculation site and in spleen, and in both sites were detected at levels greater than the inoculation dose 10^4 TCID₅₀/g equivalent, consistent with viral replication. Other PCR-positive tissues included small intestine (n=2), gonad (n=3), heart (n=1) and kidney (n=3). SUDV RNA was never detected in salivary gland or oral or rectal swabs.

Necropsy, Histology and Immunohistochemistry

Histologic findings from SUDV bats were comparable to those in the pilot study. At 3 DPI, one animal had very few, randomly scattered foci of mononuclear infiltrate in the liver, and similar foci were present in all three bats at day 6. These foci were still present in on days 9 (n=2) and 12 (n=1), and sometimes contained single to few necrotic hepatocytes. In the livers of the three MARV bats from 15 DPI, there were scattered foci of mixed infiltrate that contained few pigment-laden macrophages, without overt necrosis or hepatocellular degeneration. Also similar to the pilot study, there were small, subcutaneous aggregates of macrophages in deep adipose tissue at the inoculation site. SUDV antigen was only detected in tissues with higher viral loads (Table 2): antigen was present in very small numbers of macrophages in the deep subcutis of the inoculation site in 4 bats from 3 and 6 DPI, and one bat had a small amount of SUDV antigen in an

axillary lymph node. No MARV-antigen was detected at 15 DPI, and all control bats were negative.

Serology

Serology results are shown in Figure 4.7. One of six bats remaining at 12 DPI had seroconverted, and a second bat seroconverted on day 15. IgG was not detected in mock inoculated control bats.

Discussion

This is the first reported experimental infection study comparing the viral kinetics, tissue and cell tropism, and clinical and pathologic effects across six different filovirus species, in a bat host known to act as a natural reservoir for Marburg virus. The pilot study, in which four animals each were inoculated with identical doses of SUDV, EBOV, BDBV, TAFV, RESTV, and MARV, showed that tissue dissemination of ebolaviruses was limited in Egyptian rousettes, viremia was not detected, and there was no evidence of viral shedding via oral or fecal routes. In contrast, Marburg virus was detected in the blood, in a wide range of tissues, and in oral and rectal swabs of Egyptian rousettes in this study and in previous experiments (36). These findings suggest that Egyptian rousettes are generally refractory to ebolavirus infection, implying they are not likely to act as a natural ebolavirus reservoir despite the identification of EBOV-seropositive Egyptian rousettes in Gabon (29) and RESTV-seropositive *Rousettus amplexicaudatus* and *R. leschenaulti* species bats in Asia (32–34). Furthermore, the Egyptian rousette, which tends to breed well in captivity and can thrive in a laboratory setting, may not be

an appropriate experimental model for investigating ebolavirus-reservoir host relationships.

For Sudan virus, pilot study findings were intermediate: viral RNA was more widespread than in the other four ebolaviruses, and was detected in both liver and spleen, though animals did not become viremic, viral loads were low, and SUDV antigen was very limited in distribution. These results were replicated and confirmed in a larger serial euthanasia study, which was designed to complement our previous Marburg virus serial euthanasia study (36); day-by-day comparison of viral RNA levels in key tissues in SUDV and MARV serial euthanasia studies is provided in Figure 4.8. SUDV RNA was detected in 10 different tissues, most frequently and at highest loads at 3 and 6 DPI. All 15 bats in the SUDV serial euthanasia study were PCR-positive in at least one tissue between 3 and 15 DPI, but viremia and viral shedding were not identified, and liver and spleen remained IHC-negative. In contrast with Marburg virus, which is frequently found in liver and spleen at levels consistent with replication in these sites, SUDV RNA was only detected in liver or spleen in 3 of 15 bats, and only one bat was PCR-positive in both tissues (Figure 4.8). The only tissues in which SUDV levels were suggestive of viral replication ($TCID_{50}/g$ equivalents greater than inoculation dose) were the inoculation site at days 3 and 6, and the spleen in one bat on day 3. The presence of limited SUDV replication and relatively widespread tissue distribution (though at low levels) indicates that Egyptian rousettes could be more broadly susceptible to infection with Sudan virus than with other ebolaviruses, perhaps given a higher inoculum dose or different route of infection. However, the generally low tissue levels of viral RNA and the lack of any evidence of viral shedding suggest the virus would not be likely to persist in the

population. No SUDV outbreak has ever been associated with caves or mines inhabited by Egyptian rousettes. Moreover, SUDV-specific RNA or antibodies have never been identified in any bat species, and the natural reservoir for SUDV remains undiscovered.

Bats inoculated with ebolaviruses did not display any clinical signs or hematologic changes consistent with significant disease, and histologic lesions were minimal. In the pilot ebolavirus study, two individual bats inoculated with either TAFV or RESTV had elevated total white blood cell counts, lymphocytes, and monocytes on two days each. Given that neither bat became viremic and no significant lesions were identified at necropsy, any relationship to viral infection was considered to be unlikely. However, since both bats' WBC counts had returned to the normal range prior to euthanasia, it is possible that lesions were no longer present at necropsy. CBC values in the Sudan virus serial euthanasia study remained within normal limits for all bats.

AST was significantly elevated in one BDBV bat at 5 DPI, relative to controls and all other groups. The same animal had creatinine levels that were elevated relative to other groups, but there was no associated histologic lesion, CBC abnormality, or significant weight loss. Increased AST can be caused by liver damage, but also by damage to muscle or erythrocytes, and, in many species, AST is less liver-specific than ALT (43). In other megachiropteran bats, chemical and manual restraint have been shown to be associated with changes in blood chemistry values (44), and restraint-associated myopathy was speculated as a possible cause of increased AST in a survey of wild flying foxes (*Pteropus giganteus*). In this study, it is possible that AST elevation reflects restraint- or capture-associated myopathy rather than leakage from damaged hepatocytes. Creatine kinase (which specifically reflects muscle damage) was not measured, so was

not available for correlation. In the SUDV serial euthanasia study, AST (but not ALT) was also significantly elevated at 3 DPI relative to controls and to any other day; in the absence of significant liver lesions, this is again suggestive of possible myopathy.

The Egyptian rousette is a natural host for Marburg virus, and a known source of virus spillover to humans. Unlike Marburg virus, no infectious ebolavirus has ever been isolated from a bat. Evidence supporting a role for bats as reservoir hosts for ebolaviruses is based primarily on ecological and epidemiologic data, which has demonstrated spatiotemporal association and epidemiologic links between human cases of EVD and bats. Though EBOV- and RESTV- seropositive bats have been found in areas where filoviruses have never yet been identified (for example, China (34)), ebolaviral RNA has been detected in bats in only a single study (28). In our SUDV serial euthanasia study, we showed that two animals developed low SUDV titers without shedding virus, becoming viremic, or supporting widespread viral replication. Thus, though experimental inoculation was sufficient to induce seroconversion, there was no corroborating evidence to support this bat as a likely SUDV reservoir. Similarly, though field serosurveys have identified EBOV-seropositive Egyptian rousettes, these bats were generally refractory to EBOV infection in our pilot study. In contrast, experimental infections of Egyptian rousettes with MARV in this and previous studies (35,36) have replicated many features of natural MARV infections (22,23,25,26), and have expanded our understanding of the virus-reservoir host dynamics.

In conclusion, we have shown that Egyptian rousette bats are not likely to act as sources of ebolavirus spillover in nature. Indeed, the most likely bat candidates for ebolavirus reservoirs are the three species in which both ebolaviral IgG and RNA have

been detected (*Epomops franqueti*, *Hypsignathus monstrosus*, and *Myonictoris torquata*) (28). Our results, in particular the contrasts between ebolaviruses and Marburg virus, suggest the possibility of a one virus-one host species relationship, analogous to that in hantaviruses and rodent species.

References

1. Kuhn JH, Becker S, Ebihara H, Geisbert TW, Johnson KM, Kawaoka Y, et al. Proposal for a revised taxonomy of the family *Filoviridae*: classification, names of taxa and viruses, and virus abbreviations. *Arch Virol*. 2010 Dec;155(12):2083–103.
2. Negredo A, Palacios G, Vázquez-Morón S, González F, Dopazo H, Molero F, et al. Discovery of an ebolavirus-like filovirus in europe. *PLoS Pathog*. 2011 Oct;7(10):e1002304.
3. Towner JS, Khristova ML, Sealy TK, Vincent MJ, Erickson BR, Bawiec D a, et al. Marburgvirus genomics and association with a large hemorrhagic fever outbreak in Angola. *J Virol*. 2006 Jul;80(13):6497–516.
4. World Health Organization. Ebola haemorrhagic fever in Sudan, 1976. *Bull World Health Organ*. 1978;56(2):247–70.
5. Baron RC, McCormick JB, Zubeir OA. Ebola virus disease in southern Sudan: Hospital dissemination and intrafamilial spread. *Bull World Health Organ*. 1983;61(6):997–1003.
6. Towner JS, Rollin PE, Bausch DG, Sanchez A, Crary SM, Vincent M, et al. Rapid Diagnosis of Ebola Hemorrhagic Fever by Reverse Transcription-PCR in an Outbreak Setting and Assessment of Patient Viral Load as a Predictor of Outcome. *J Virol*. 2004;78(8):4330–41.

7. Towner JS, Sealy TK, Khristova ML, Albariño CG, Conlan S, Reeder S a, et al. Newly discovered ebola virus associated with hemorrhagic fever outbreak in Uganda. *PLoS Pathog.* 2008 Nov;4(11):e1000212.
8. MacNeil A, Farnon EC, Wamala J, Okware S, Cannon DL, Reed Z, et al. Proportion of deaths and clinical features in Bundibugyo Ebola virus infection, Uganda. *Emerg Infect Dis.* 2010 Dec;16(12):1969–72.
9. Albariño CG, Shoemaker T, Khristova ML, Wamala JF, Muyembe JJ, Balinandi S, et al. Genomic analysis of filoviruses associated with four viral hemorrhagic fever outbreaks in Uganda and the Democratic Republic of the Congo in 2012. *Virology.* 2013;442(2):97–100.
10. Siegert R, Shu HL, Slenczka HL, Peters D, Muller G. The aetiology of an unknown human infection transmitted by monkeys (preliminary communication). *Ger Med Mon.* 1968;13(1):1–2.
11. Pattyn S, Jacob W, ven der Groen G, Piot P, Courteille G. Isolation of Marburg-like virus from a case of hemorrhagic fever in Zaire. *Lancet.* 1977;309:573–4.
12. Johnson KM, Lange J V, Webb PA, Murphy FA. Isolation and partial characterisation of a new virus causing acute haemorrhagic fever in Zaire. *Lancet.* ENGLAND; 1977 Mar;1(8011):569–71.
13. Okware SI, Omaswa FG, Zaramba S, Opio A, Lutwama JJ, Kamugisha J, et al. An outbreak of Ebola in Uganda. *Trop Med Int Health.* 2002 Dec;7(12):1068–75.

14. Formenty P, Boesch C, Wyers M, Steiner C, Donati F, Walker F, et al. Ebola Virus Outbreak among Wild Chimpanzees Living in a Rain Forest of Cote d'Ivoire. *J Infect Dis.* 1999;179(Suppl 1):120–6.
15. Formenty P, Hatz C, Le Guenno B, Stoll A, Rogenmoser P, Widmer A. Human infection due to Ebola virus, subtype Côte d'Ivoire: clinical and biologic presentation. *J Infect Dis.* 1999;179(Suppl 1):S48–53.
16. Jahrling PB, Geisbert TW, Dalgard DW, Johnson ED, Ksiazek TG, Hall WC, et al. Preliminary report: isolation of Ebola virus from monkeys imported to USA. *Lancet.* 1990;335(8688):502–5.
17. Rollin PE, Williams RJ, Bressler DS, Pearson S, Cottingham M, Pucak G, et al. Ebola (subtype Reston) virus among quarantined nonhuman primates recently imported from the Philippines to the United States. *J Infect Dis.* 1999;179(Suppl):S108–14.
18. Miranda MEG, Yoshikawa Y, Manalo DL, Calaor AB, Miranda NLJ, Cho F, et al. Chronological and spatial analysis of the 1996 Ebola Reston virus outbreak in a monkey breeding facility in the Philippines. *Exp Anim.* 2002;51(2):173–9.
19. Miranda ME, Ksiazek TG, Retuya TJ, Khan SA, Sanchez A, Fulhorst CF, et al. Epidemiology of Ebola (subtype Reston) virus in the Philippines, 1996. *J Infect Dis.* 1999;179(Suppl):S115–9.

20. Barrette RW, Metwally SA, Rowland JM, Xu L, Zaki SR, Nichol ST, et al. Discovery of swine as a host for the Reston ebolavirus. *Science* (80-). 2009 Jul 10;325(5937):204–6.
21. Centers for Disease Control and Prevention. 2014 Ebola Outbreak in West Africa - Case Counts [Internet]. 2015 [cited 2015 Apr 4]. Available from: <http://www.cdc.gov/vhf/ebola/outbreaks/2014-west-africa/case-counts.html>
22. Towner JS, Amman BR, Sealy TK, Carroll SAR, Comer JA, Kemp A, et al. Isolation of genetically diverse Marburg viruses from Egyptian fruit bats. *PLoS Pathog*. 2009;5(7):e1000536.
23. Amman BR, Carroll SA, Reed ZD, Sealy TK, Balinandi S, Swanepoel R, et al. Seasonal pulses of Marburg virus circulation in juvenile *Rousettus aegyptiacus* bats coincide with periods of increased risk of human infection. *PLoS Pathog*. 2012;8(10):e1002877.
24. Swanepoel R, Smit SB, Rollin PE, Formenty P, Leman PA, Kemp A, et al. Studies of reservoir hosts for Marburg virus. *Emerg Infect Dis*. 2007;13(12):1847–51.
25. Towner JS, Pourrut X, Albariño CG, Nkogue CN, Bird BH, Grard G, et al. Marburg virus infection detected in a common African bat. *PLoS One*. 2007;2(8).
26. Amman BR, Nyakarahuka L, McElroy AK, Dodd KA, Sealy TK, Schuh AJ, et al. Marburgvirus resurgence in Kitaka Mine bat population after extermination attempts, Uganda. *Emerging infectious diseases*. 2014. p. 1761–4.

27. Arata A, Johnson B. Approaches towards studies on potential reservoirs of viral haemorrhagic fever in southern Sudan (1977). *Ebola Virus Haemorrhagic Fever*. 1978.
28. Leroy EM, Kumulungui B, Pourrut X, Rouquet P, Hassanin A, Yaba P, et al. Fruit bats as reservoirs of Ebola virus. *Nature*. 2005 Dec 1;438(7068):575–6.
29. Pourrut X, Souris M, Towner JS, Rollin PE, Nichol ST, Gonzalez J-P, et al. Large serological survey showing cocirculation of Ebola and Marburg viruses in Gabonese bat populations, and a high seroprevalence of both viruses in *Rousettus aegyptiacus*. *BMC Infect Dis*. 2009;9:159.
30. Pourrut X, Délicat A, Rollin PE, Ksiazek TG, Gonzalez J-P, Leroy EM. Spatial and temporal patterns of Zaire ebolavirus antibody prevalence in the possible reservoir bat species. *J Infect Dis*. 2007 Nov 15;196(Suppl 2):S176–83.
31. Hayman DTS, Emmerich P, Yu M, Wang L-F, Suu-Ire R, Fooks AR, et al. Long-term survival of an urban fruit bat seropositive for Ebola and Lagos bat viruses. *PLoS One*. 2010 Jan;5(8):e11978.
32. Taniguchi S, Watanabe S, Masangkay JS, Omatsu T, Ikegami T, Alviola P, et al. Reston Ebolavirus antibodies in bats, the Philippines. *Emerging infectious diseases*. 2011. p. 1559–60.
33. Olival KJ, Islam A, Yu M, Anthony SJ, Epstein JH, Khan SA, et al. Ebola virus antibodies in fruit bats, Bangladesh. *Emerg Infect Dis*. 2013;19(2):270–3.

34. Yuan J, Zhang Y, Li J, Zhang Y, Wang L-F, Shi Z. Serological evidence of ebolavirus infection in bats, China. *Virology Journal*. 2012. p. 236.
35. Paweska JT, Jansen van Vuren P, Masumu J, Leman PA, Grobbelaar AA, Birkhead M, et al. Virological and serological findings in *Rousettus aegyptiacus* experimentally inoculated with vero cells-adapted hogan strain of Marburg virus. *PLoS One*. 2012;7(9):e45479.
36. Amman BR, Jones MEB, Sealy TK, Uebelhoer LS, Schuh AJ, Bird BH, et al. Oral Shedding of Marburg Virus in Experimentally Infected Egyptian Fruit Bats (*Rousettus aegyptiacus*). *J Wildl Dis*. 2015;51(1):113–24.
37. Swanepoel R, Leman PA, Burt FJ, Zachariades NA, Braack LE, Ksiazek TG, et al. Experimental inoculation of plants and animals with Ebola virus. *Emerg Infect Dis. Centers for Disease Control*; 1996;2(4):321–5.
38. Saéz AM, Weiss S, Nowak K, Lapeyre V, Kaba M, Regnaut S, et al. Investigating the zoonotic origin of the West African Ebola epidemic. *EMBO Mol Med*. 2015;7(1):17–23.
39. Krähling V, Dolnik O, Kolesnikova L, Schmidt-Chanasit J, Jordan I, Sandig V, et al. Establishment of fruit bat cells (*Rousettus aegyptiacus*) as a model system for the investigation of filoviral infection. *PLoS Negl Trop Dis*. 2010 Jan;4(8):e802.
40. National Research Council. *Guide for the Care and Use of Laboratory Animals*. 8th Ed. Washington, DC: National Academies Press; 2011.

41. Ksiazek TG, Rollin PE, Williams a J, Bressler DS, Martin ML, Swanepoel R, et al. Clinical virology of Ebola hemorrhagic fever (EHF): virus, virus antigen, and IgG and IgM antibody findings among EHF patients in Kikwit, Democratic Republic of the Congo, 1995. *J Infect Dis.* 1999 Mar;179(Suppl 1):S177–87.
42. Ksiazek TG, West CP, Rollin PE, Jahrling PB, Peters CJ. ELISA for the detection of antibodies to Ebola viruses. *J Infect Dis.* 1999 Feb;179(Suppl):S192–8.
43. Latimer KS, Duncan JR. Duncan and Prasse's Veterinary Laboratory Medicine: Clinical Pathology. 5th Ed. Chichester, West Sussex, UK: Wiley-Blackwell; 2011.
44. Heard DJ, Huft VJ. The Effects of Short-Term Physical Restraint and Isoflurane Anesthesia on Hematology and Plasma Biochemistry in the Island Flying Fox (*Pteropus hypomelanus*). 1998;29(1):14–7.

Table 4.1. Pilot Study: Tissue viral loads as determined by quantitative reverse-transcriptase PCR (Q-RT-PCR)^{a,b} for Egyptian rousette bats (*Rousettus aegyptiacus*) experimentally inoculated with Marburg virus or one of five species of ebolavirus, and euthanized at days 5 or 10 post-inoculation. Tissues in which viral antigen was detected are marked with an asterisk (*).

Virus	DPI	Bat ID	Sex	Skin (inoc)			Ax	Saliv	UrBl	S	Mes		Hrt	Kid	Bld
				Liv	Spl	LN	G	Int		LN	G				
Mock	10	85334	f	-	-	-	-	-	-	-	-	-	-	-	-
		91271	m	-	-	-	-	-	-	-	-	-	-	-	-
MARV	5	86433	f	++++*	++++*	++++*	++	++	++	-	-	-	-	-	++
		50542	m	++++*	++++*	++++*	-	-	++	-	-	++	++	-	++
	10	91482	f	++++*	++	-	-	++	-	++	-	-	-	+++	-
		91547	m	+++*	+++	+++	-	+++	-	++	++	++	-	-	-
SUDV	5	56380	f	+++*	+	+	+	-	-	-	-	-	-	-	-
		16107	m	++	+	+	-	-	-	-	-	-	-	-	-
	10	43612	f	+	-	-	+	-	+	-	-	-	-	-	-
		20778	m	-	-	-	+	-	-	-	-	-	-	-	-
EBOV	5	85933	f	+++*	-	-	-	-	-	-	-	-	-	-	-
		52392	m	-	-	-	-	-	-	-	-	-	-	-	-
	10	41902	f	++	-	-	++	-	-	-	-	-	-	-	-
		26060	m	+	-	-	-	-	-	-	-	-	-	-	-
BDBV	5	41354	f	++	-	-	-	-	-	-	-	-	-	-	-
		91128	m	++	-	-	-	-	-	-	-	-	-	-	-
	10	23796	f	-	-	-	-	-	-	-	-	-	-	-	-
		25844	m	-	-	-	++	-	-	-	-	-	-	-	-
TAFV	5	42084	f	++	-	-	-	-	-	-	-	-	-	-	-
		35825	m	+++	-	-	-	-	-	-	-	-	-	-	-
	10	42348	f	-	-	-	-	-	-	-	-	-	-	-	-
		26015	m	+	-	-	-	-	-	-	-	-	-	-	-
RESTV	5	86551	f	++++*	-	-	-	-	-	-	-	-	-	-	

	38558	m	++	-	-	-	-	-	-	-	-	-	-	-
10	50188	f	++	-	-	-	-	-	-	-	-	-	-	-
	45164	m	-	-	-	++	-	-	-	-	-	-	-	-

^aAbbreviations for tissues: Skin (inoc) = skin taken from inoculation site; Liv = liver, Spl = spleen, Ax LN = axillary lymph node, Saliv G = salivary gland, UrBl = urinary bladder, S Int = small intestine, Mes LN = mesenteric lymph node, Gnd = gonad, Hrt = heart, Kid = kidney, and Bld = blood at time of euthanasia. Abbreviations for viruses: Mock = mock inoculated (control), MARV = Marburg virus, SUDV = Sudan Virus, EBOV = Ebola virus, BDBV = Bundibugyo virus, TAFV = Taï Forest virus, RESTV = Reston virus. DPI = day post-inoculation.

^bTissue viral load as indicated by cycle threshold (Ct) value from Q-RT-PCT assay: + = Ct 35-40, ++ = Ct 30-34.9, +++ Ct 25-29.9, ++++ Ct 20-24.9.

^cTissues also tested that were negative for all animals included adrenal gland, lung, large intestine, brain, and skin from antebrachium.

Table 4.2. Tissue viral loads^a for Egyptian rousette bats (*Rousettus aegyptiacus*) inoculated with Sudan virus (Gulu) in a serial euthanasia study. Tissues in which Sudan virus antigen was identified are marked with an asterisk (*).^{b,c}

Group	DPI	Bat ID	Skin (inoc)	Liv	Spl	Ax LN	Ur Bl	S Int	Lg Int	Gnd	Hrt	Kid
SUDV	3	546948	++++*	-	+	++	+	+	++	++	-	+
		684640	++++*	-	-	+++	+	-	+	+	-	+
		720747	++++*	++	++++	+++*	-	-	+	+	-	+
	6	550595	+++	-	+	+++	-	-	-	-	-	-
		556705	++++	-	-	++	+	+	++	-	-	-
		690641	++++*	+	-	-	++	-	+	-	+	-
	9	725908	+++	-	-	-	-	-	-	-	-	-
		845660	++	-	-	-	-	-	-	-	-	-
		546543	+	-	-	-	-	-	-	-	-	-
	12	721126	++	-	-	+++	-	-	-	-	-	-
		724099	+	-	-	-	-	-	-	-	-	-
		684978	-	-	-	+	-	-	-	-	-	-
	15	642832	++	-	-	-	-	-	-	-	-	-
		721018	++	-	-	-	-	-	-	-	-	-
		723995	-	+	-	-	-	-	-	-	-	-
Mock	15	214528	-	-	-	-	-	-	-	-	-	-
		550277	-	-	-	-	-	-	-	-	-	-
		684727	-	-	-	-	-	-	-	-	-	-

^aViral loads are expressed as 50% tissue culture infective dose (TCID₅₀) equivalents per gram, derived from standard curves of the diluted stock viruses assayed using the identical Q-RT-PCR protocols as that for tissues: + <100 TCID₅₀ eq.; ++ 100-999 TCID₅₀ eq.; +++ 1000-9,999 TCID₅₀ eq.; ++++ 10,000-100,000 TCID₅₀ eq.

^bAbbreviations: Skin (inoc) = skin from the inoculation site (ventral abdomen); Liv = liver; Spl = spleen; Ax LN = axillary lymph node; Ur Bl = urinary bladder; S Int = small intestine; Gnd = gonad; Hrt = heart; Kid = kidney; SUDV = Sudan virus.

^cTissues also tested that were negative in all animals: lung, salivary gland.

Figure Legends

Figure 4.1. Blood chemistry measurements for bats inoculated with six different filoviruses in the pilot study and euthanized at 5 (black bars) or 10 (open bars) days post inoculation (DPI). Mock = mock-inoculated controls, MARV=Marburg virus, SUDV=Sudan virus, EBOV=Ebola virus, BDBV=Bundibugyo virus, TAFV=Taï Forest virus, and RESTV=Reston virus. ALT=alanine aminotransferase, AST=aspartate aminotransferase, ALP=alkaline phosphatase, ALB=albumin, BUN=blood urea nitrogen.

Figure 4.2. Complete white blood cell (WBC) counts for bats inoculated with six different filoviruses in the pilot study and euthanized at 5 and 10 days post inoculation (DPI). Mock = mock-inoculated controls, MARV=Marburg virus, SUDV=Sudan virus, EBOV=Ebola virus, BDBV=Bundibugyo virus, TAFV=Taï Forest virus, and RESTV=Reston virus.

Figure 4.3. Viral RNA, as determined by Q-RT-PCR, in four bats inoculated with Marburg virus and euthanized at 5 (n=2) or 10 (n=2) days post inoculation. **A.** Marburg viral RNA in blood is evidence of viremia in all four Marburg virus-inoculated bats. **B.** Marburg viral RNA in oral (filled bars) and rectal (open bars) swabs.

Figure 4.4. Photomicrographs of liver and spleen from Marburg-virus inoculated Egyptian rousette bats in a pilot study. Tissue in panel A is stained with hematoxylin and in panels B-F with immunoalkaline phosphatase with naphthol fast red and hematoxylin counterstain. **A.** Liver, MARV-inoculated bat, day 5 post-inoculation. A focus of mixed cellular infiltrate and rare necrotic hepatocytes disrupts the parenchyma. **B.** Liver, MARV-inoculated bat, day 5 post-inoculation. Marburgviral antigen is present in a focus of mild hepatic inflammation (arrow). Inset: positive immunostaining in the cytoplasm of

a necrotic hepatocyte. **C and D.** Liver, MARV-inoculated bat, 5 days post-inoculation. Antigen is present perimembranous regions around hepatocytes and in foci of mononuclear cell aggregation in the liver. **E.** Spleen, MARV-inoculated bat, 5 days post-inoculation. MARV antigen is present in small numbers of red pulp macrophages (arrows). **F.** Spleen, MARV-inoculated bat, 5 days-post inoculation. Higher magnification of (E). MARV antigens are localized in the cytoplasm of cells morphologically consistent with macrophages.

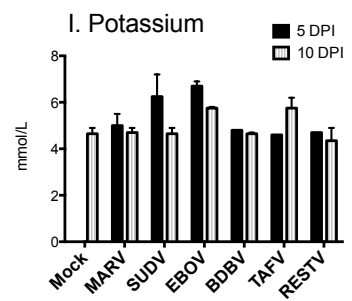
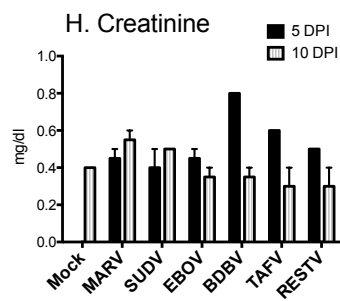
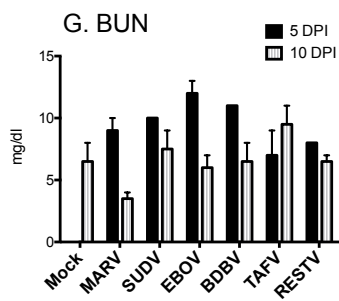
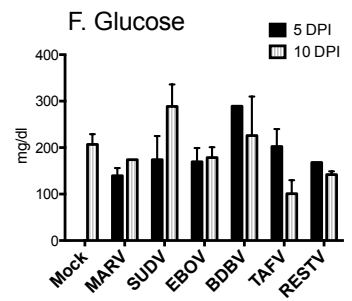
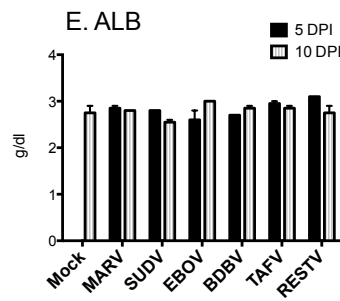
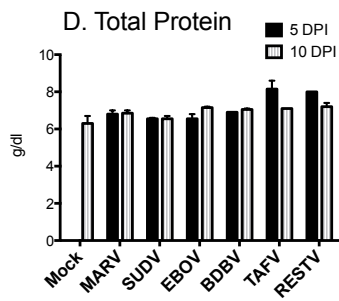
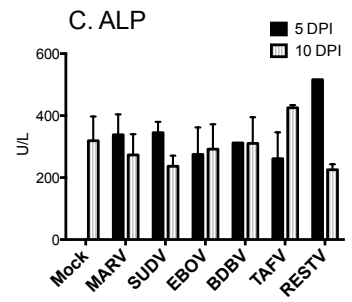
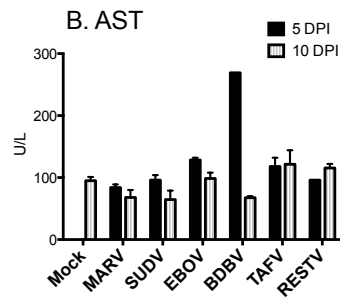
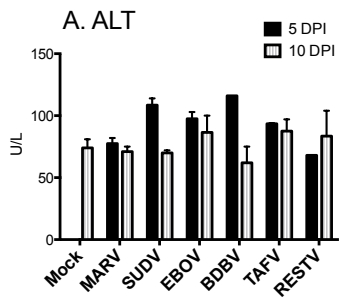
Figure 4.5. Complete blood count data for Egyptian rousette bats inoculated with Sudan virus (n=15, green triangles), Marburg virus (N=3, red squares) and mock-inoculated controls (n=3, open circles/dashed line) in a serial euthanasia study. WBC=white blood cell count, RBC=red blood cell count, MARV=Marburg virus, SUDV=Sudan virus.

Figure 4.6. Blood chemistry measurements Egyptian rousette bats inoculated with Sudan virus. Three Sudan virus-inoculated bats were euthanized on each of days 3, 6, 9, 12 and 15 post-inoculation. Mock-inoculated bats were euthanized on day 15. Mock=mock-inoculated controls, SUDV=Sudan virus, ALT=alanine aminotransferase, AST=aspartate aminotransferase, ALP=alkaline phosphatase, ALB=albumin, BUN=blood urea nitrogen.

Figure 4.7. Serology results for Egyptian rousette bats inoculated with Sudan virus in a serial euthanasia study. Results for anti-SUDV IgG measured by enzyme linked immunosorbent assay are shown as adjusted sum optical densities (OD) by day post-inoculation for 15 SUDV inoculated bats (black circles) and 3 mock-inoculated control bats (open squares).

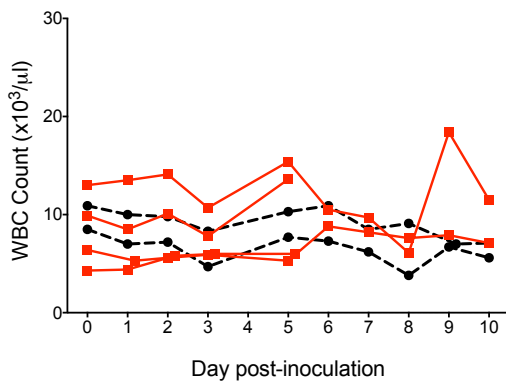
Figure 4.8. Comparison of Sudan viral and Marburg viral RNA levels in Egyptian rousette tissues (skin at the inoculation site, liver, spleen, and kidney) compared at days

3, 6, 9, 12, and 15 post-infection. Viral loads are expressed as \log_{10} 50% tissue culture infective dose (TCID₅₀) equivalents per gram, derived from quantitative reverse-transcriptase PCR. Data for days 3-12 for Marburg virus-inoculated bats are from Amman *et al.*, 2015 (36) and see Supplemental Data in Appendix A.

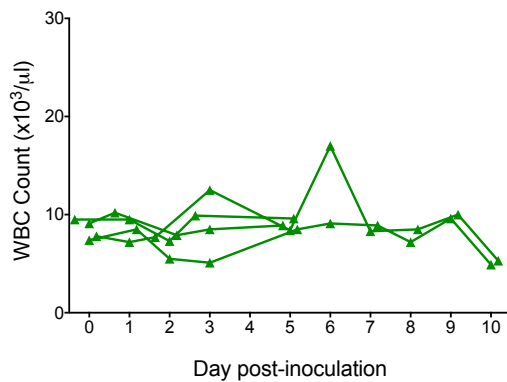


4.1

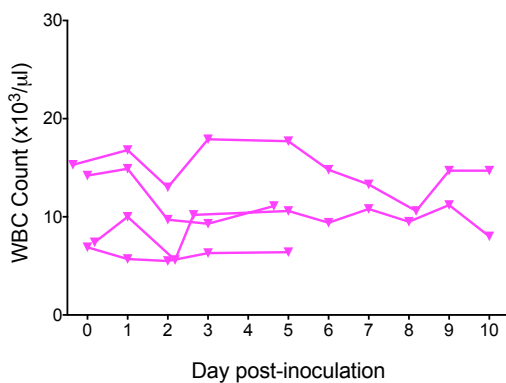
MARV



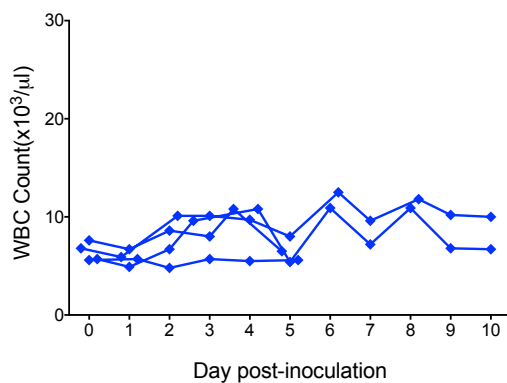
SUDV



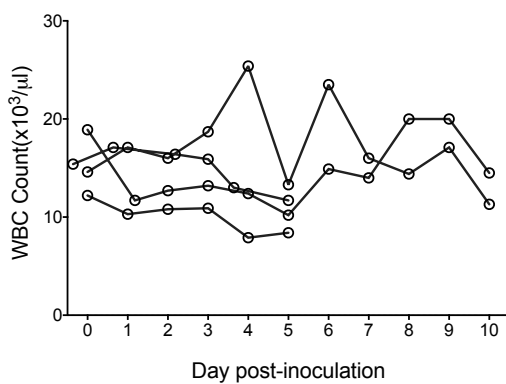
EBOV



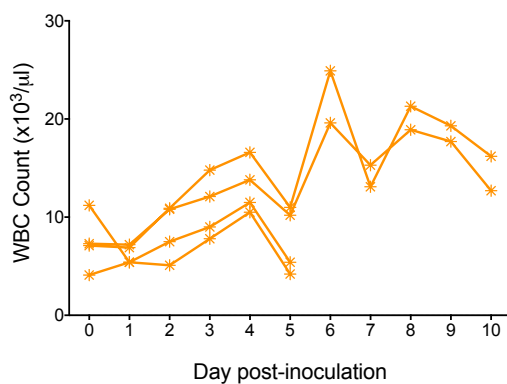
BDBV



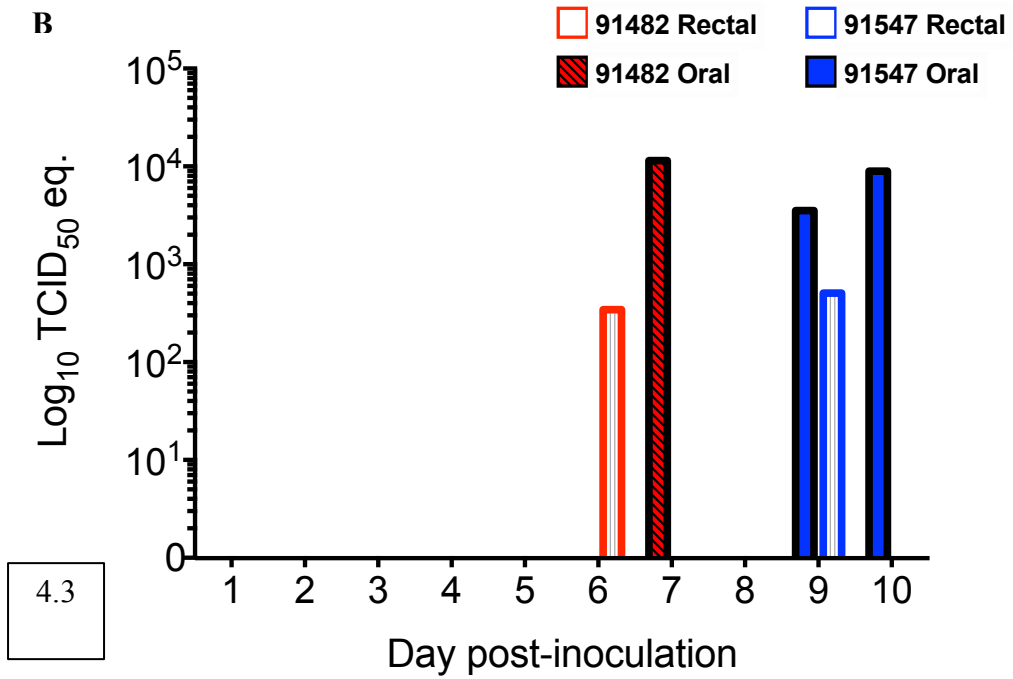
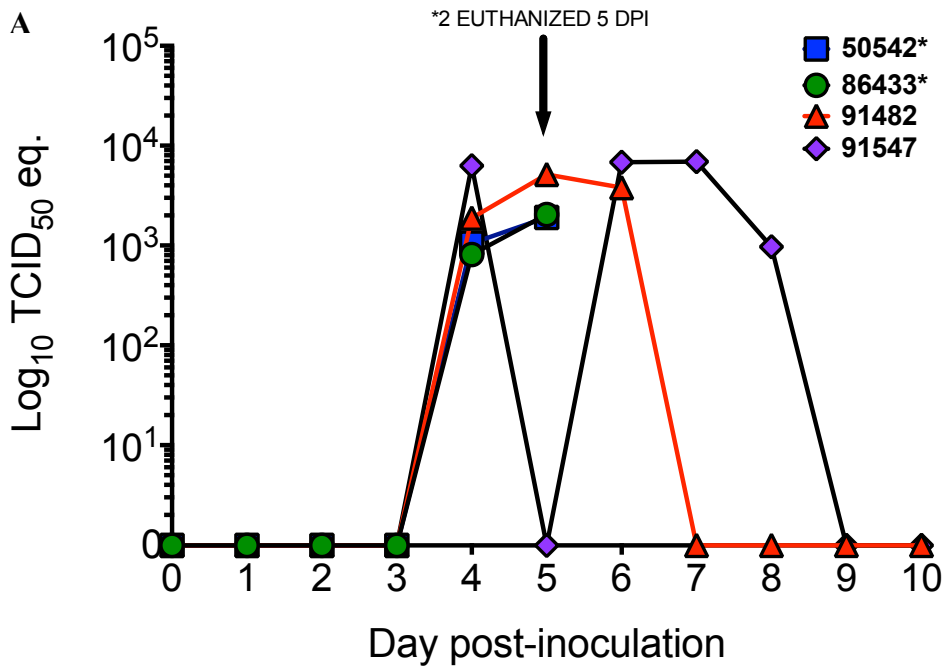
TAFV



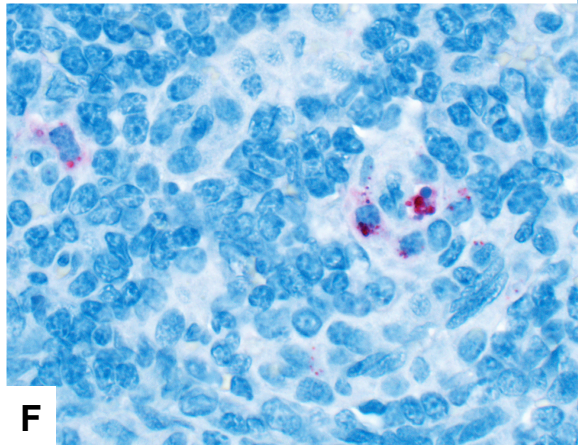
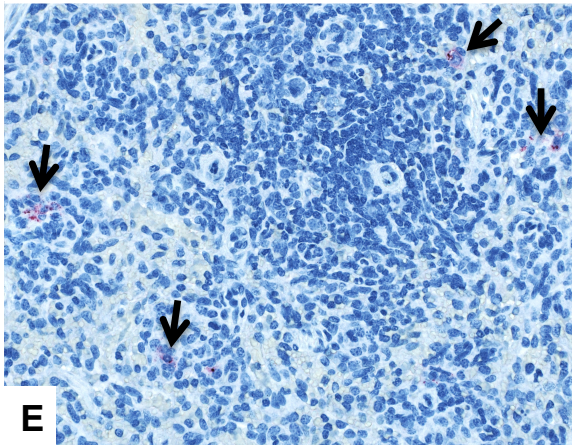
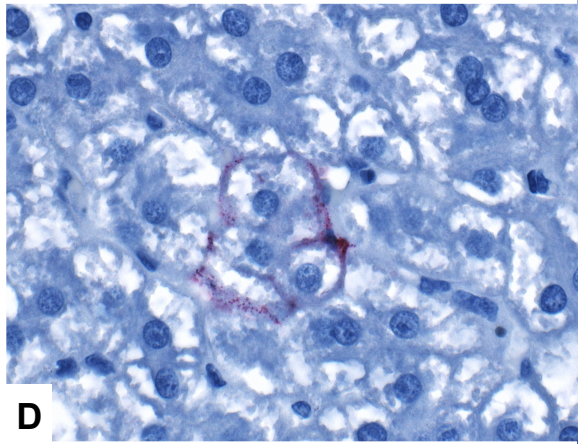
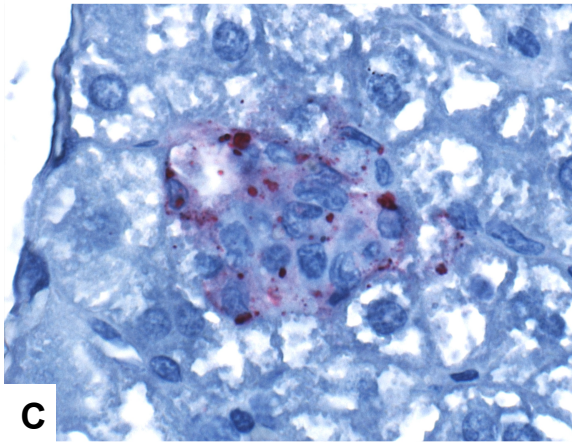
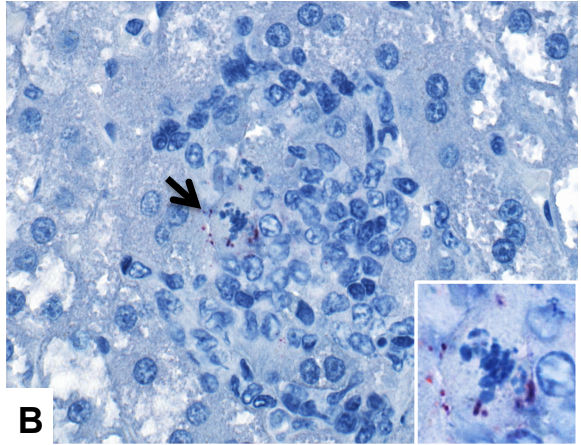
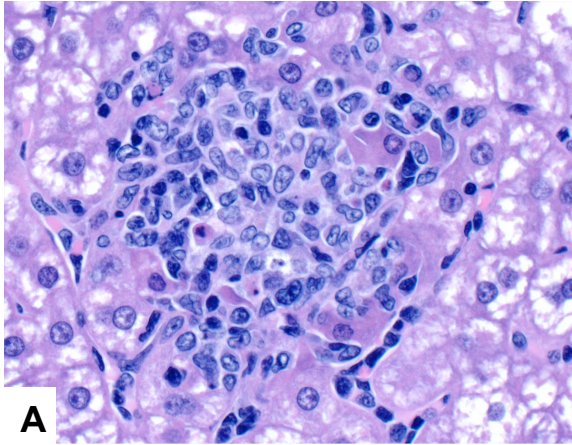
RESTV



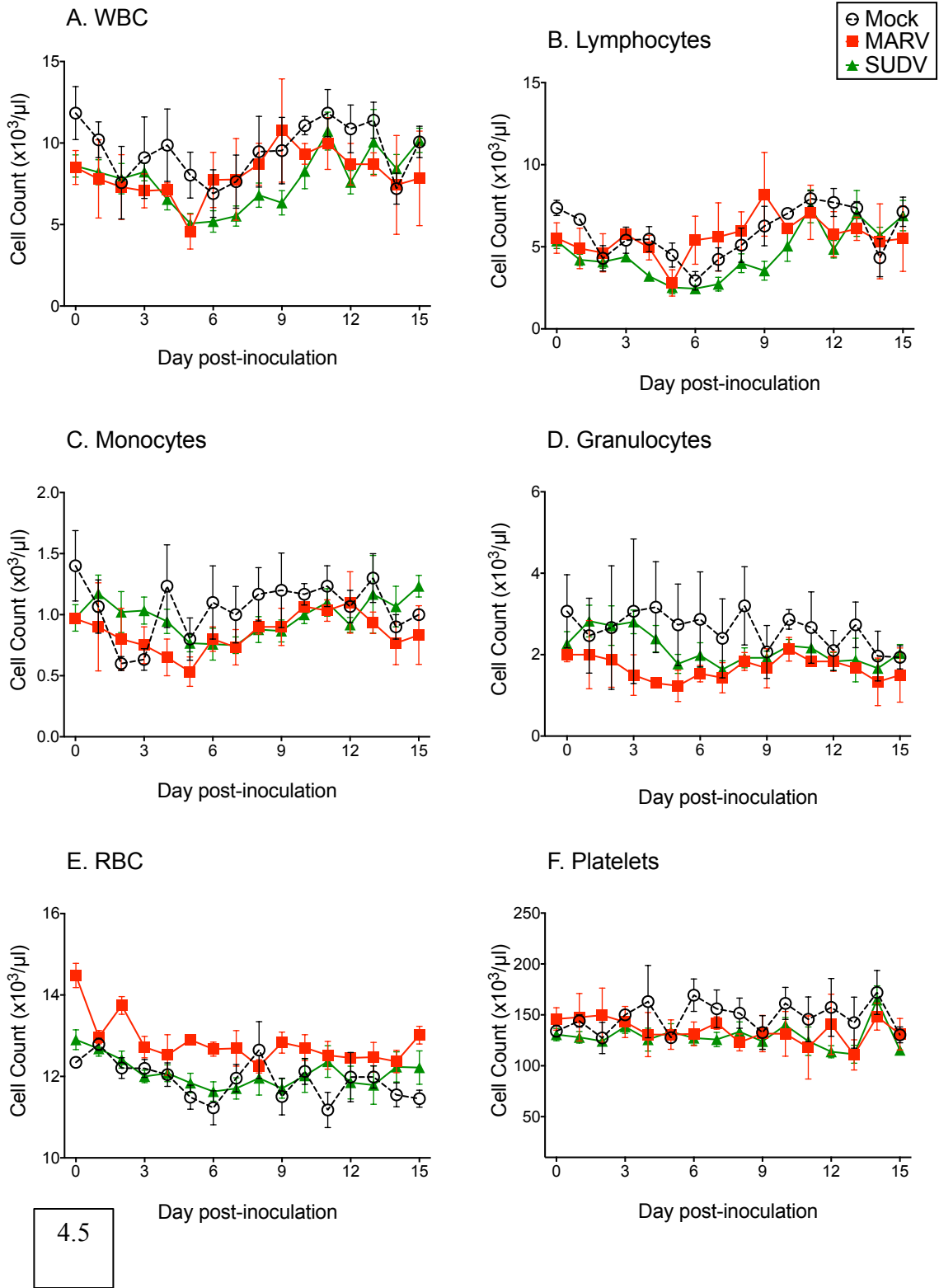
4.2

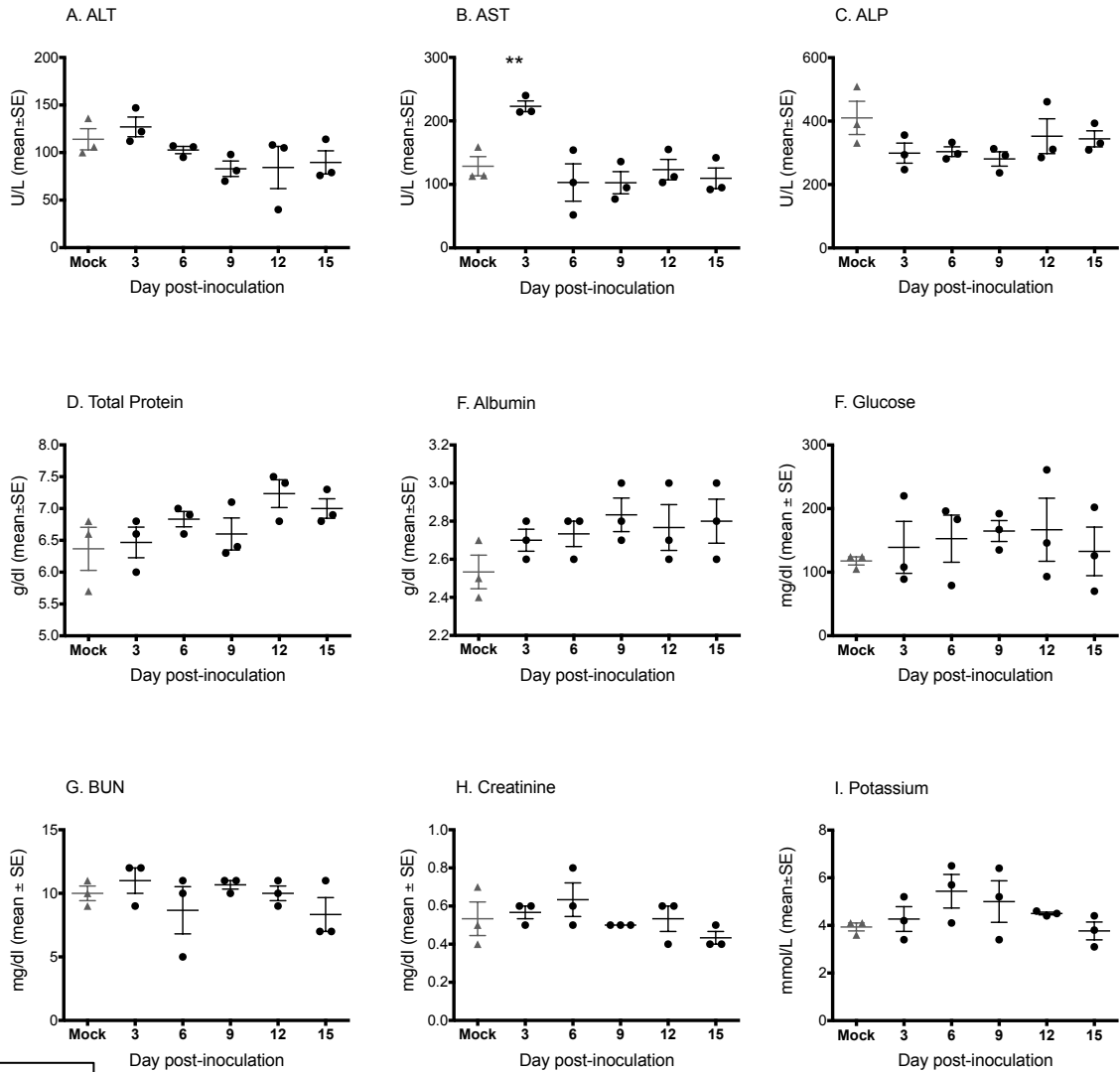


4.3

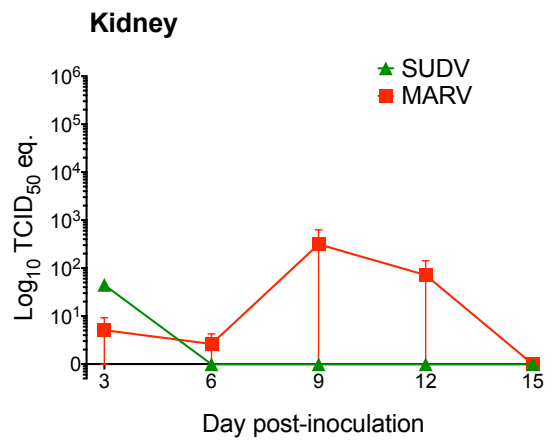
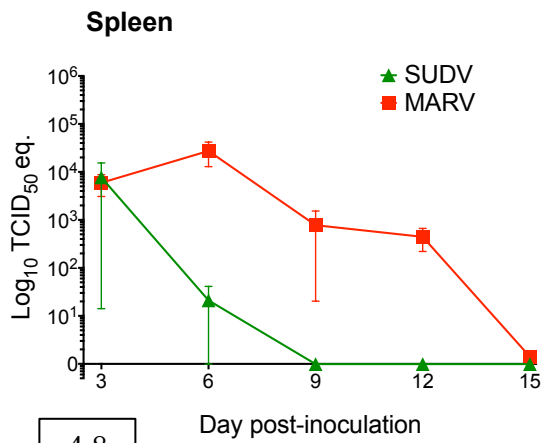
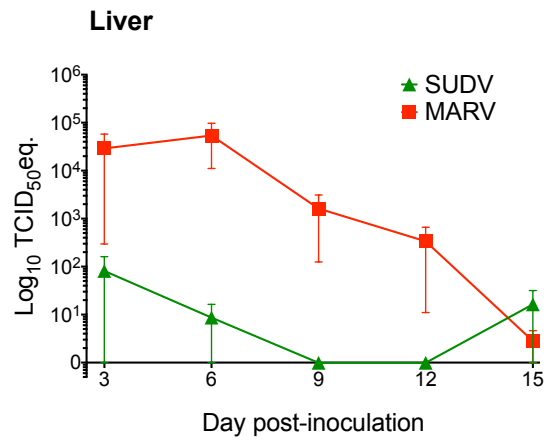
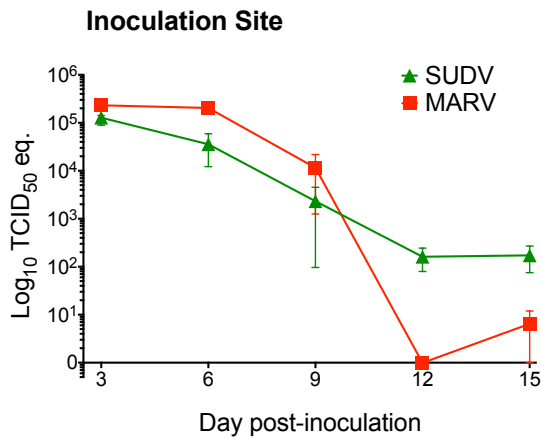


4.4





4.6



4.8

CHAPTER 5

CONCLUSIONS

The ongoing Ebola virus outbreak in West Africa is, by orders of magnitude, the largest filovirus outbreak recorded, and the first to occur in that region. The marked expansion in case numbers and new geographic range demonstrate the potential for filoviruses to become threats to public health on a global scale. Until the last decade, the identity of the reservoir host(s) for filoviruses has remained elusive. Significant gaps in the understanding of filoviral natural history have interfered with prediction or prevention of filoviral disease outbreaks.

A role for bats in the filovirus life cycle has long been postulated, but has only been confirmed for marburgviruses. Our research has advanced the understanding of the relationship between filoviruses and one bat species that is implicated as a potential source of both marburgviruses and ebolaviruses in nature, the Egyptian rousette.

In the first set of experiments, we built upon the key findings of recent longitudinal field studies that established the Egyptian rousette as a marburgvirus reservoir and consistent source of virus spillover to humans. Experimental infection studies were essential for elucidating the dynamics of this virus-reservoir host relationship. In our Marburg virus serial euthanasia study, we replicated as closely as possible the natural infection patterns observed in the wild. We used a low-passage, wild-type virus originally isolated from a Ugandan rousette bat, and our study animals were same-cohort, first generation captive-born juveniles. We showed that experimentally

inoculated bats exhibit viremia, widespread virus dissemination, and viral shedding, and we demonstrated viral antigen in tissues. Very mild liver lesions and splenic and hepatic antigen distribution were comparable to observations in naturally infected bats.

Furthermore, we demonstrated that Marburg virus exhibits tropism for macrophages, fibroblasts, and hepatocytes in Rousette bats. These cell types are also infected in natural cases of Marburg virus disease in humans and nonhuman primates. However, despite early infection of macrophages, viremia, dissemination to lymph nodes, replication in spleen, skin, and liver, and evidence of direct virus-induced hepatocyte damage, Marburg virus infection causes minimal disease in bats, and the duration of infection appears to be limited.

This was the first ever comprehensive study of the clinical and pathologic effects of a filovirus in its reservoir host. Our findings establish that this experimental model recapitulates natural infections. This model will be an essential tool for investigating the molecular and immunologic determinants of filovirus circulation in nature, and spillover to humans and nonhuman primates. This is a fundamental first step for understanding the innate and adaptive mechanisms by which these bats control infection, and for addressing numerous still-unanswered questions such as the potential for bats to be persistently infected, dynamics of bat-to-bat transmission, and potential for long-term viral maintenance in the population.

In contrast to marburgviruses, none of the five known ebolaviruses (Sudan virus, Ebola virus, Bundibugyo virus, Tai Forest virus, Reston virus) has ever been isolated from a potential reservoir host, and the source of ebolavirus infection in nature is not known. In our second set of experiments, we showed that Egyptian rousette bats are

generally refractory to experimental ebolavirus infection, and demonstrated a clear contrast between findings for all five known ebolaviruses and Marburg virus. In another set of experiments, we showed that inoculation of rousettes with Sudan virus elicited low-level tissue dissemination of virus and seroconversion, without viremia or evidence of viral shedding. These findings suggest that Egyptian rousette bats are not likely to act as sources of ebolavirus spillover in nature. Cumulatively, our results, in particular the contrasts between ebolaviruses and Marburg virus, suggest the possibility of a one virus-one host species relationship, analogous to that in hantaviruses and rodent species.

APPENDIX A

SUPPLEMENTAL DATA:

VIREMIA, VIRAL TISSUE DISSEMINATION, AND EVIDENCE OF ORAL
SHEDDING IN EGYPTIAN ROUSETTE BATS EXPERIMENTALLY INOCULATED
WITH MARBURG VIRUS*

* Selected data published in different format in Amman BR, Jones MEB, Sealy TK, Uebelhoer LS, Schuh AJ, Bird BH, Coleman-McCray JD, Martin BE, Nichol ST, and Towner, JS. Oral Shedding of Marburg Virus in Experimentally Infected Egyptian Fruit Bats (*Rousettus aegyptiacus*). J Wildl Dis. 2015;51(1):113–24.

Supplemental Data

As described in Chapter 3, we performed a serial euthanasia experiment in which 27 (three groups of nine) juvenile, male Egyptian rousettes were inoculated with 10^4 TCID₅₀ of low-passage, wild-type Marburg virus derived from an isolate originally obtained from a rousette bat from Kitaka Cave, Uganda (Towner et al 2009). Three control bats were mock-inoculated. 3 bats per time point were euthanized at days 3, 5-10, 12, and 28 post-inoculation, and mock-inoculated controls were euthanized on day 28. This study was divided into two components, one detailing the Q-RT-PCR findings (Amman et al 2015), and the other detailing clinical, pathologic, and immunohistochemical findings (Chapter 3 in this dissertation). Blood, oral, and rectal swabs were collected for quantitative reverse-transcriptase PCR (Q-RT-PCR) between days 0 and 14, then weekly until day 28. Tissues were collected for Q-RT-PCR at the time of euthanasia and necropsy. Presented below for completeness, and for correlation with findings in Chapters 3 and 4, are key Q-RT-PCR data modified from Amman *et al*, 2015, in which MEBJ is listed as second author for significant contributions to experimental design, performing the experiments, developing standard curves for determination of viral load from cycle threshold (Ct) values, performing data analysis, and writing the manuscript.

Table A.1. Viral loads^a in tissues from Egyptian rousette bats inoculated with Marburg virus in a serial euthanasia study^b.

Day	Bat ID	Li	Spl	Bld	Hrt	Kid	Adr	Lu	LI	SI	MesLN	Tes	SkIn	UrBl	SG
3	40088	++	+++	++	+	+	--	+	+	--	+	+	+++++	+	--
	42250	++	++	+	--	--	--	--	--	--	+	--	+++++	--	--
	42336	++++	+++	--	--	--	--	--	--	--	--	--	+++++	--	+
5	19854	+++	+++++	+++	+	+	--	+	+	--	+	--	+++++	+	+
	42919	++++	++++	++	+	--	--	--	+	--	+	--	+++++	+	--
	56159	+++++	+++++	+++	--	--	--	--	--	--	++	--	+++++	++	--
6	42672	++	++++	++	--	+	--	+	+	--	--	--	+++++	--	--
	38666	++++	+++	++	--	--	--	--	--	--	+	--	+++++	+	--
	36412	+++++	++++	+++	--	--	--	--	++	--	--	--	+++++	+	+
7	40896	+++	+++	--	--	+++	--	--	--	--	--	+	++++	--	++
	43165	++++	+++	+	++	+	--	--	+	+++	--	--	+++++	+	--
	38702	++++	+++	--	--	--	--	--	+	--	--	--	++++	--	--
8	42853	+++++	+++	+	+	++	++	++	+++	++	++++	++++	+++++	+	+++
	41032	++	+++	--	--	--	--	++	--	--	+	--	++++	--	+
	90906	++++	++	--	--	--	--	--	--	--	--	--	++	--	--
9	36089	+++	+++	+	--	++	+	--	++	+	+++	--	++++	--	--
	43133	+	+	--	--	--	--	--	--	--	--	--	+++	--	--
	20712	++	--	--	--	--	--	--	--	--	--	--	+++	--	--
10	41880	+	++	--	--	--	--	--	+	--	--	--	+++	--	+
	42030	++	++	--	--	++	--	--	+	+	--	++	++	--	++
	40002	--	--	--	--	--	--	--	--	--	--	--	--	--	--
12	43662	+	++	--	+	--	--	--	--	--	--	--	--	--	--
	41671	++	++	--	+	++	--	+	--	--	--	--	--	--	--
	42509	--	--	--	--	--	--	--	--	--	--	--	--	--	--
28	41468	--	+	--	--	--	--	--	--	--	--	--	--	--	--
	41412	--	+	--	--	--	--	--	--	--	--	--	--	--	--

85963	--	--	--	--	--	--	--	--	--	--	--	--	--	--	--
-------	----	----	----	----	----	----	----	----	----	----	----	----	----	----	----

^aViral loads are expressed as 50% tissue culture infective dose (TCID₅₀) equivalents derived from standard curves of the diluted stock viruses assayed using the identical Q-RT-PCR protocols as that for tissues: + <100 TCID₅₀ eq.; ++ 100-999 TCID₅₀ eq.; +++ 1000-9,999 TCID₅₀ eq.; ++++ 10,000-99,999 TCID₅₀ eq.; +++++ 100,000 to 1,000,000 TCID₅₀ eq.

^bAbbreviations: Li=liver, Spl=spleen, Bld=blood (at time of terminal bleed), Hrt=heart, Kid=kidney, Lu=lung, MesLN=mesenteric lymph node, Tes=testis, SkIN=skin from the inoculation site, UrBl=urinary bladder, SG=salivary gland.

Figure Legends

Figure A.1. Viral RNA load in blood (Q-RT –PCR derived 50% tissue culture infective dose (TCID₅₀) equivalents (eq.)/gram) in 27 bats inoculated with Marburg virus in a serial euthanasia study. Mean±SEM TCID₅₀ eq. for each group (A, B, or C) are shown with the overall mean for all 27 bats (dashed line), by day post-inoculation.

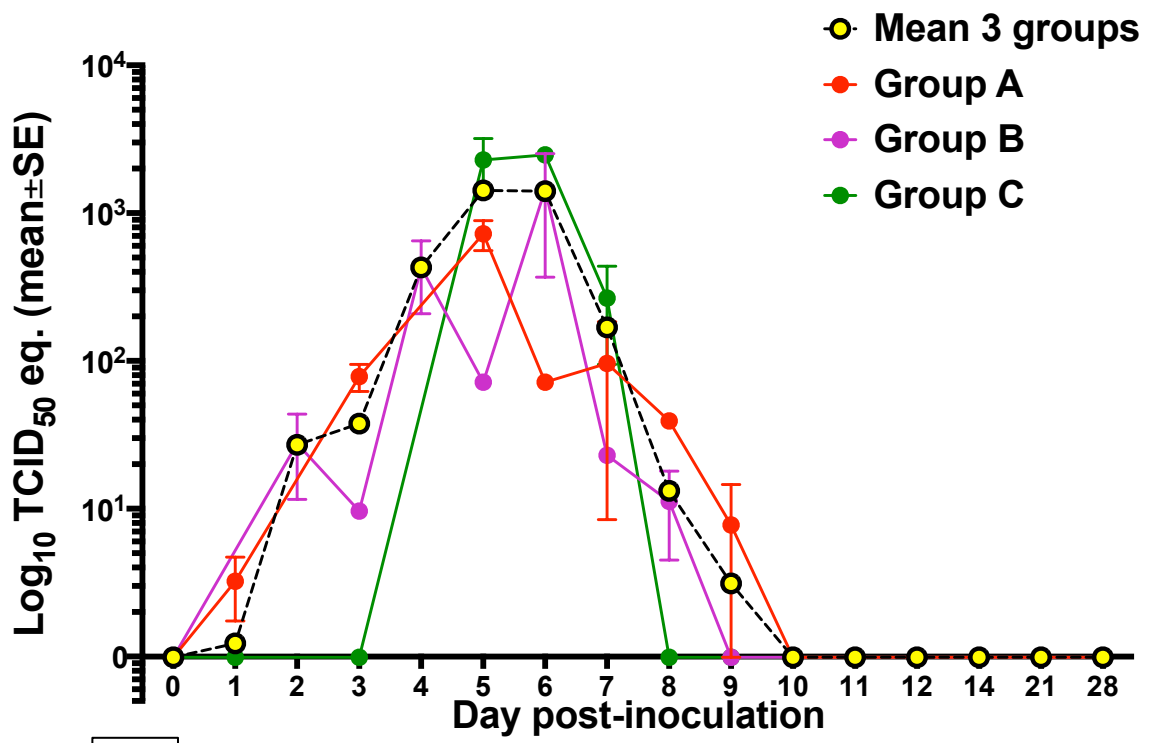
Figure. A.2. Viral RNA loads for spleen, liver, kidney, and skin at the inoculation site, compared with blood levels at the time of euthanasia. Results for Q-RT-PCR are shown as 50% tissue culture infective dose (TCID₅₀) equivalents (eq.)/g by day post-inoculation. RNA levels for spleen, liver, and skin at the inoculation site were greater than the inoculation dose of virus, consistent with viral replication.

Figure A.3. Viral RNA loads for tissues potentially involved in viral shedding (large intestine, urinary bladder, and salivary gland) for 27 bats inoculated with Marburg virus in a serial euthanasia study. Results for Q-RT-PCR are shown as 50% tissue culture infective dose (TCID₅₀) equivalents (eq.)/g by day post-inoculation.

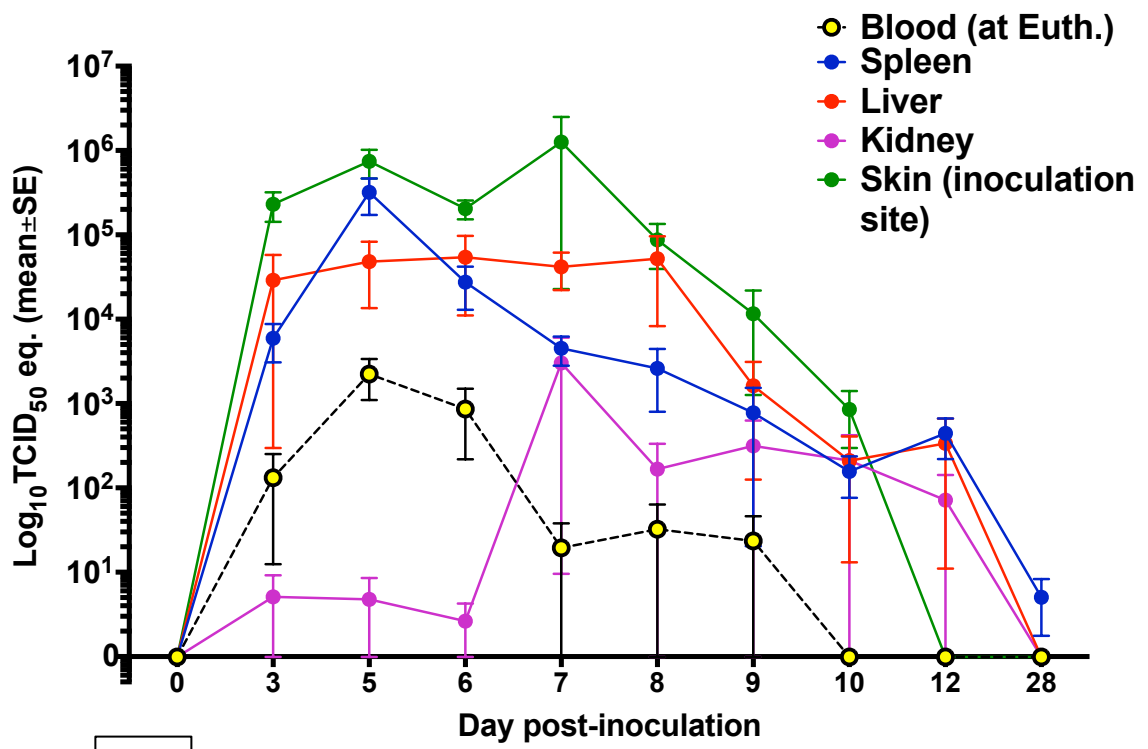
Figure A.4. Viral loads for oral and rectal swabs taken from bats experimentally inoculated with Marburg virus. Results for Q-RT-PCR are shown as 50% tissue culture infective dose (TCID₅₀) equivalents (eq.)/mL by day. RNA was detected in both oral and rectal swabs in four bats. Marburg virus was isolated from two oral swabs from day 8 and one from day 11, marked with asterisks (*).

Figure A.5. Serology results for bats inoculated with Marburg virus in a serial euthanasia study. All bats had seroconverted by 12 days post-inoculation. Results for anti-Marburg virus IgG measured by enzyme-linked immunosorbent assay (ELISA) are shown as adjusted sum optical densities (OD) by day post-inoculation. Serum for ELISA was taken

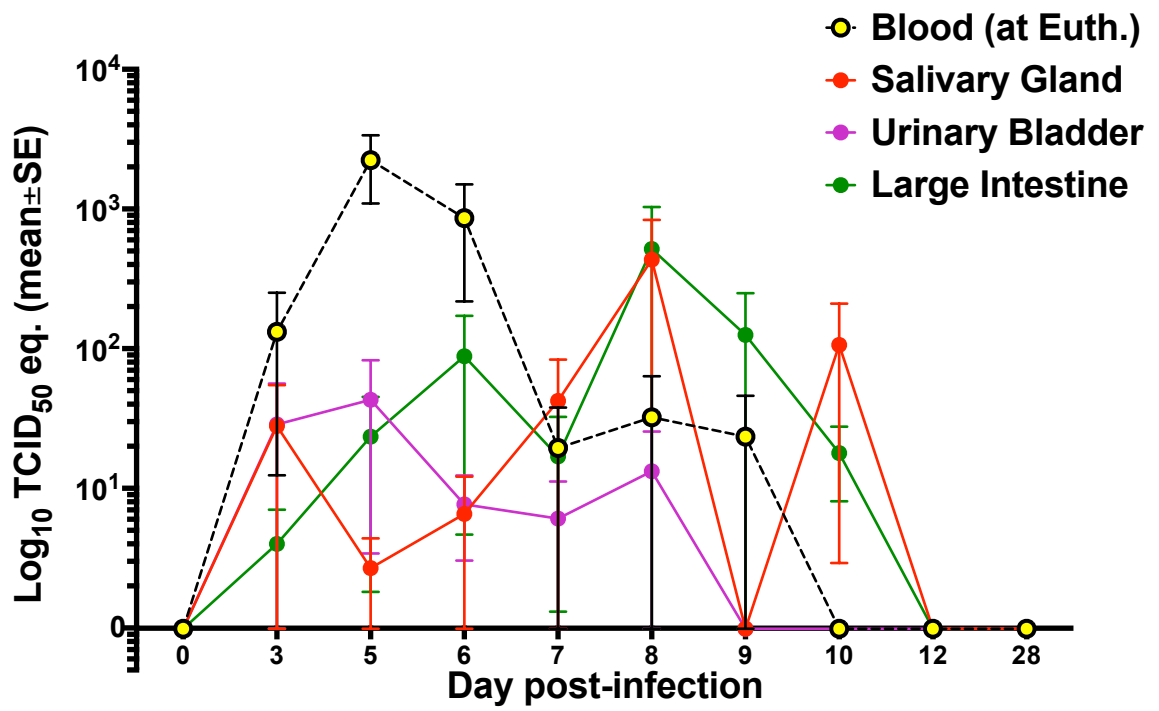
at the time of euthanasia (n=3 bats per time point). The mean adjusted sum OD is shown as a black curve.



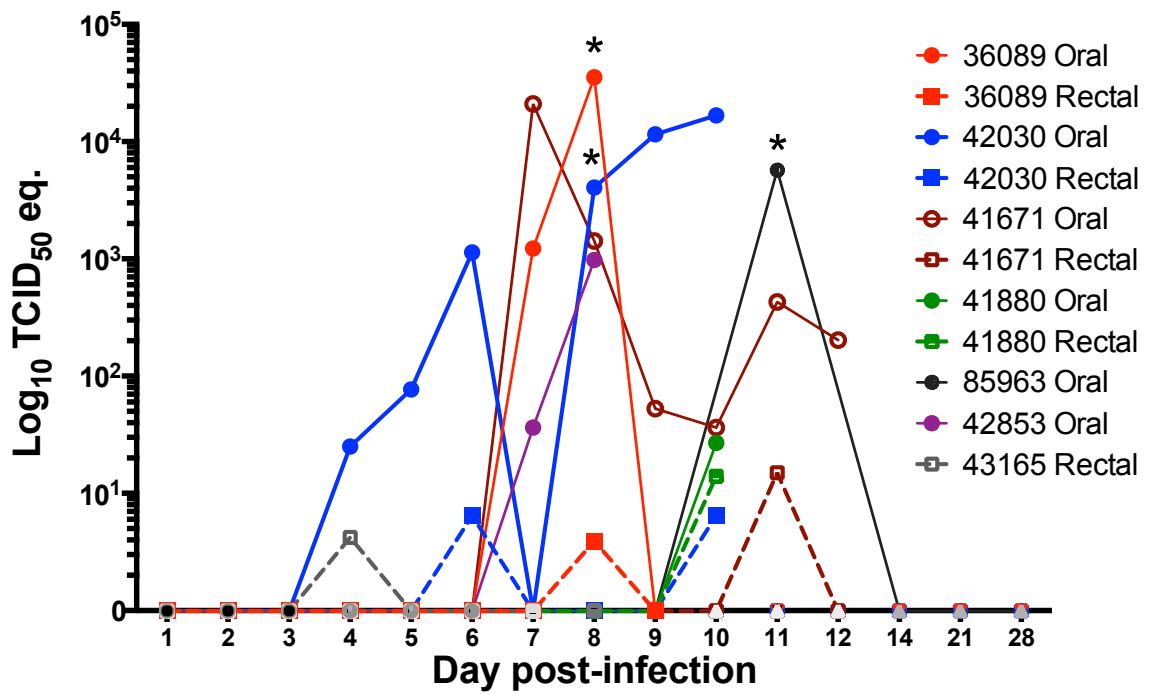
A.1



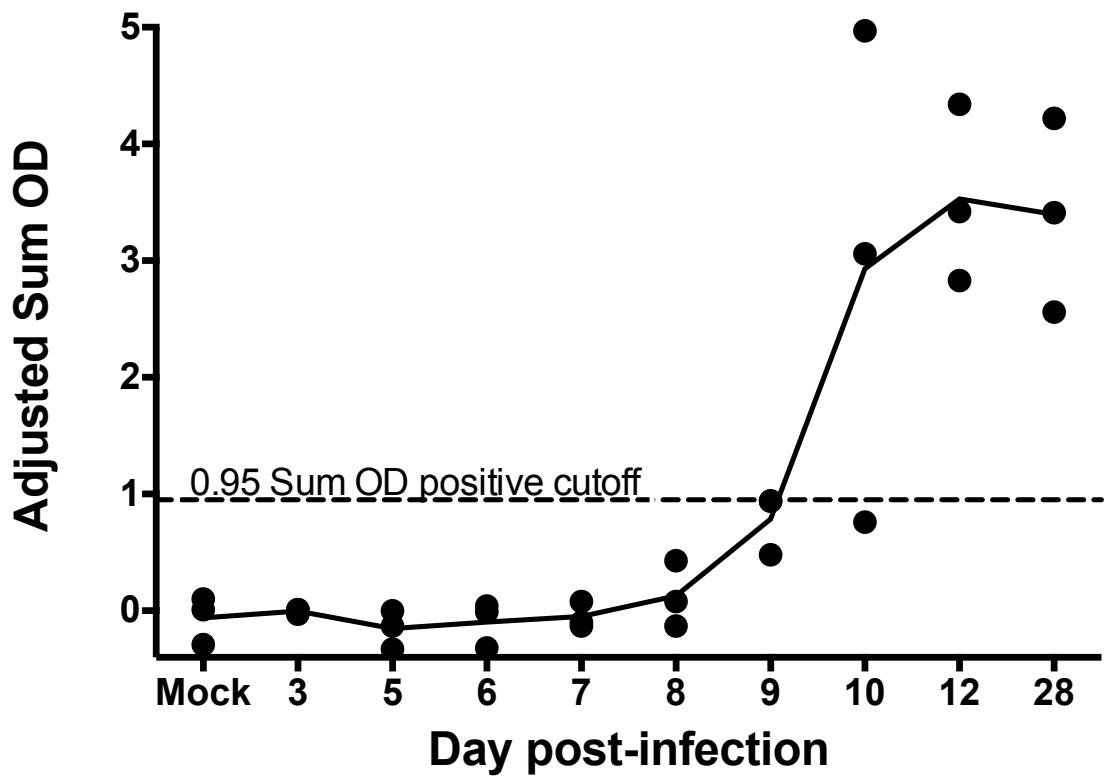
A.2



A.3



A.4



A.5